Establishment of a hiPSC-based *in vitro* model to study environmental and genetic disturbances of neurodevelopmental processes

Inaugural-Dissertation

zur Erlangung des Doktorgrades
der Mathematisch-Naturwissenschaftlichen Fakultät

der Heinrich-Heine-Universität Düsseldorf

vorgelegt von

Maxi Hofrichter

aus Halle an der Saale

Düsseldorf, April 2016

Angefertigt am Leibniz-Institut für umweltmedizinische Forschung (IUF)

an der Heinrich-Heine-Universität Düsseldorf

Gedruckt mit der Genehmigung der

Mathematisch-Naturwissenschaftlichen Fakultät der

Heinrich-Heine-Universität Düsseldorf

Referent: Prof. Dr. Ellen Fritsche

Korreferent: Prof. Dr. Dieter Willbold

Tag der mündlichen Prüfung: 29.06.2016

Table of Contents

Abstract

Studying mechanisms causing human brain disorders remains to be challenging due to the difficulty in obtaining neural tissue from patients. Despite the availability of an enormous variety of transgenic animals, these do not necessarily reflect human disease. Thus, the novel technique of human induced pluripotent stem cells (hiPSCs) represents a promising alternative method for patient-specific disease modeling. Cockayne syndrome B (CSB) is a rare autosomal recessive disease caused by mutations in the *CSB* gene, leading to severe neurodevelopmental defects. How *CSB* mutations impair brain development is so far enigmatic due to a lack of models to investigate CSB because compared to humans CSB-deficient animal models reveal a significantly milder neurological phenotype.

Therefore, the goal of this study was to create a hiPSC-derived *in vitro* method that allows investigations on the neurodevelopmental pathophysiological mechanisms underlying the severe neurological symptoms of CSB patients. In analogy to primary human neurospheres, which represent a well-studied *in vitro* method for studying basic processes of brain development, like proliferation, migration, neuronal and glial differentiation, hiPSCs were differentiated into three-dimensional neurospheres. Therefore, two different protocols were compared: one neural induction protocol using noggin (Noggin protocol) and one cultivating cells in neural induction medium containing B27 and N2 medium supplements (NIM protocol). Flow cytometry analyses revealed that both methods resulted in the differentiation of hiPSCs to $Nestin^{+}/SOX2^{+}$ neural progenitor cells (NPC), forming neurospheres. To test their performance, both hiPSC-derived neurospheres were compared to primary neurospheres generated directly from fetal brains. The comparative studies revealed that with regard to NPC proliferation and neuronal differentiation hiPSC-derived neurospheres created with the NIM protocol are more similar to primary human neurospheres than hiPSC-derived neurospheres generated with the Noggin protocol. Using the NIM protocol, hiPSCs derived from two different CSB patients with two different mutations (p.0 and pArg683x) and two healthy controls were differentiated into neurospheres. CSB-deficient hiPSC-derived neuropsheres display impaired proliferation as measured by the increase of sphere diameter over a time period of 14 days. Moreover, they show a decreased migration capacity and impaired differentiation compared to healthy controls.

In summary, this hiPSC-based neurosphere method allows investigations of mechanisms causing human neurodevelopmental disease. Thus, it can be used for studying the pathophysiological mechanisms underlying the neurodevelopmental phenotypes of CSB patients in the future.

Zusammenfassung

Molekulare Untersuchungen von Störungen der menschlichen Gehirnentwicklung werden derzeit hauptsächlich an Tiermodellen durchgeführt. Durch Speziesunterschiede ist jedoch eine direkte Übertragbarkeit der Resultate auf den Menschen nicht immer gegeben. Humane induzierte pluripotente Stammzellen (hiPS) stellen eine vielversprechende Alternativmethode zur Patienten-spezifischen Krankheitsmodellierung dar, da sie auf humanen Zellen basieren, sich in quasi alle Zelltypen des Körpers differenzieren können und in unbegrenzter Menge zur Verfügung stehen. Das Cockayne Syndrom B (CSB) ist eine seltene, autosomal-rezessive Krankheit, die durch Mutationen im *CSB* Gen ausgelöst wird und zu schweren neuralen Entwicklungsstörungen führt. In welcher Weise *CSB* Mutationen jedoch die Gehirnentwicklung beeinträchtigen, ist bisher nicht bekannt, da es keine geeigneten Tiermodelle zur Untersuchung der Gehirnentwicklung von CSB gibt. CSB-defiziente Mäuse zeigen einen signifikant schwächeren neurologischen Phänotyp als CSB Patienten. Das Ziel dieser Arbeit war daher die Entwicklung eines hiPS-basierten *in vitro* Modells zur Untersuchung der Mechanismen, die den pathophysiologischen Veränderungen von CSB Patienten bei der Gehirnentwicklung zugrunde liegen. Analog zu primären humanen Neurosphären, die eine gut erforschte *in vitro* Methode zur Untersuchung von Gehirnentwicklungsprozessen wie Proliferation, Migration, neuronale und gliale Differenzierung darstellen, wurden hiPS Zellen in drei-dimensionale Neurosphären differenziert. Dazu wurden zwei verschiedene neurale Induktionsprotokolle miteinander verglichen: Im ersten Protokoll wurden die Zellen mit Hilfe von Noggin induziert (Noggin Protokoll), während für das zweite Protokoll ein spezielles neurales Induktionsmedium mit B27 und N2 Mediumzusätzen (NIM Protokoll) verwendet wurde. Beide Protokolle resultierten in der Differenzierung von hiPS Zellen zu neuralen $Nestin^{+}/SOX2^{+}$ Progenitorzellen. Vergleichende Analysen mit primären humanen Neurosphären zeigten jedoch, dass hiPS-Neurosphären aus dem NIM Protokoll hinsichtlich der Proliferation und Differenzierung den primären Zellen stärker ähnelten als die hiPS-Neurosphären aus dem Noggin Protokoll. Mit Hilfe des NIM Protokolls wurden anschließend hiPS Zellen von zwei verschiedenen CSB Patienten mit zwei verschiedenen Mutationen (p.0 und pArg683x) und zwei gesunden Kontrollen zu Neurosphären differenziert. CSB-defiziente hiPS-Neurosphären zeigten eine veränderte Proliferation über eine Zeitspanne von 14 Tagen. Außerdem konnte eine verringerte Migration und eine Beeinträchtigung der Differenzierung im Vergleich zu den gesunden Kontrollen gemessen werden.

Zusammengefasst scheint diese hiPS-basierte *in vitro* Methode die Untersuchung von Prozessen der Gehirnentwicklung zu erlauben, die zu neuropathologischen Veränderungen bei CSB Patienten führen. Weiterführende Untersuchungen werden die den funktionellen Defekten zu Grunde liegenden Signalwege aufdecken.

1. Introduction

1.1 Brain development

The brain is a highly complex organ that forms together with the spinal cord the central nervous system (CNS). It is composed of different specialized cell types which intensively interact with each other to ensure a proper brain function. These cell types include neurons and glial cells, further separated into astrocytes, oligodendrocytes and microglia (Kandel 2000). Whereas neurons, astrocytes and oligodendrocytes originate from the ectodermal germ layer, microglia are known to derive from monocytes and belong to the mesodermal cell lineage (Guillemin and Brew 2004).

Neurons represent the core of the brain due to their ability to communicate with each other via synaptic transmission (Fatt and Katz 1950, Kavalali 2015). They are composed of the cell body, dendrites and the axon which ensures the transmission over long distances (Holcomb et al. 2013). At the pre-synaptic end of the axon the neuron releases neurotransmitters which bind at receptors of the post-synaptic end of the receiver neuron and thereby forward their information from one neuron to another (Holz and Fisher 1999).

Astrocytes are one of the major types of glial cells present in the brain (Ransom and Ransom 2012). Together with endothelial cells, astrocytes are contributing to the blood-brain-barrier to protect the brain from invading cells or toxic compounds (Wosik et al. 2007, Alvarez et al. 2011, Keaney and Campbell 2015). Generally, astrocytes are described as the supporter cells for neurons and play a crucial role in maintaining the extracellular environment (Brooks et al. 2008). They not only regulate cerebral blood flow by surrounding all parts of the vasculature (Zonta et al. 2003), but also clear the extracellular environment of glutamate and gamma-aminobutyric acid (GABA) to ensure proper neuronal function (Takagaki et al. 1961, Levi et al. 1983). Additionally, astrocytes are thought to possess important antioxidant functions due to neutralization of damaging reactive oxygen species (ROS)(Aschner 2000). However, the most important function of astrocytes is their contribution to the formation of neuronal circuits by secreting synaptogenic factors (Kucukdereli et al. 2011, Risher et al. 2014). Thereby, astrocytes play a crucial role in the development of excitatory and inhibitory synaptogenesis (Jiang and Nardelli 2015).

Oligodendrocytes form the myelin sheath that surrounds neuronal axons and thereby increase transmission speed extensively (Aggarwal et al. 2011). Myelin has a high fat ratio and therefore a white appearance in the brain leading to the expression of the ‘white matter’ (Brooks et al. 2008). Oligodendrocytes are able to myelinate different axons with numerous internodes, also known as nodes of Ranvier (Sherman and Brophy 2005).

Microglia are not derived from the ectodermal germ layer but originate from the hematopoietic cell lineage (Guillemin and Brew 2004) and therefore belong to the mesoderm. They exhibit the same properties as macrophages and are usually described as the immune cells of the brain (Kreutzberg 1996).

1.1.1 Processes of brain development

In contrast to the previous assumption that brain development is completed with birth, it is known that brain development continues until after birth (Kolb and Gibb 2011). Human brain development starts at about three weeks after fertilization with the formation of the neural tube and continuous with enormous cell proliferation, migration and brain expansion (Linderkamp et al. 2009, Jiang and Nardelli 2015). Neurogenesis is mostly completed after five months and neural cells start to migrate until they reach their final location (Kolb and Gibb 2011). Finally, neurons begin to grow dendrites and axons to build a neuronal network with other neurons by the formation of synapses (Sidman and Rakic 1973). Dendritic outgrowth as well as synaptic production start prenatally but continue for an extended time after birth (Jung and Bennett 1996). Effectively, neurogenesis in specific regions of the brain like the hippocampus persists until old age (Eriksson et al. 1998).

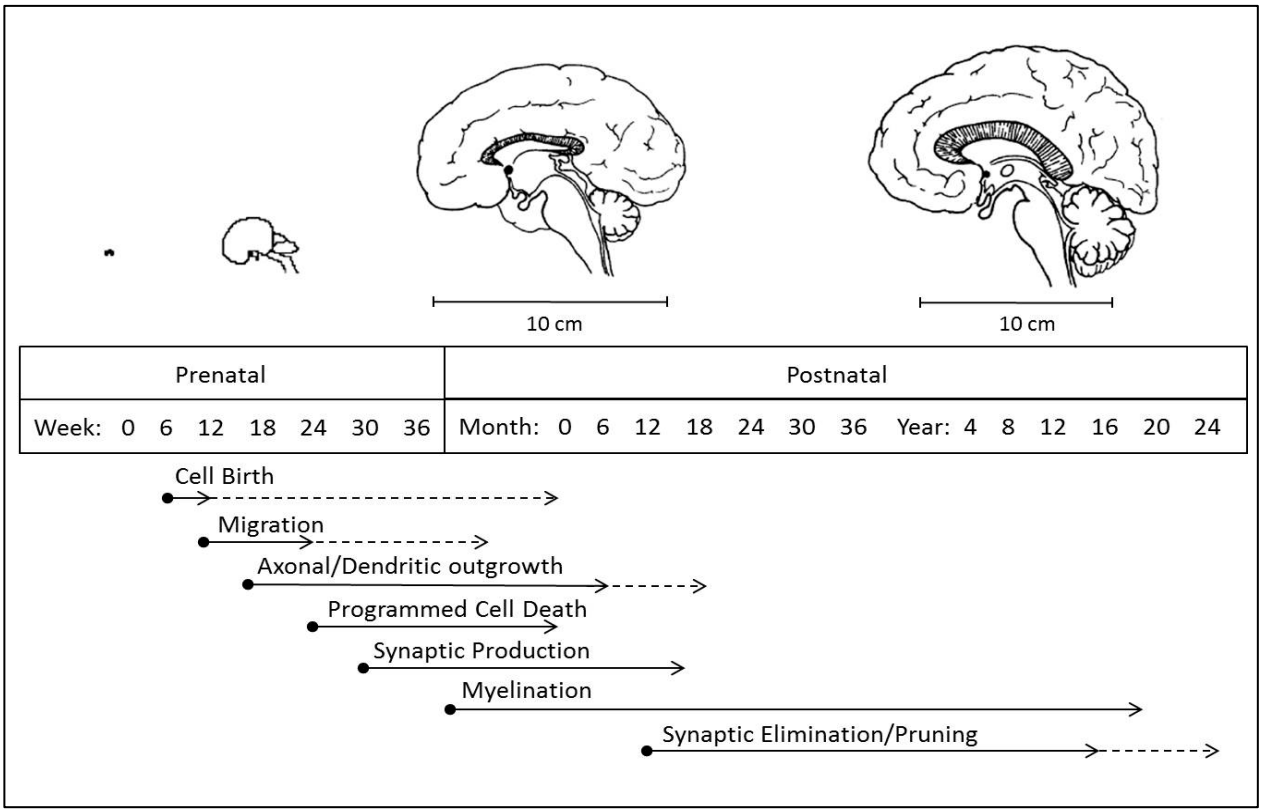

Fig. 1.1: The different stages of brain development. Brain development occurs in different stages and altered developmental processes may appear in different stages and time points. Modified from (Andersen 2003).

After the major part of neurogenesis is completed, astrocytes and oligodendrocytes start to develop, which are processes that also last throughout life (Kolb and Gibb 2011). Especially myelination is a very late-onset process that mostly starts at around birth and regularly changes during life dependent on individual learning processes (de Hoz and Simons 2015). This pre- and postnatal plasticity of the human brain clearly shows how complex the developmental phases are (Fig. 1.1). Moreover, it points out that any adverse effect on any signaling pathway responsible for brain development either before or after birth might lead to tremendous defects.

1.1.2 Neurospheres as an *in vitro* model for neurodevelopment

In 1992, Reynolds and colleagues first described that cells from the CNS of adult and embryonic mice could be isolated and maintained as a self-renewing *in vitro* culture (Reynolds et al. 1992, Reynolds and Weiss 1992). Cultured with epidermal growth factor (EGF), these isolated neural cells formed agglomerations, also called neurospheres, consisting of undifferentiated multipotent progenitor cells. The cultured neurospheres were positive for the neural stem/progenitor marker Nestin and had the potential to differentiate into neurons and astrocytes (Reynolds et al. 1992). Such neural progenitor cells (NPCs) also can be isolated from human fetal brains and mimic neurodevelopmental processes *in vitro* (Moors et al. 2009).

Neurospheres are thought to represent a more physiological model compared to monolayers due to their three-dimensional structure (Alepee et al. 2014) and the ability to differentiate into the three major cell types of the brain: neurons, astrocytes and oligodendrocytes (Moors et al. 2007). With the so-called Neurosphere assay (Fig. 1.2) the main processes of neurodevelopment, apoptosis, proliferation, migration and differentiation can be studied *in vitro* (Fritsche et al. 2011, Baumann et al. 2014). The Neurosphere assay also represents a valuable tool for developmental neurotoxicity (DNT) testing (Moors et al., 2009; Baumann et al., 2015). Especially the fetal brain is highly vulnerable towards toxic effects of drugs and chemicals (Longo 1980). Therefore, good-working testing strategies are needed to efficiently predict possible adverse effects of chemicals on neurodevelopmental processes (Bal-Price et al. 2015a). Current DNT testing methods are mostly based on animal experiments which do not only pose ethical concerns but are also time- and cost-intensive (Coecke et al. 2007, Lein et al. 2007). Moreover, potential species differences might result in non-predictive results from animals for human health (Seok et al. 2013, Baumann et al. 2014). Therefore, alternative methods based on human cells are urgently needed and are addressed in the Neurosphere assay using primary fetal human NPCs (hNPCs) (Moors et al. 2009, Gassmann et al. 2010, Fritsche et al. 2011, Baumann et al. 2015). However, fetal hNPCs are rather restricted in material and also can generate ethical concerns (Dunnett and Rosser 2014).

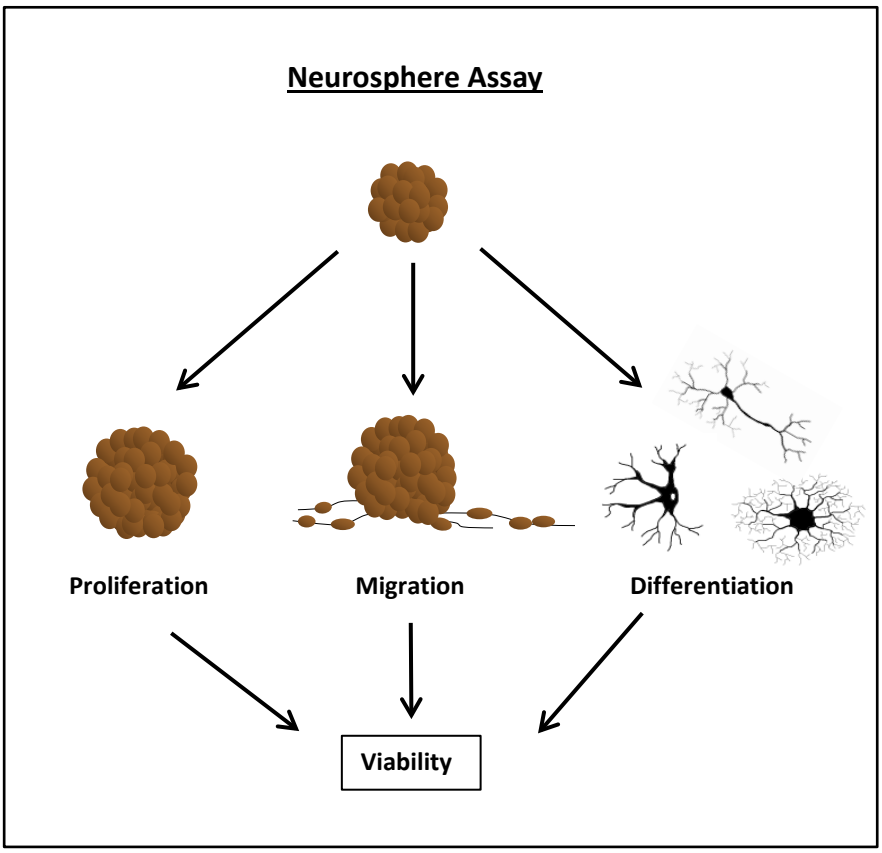

Fig. 1.2: The Neurosphere assay. Using the Neurosphere assay neurospheres are able to mimic the main processes of neurodevelopment: proliferation, migration, differentiation and apopotosis (viability) *in vitro*.

1.2 Human induced pluripotent stem cells

In 2012 Shinya Yamanaka and John Gurdon were awarded with the Nobel Prize for Physiology or Medicine for the discovery that differentiated cells have the potential to restore a pluripotent character. Yamanaka's group showed for the first time in 2006 that mouse fibroblasts can be reprogrammed into so-called induced pluripotent stem cells (iPSCs) by simultaneously introducing the four genes *octamer-binding transcription factor 4* (*Oct4*), *sex determining region Y-box 2* (*Sox2*), *kruppel-like factor 4* (*Klf4*) and *myelocytomatosis oncogene* (*c-Myc*) (Takahashi and Yamanaka 2006) by retroviral delivery. These mouse iPSCs exhibited most characteristics of embryonic stem cells (ESCs). One year later, in 2007, already two different groups published the ability to reprogram human dermal fibroblasts into human iPSCs (hiPSCs) using a similar approach. However, whereas Yamanaka's group introduced the genes *Oct4*, *Sox2*, *Klf4* and *c-Myc* (Takahashi et al. 2007), James Thomson's group achieved the same result by also using *Oct4*, *Sox2* combined with *Nanog homeobox* (*Nanog*) and *lineage protein 28* (*Lin28*) instead of *Klf4* and *c-Myc* (Yu et al. 2007). These results opened a broad spectrum of opportunities including the

usage of hiPSCs in basic research, toxicity testing, disease modeling or autologous cell therapy (Gonzalez et al. 2011).

1.2.1 The main characteristics of hiPSCs

Both types of undifferentiated cells, ESCs and iPSCs, are generally defined by their unlimited self-renewal capacity and potential to differentiate into all cell types of the body (Zhang et al. 2012). Undifferentiated cells exhibit a high ratio of nucleus to cytoplasm with prominent nuclei (Smith et al. 2009) and they usually grow in multi-layered colonies (Courtot et al. 2014). They are characterized by an abbreviated GI phase of the cell cycle resulting in a rapid proliferation rate (Becker et al. 2006, Ghule et al. 2007). Moreover, iPSCs express the cell surface markers stage-specific embryonic antigen (SSEA)-3, SSEA-4, tumor rejection antigen (Tra)-1-60 and Tra-1-81 (Chan et al. 2009, Zhao et al. 2013). Other markers that are commonly used to identify pluripotent stem cells are alkaline phosphatase but also Oct4, Sox2 and Nanog (Nichols et al. 1998, Chambers et al. 2003, Mitsui et al. 2003).

To prove their pluripotent potential, iPSCs need to be able to differentiate into cell types of all three germ layers - ectoderm, mesoderm and endoderm (Sheridan et al. 2012, Fukusumi et al. 2013). This ability can be tested *in vitro* by the formation of embryoid bodies (EBs), spontaneously formed spherical clusters cultured in suspension, which express genes specific for each germ layer (Itskovitz-Eldor et al. 2000). The corresponding *in vivo* approach, which is up to date the gold standard method for proving pluripotency, is the ability of iPSCs to spontaneously differentiate through teratoma formation if introduced into immunodeficient mice (Przyborski 2005, Wesselschmidt 2011). Teratoma are tumor-like formations consisting of tissue derived from the three germ layers (Prokhorova et al. 2009). Even though teratoma formation was considered to be one of the most important evidences of pluripotency it is a time-consuming method with high variability depending on the implantation site (Cooke et al. 2006, Prokhorova et al. 2009). Furthermore, the identification of specific tissues inside the teratoma requires a lot of experience (Smith et al. 2009).

1.2.2 Methods for producing hiPSCs

Even though the reprogramming mechanism is easy and reproducible, it is an extremely slow and inefficient process (Yamanaka 2012). Due to the simplicity of reprogramming somatic cells into iPSCs through ectopic expression of defined transcription factors, many research groups started to reproduce and modify the iPSC technique. This led to a high number of different reprogramming methods varying in donor cell type, reprogramming cocktail and technique as well as culture conditions (Gonzalez et al. 2011).

The first observation revealed that reprogramming efficiency was highly dependent on the donor cell type. To produce iPSCs from mouse embryonic fibroblasts (MEFs) reprogramming treatment needed to be performed for 8 – 12 days whereas the reprogramming process for human foreskin fibroblasts took 20 – 25 days using the same technique (Gonzalez et al. 2011). Even though dermal fibroblasts represent the most popular donor cell type to be reprogrammed, keratinocytes showed a hundredfold higher efficiency (Aasen et al. 2008). Moreover, the differentiation state of the donor cell also seems to have a significant effect on reprogramming efficiency resulting in lower efficiency with increasing maturation. For example, terminally differentiated B and T cells showed a decreased reprogramming efficiency compared to hematopoietic stem cells (Eminli et al. 2009).

Another important parameter is the choice of transcription factors used for reprogramming. The most widely used are the aforementioned Yamanaka factors OSKM (Oct4, Sox2, Klf4 and c-Myc; (Takahashi and Yamanaka 2006, Park et al. 2008, Kahler et al. 2013). However, the transcription factors found by Thomson's laboratory have also been repeatedly successfully employed (Yu et al. 2007, Si-Tayeb et al. 2010, Zhang et al. 2010). Furthermore, studies have been published with less or additional transcription factors. For example, c-Myc represents an oncogene that likely bears the risk for tumorigenesis (Okita et al. 2007) and therefore is often removed from the reprogramming cocktail (Nakagawa et al. 2008, Wernig et al. 2008). On the other hand, additional transcription factors like undifferentiated embryonic cell transcription factor 1 (UTF1) or spalt-like transcription factor 4 (SALL4) were able to increase the number of iPSC colonies if added to the OSK or OSKM cocktail (Zhao et al. 2008, Tsubooka et al. 2009).

Besides the donor cell type and transcription factors, culture conditions play an important role during the reprogramming process. Cells can be cultured on MEFs, also called feeder cells, which secrete supportive growth factors, required for ESC and iPSC survival, and inhibit spontaneous differentiation (Dravid et al. 2005). Moreover, hypoxic conditions with 5% O_2, resembling the conditions in some stem cell niches of the body, were found to be highly supportive for reprogramming efficiency (Yoshida et al. 2009).

In addition, there are many reprogramming methods to obtain iPSCs from somatic cells. In general, they can be divided into two classes. The first class includes the integration of exogenous genetic material into the donor cell (Gonzalez et al. 2011). The original reprogramming process was achieved using Moloney murine leukemia virus (MMLV)-derived retroviruses (Takahashi and Yamanaka 2006). Other integrative reprogramming methods include the usage of lentiviruses derived from human immunodeficiency virus (HIV) (Blelloch et al. 2007, Yu et al. 2007), transfection of linear DNA (Kaji et al. 2009) or piggyBack transposons (Wilson and Bohr 2007, Woltjen et al. 2009).

Even though integration of exogenous genetic material allows a relative efficient generation of iPSCs it also produces stem cells with viral transgene insertions which could lead to mutations and therefore impair genetic stability (Gonzalez et al. 2011). Safety of produced iPSCs is a fundamental issue especially with regard to the possible usage in cell therapy (Gonzalez et al. 2011). Therefore, various reprogramming methods have been published without genetic modification of the donor cell. These non-integrative approaches include integration-defective viral, episomal, RNA and protein delivery (Okita et al. 2008, Stadtfeld et al. 2008, Kim et al. 2009, Yu et al. 2009, Zhou and Freed 2009, Jia et al. 2010, Warren et al. 2010). Even though they represent a possible solution to avoid the permanent genetic modification they are usually much more inefficient and less reproducible compared with integration-based techniques (Zhou and Zeng 2013).

One of the major concerns of hiPSCs is the high variability between the cell lines. Besides the various genetic backgrounds, different reprogramming and culturing methods might result in different iPSC quality (Gonzalez et al. 2011).

1.2.3 hiPSCs as a model for neurological diseases

The discovery that differentiated somatic cells can be reprogrammed into iPSCs with the potential to self-renew and differentiate into any cell type of the body rendered the possibility for various applications. Thus, hiPSCs can be used for basic research, autologous cell therapy, drug and toxicity screening as well as disease modeling (Robinton and Daley 2012) (Fig. 1.3). Especially neurological diseases are often difficult to study due to the limited sources of relevant human brain tissue. Therefore, many studies of neurological diseases were performed in post mortem tissue that is mostly not well preserved and only exhibits a picture of the diseases end-stage (Marchetto et al. 2011). Mouse models represent a possible source to study the development of the neurological disease but also have several limitations. Not every human neurological disease has an adequate mouse model and even if, there are still differences between human and mouse signaling networks during brain development (Wang and Doering 2012).

Patient-specific hiPSCs offer the opportunity to obtain neuronal cells based on the genetic background of the patient. They can be derived from any patient and theoretically differentiated into any brain cell type. This makes them a valuable tool to allow human-based studies and circumvent ethical issues connected with hESCs (Kastenberg and Odorico 2008). However, not even hiPSCs are limitation-free. High variability has been observed between individual hiPSC lines even from the same donor depending on the reprogramming technique as well as on culture conditions (Bellin et al. 2012, Yamanaka 2012). Moreover, increasing culture time also

increases the possibility of epigenetic and genetic instability in hiPSCs (Mummery 2011, Pera 2011). Especially the high variability between hiPSC lines raises the question for proper controls. Genetic modification for gain- and loss-of-function studies, hiPSCs derived from siblings and high numbers of hiPSC lines have been discussed to enable reliable results (Bellin et al. 2012, Okano and Yamanaka 2014).

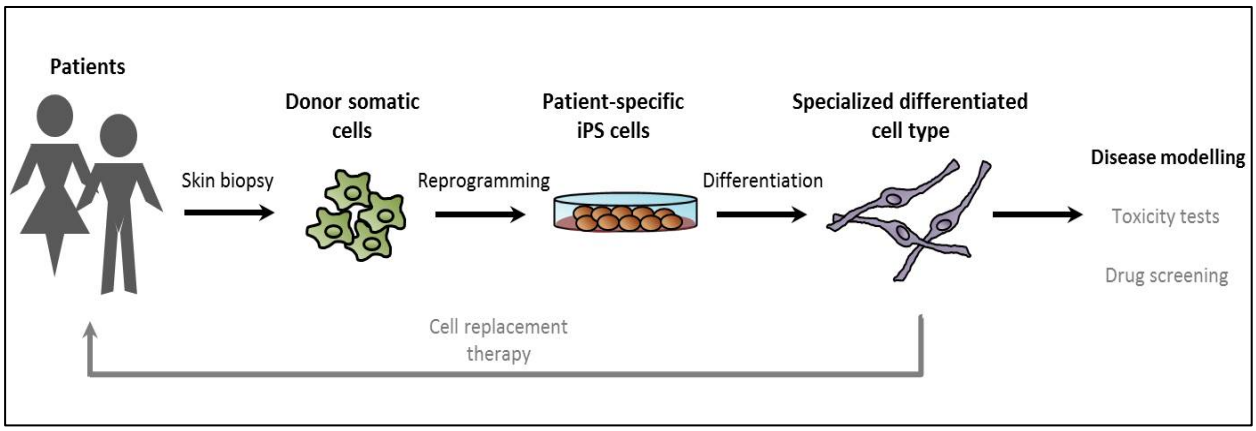

Fig. 1.3: The potential of hiPSCs to treat and study neurological diseases. Somatic cells obtained from patients can be reprogrammed into hiPSCs and further differentiated into disease-relevant cell types. These patient-specific hiPSC-derived cell types can be either used for disease modeling, toxicity testing, drug screening or cell replacement therapy.

Despite these concerns, hiPSCs have already been used for the study of neurodevelopmental and neurodegenerative disorders including Down syndrome (Shi et al. 2012), Angelman syndrome (Chamberlain et al. 2010), Prader-Willi syndrome (Yang et al. 2010), Parkinson's disease (PD) (Nguyen et al. 2011), Alzheimer's disease (AD) (Israel et al. 2012) and amyotrophic lateral sclerosis (ALS) (Dimos et al. 2008, Mitne-Neto et al. 2011). A good example to demonstrate the great potential of hiPSC-based disease models is the Rett syndrome (RTT), which is a rare monogenetic neurodevelopmental disorder caused by a mutation in the methyl CpG-binding protein (MeCP2) gene (Amir et al. 1999). Studies showed that hiPSC-derived neurons from RTT patients exhibited a decrease in the soma size of RTT neurons compared to healthy controls (Chen et al. 2010, Cheung et al. 2011). This phenotype could also be observed in the animal model as well as in RTT post mortem human brain tissue (Chen et al. 2001). Moreover, synaptic defects observed in RTT could be rescued by treatment with insulin growth factor 1 (IGF-1) in both hiPSC-derived neurons and RTT mice (Tropea et al. 2009, Marchetto et al. 2010). These results clearly indicate that patient-specific hiPSCs represent a suitable model for neurological diseases.

Even though hiPSCs are also used to study neurodegenerative diseases like AD (Israel et al. 2012), hiPSC-derived somatic cells potentially need extensive time to mature complicating the studying of age-related diseases (Bellin et al. 2012). In contrast, hiPSCs bear great potential

studying early-onset neurodevelopmental diseases, especially diseases without adequate mouse models.

1.3 Cockayne syndrome

1.3.1 Clinical picture and classification of Cockayne syndrome patients

Cockayne syndrome (CS) is a rare hereditary autosomal recessive disease which is characterized by an increased photosensitivity, an extremely short stature and premature aging (Newman et al. 2006, Melis et al. 2013). Furthermore, patients who suffer from CS exhibit several neurological defects, like ataxia, microcephaly, sensorineural deafness and retinal degeneration. They also show signs of mental retardation and are characterized by neuronal demyelination (Kraemer et al. 2007). Other neurological symptoms include calcification in basal ganglia and cerebral cortex as well as loss of Purkinje cells and granule neurons in the cerebellum (Jeppesen et al. 2011). The reason for these severe neurological defects is still unknown because there is a lack of adequate animal models representing the human neurological phenotypes (van der Horst et al. 1997). Specifically, the mouse model only shows very mild neurological symptoms like reduced motor function or defects in sensorimotor coordination and completely lacks neuronal demyelination (Niedernhofer 2008). Moreover, $CSB^{-/-}$ mice develop normally, do not show a microcephaly, and only exhibit a slight reduction in body weight compared to their wild-type (wt) littermates (van der Horst et al. 1997).

The classical CS phenotype (CS I) was characterized by a normal appearance of patients at birth with first symptoms occurring during early childhood development (Nance and Berry 1992). These children developed the classical symptoms, like growth failure, neurologic abnormalities, sensorineural hearing loss, cataracts, pigmentary retinopathy and cutaneous photosensitivity. With increasing possibilities for clinical diagnosis, the clinical spectrum of CS has been continuously expanded (Laugel 2013). In addition to the 'classical CS I phenotype' also early-onset (Lowry 1982, Moyer et al. 1982) as well as late-onset cases (Kennedy et al. 1980, Rapin et al. 2006) entitled CS II and CS III, respectively, were identified. All patients exhibit a similar spectrum of symptoms; however, the time of onset and the rate of progression vary extensively among the different groups. Whereas the early-onset cases show congenital symptoms, late-onset cases only exhibit signs of the disease later in life (Nance and Berry 1992). The discovery of the very severe form 'Cerebro-oculofacio-skeletal syndrome' (COFS) and the very mild form 'UV-sensitive syndrome' (UVSS) were even more challenging. First they were described as independent diseases (Lowry et al. 1971, Pena and Shokeir 1974, Fujiwara et al. 1981) but later proved to share mutations in the same genes as CS patients (Meira et al. 2000, Horibata et al. 2004, Laugel et al. 2008b, Nardo et al. 2009).

Whereas COFS and UVSS border the broad spectrum of CS on both ends, clear separation of the different CS subtypes is often not possible (Laugel 2013). The molecular reasons underlying the different CS phenotypes are fairy unclear.

1.3.2 The role of CS proteins in the nucleotide excision repair (NER)

CS is caused by mutations in either the *CSA* (Cockayne syndrome A), also called excision-repair cross complementing group 8 (*ERCC8*) or the *CSB* (Cockayne syndrome B) gene, also called *ERCC6* (Troelstra et al. 1992b, Henning et al. 1995). The majority of patients (around two thirds of the CS cases) exhibit mutations in the *CSB* gene (Laugel et al. 2010). To date there is no clear separation between the clinical phenotype of CSB and CSA patients (Laugel 2013). The *CSB* gene is located on chromosome 10q11-21 and encodes a 168 kDa protein (Troelstra et al. 1992a). It belongs to the SWI2/SNF2 family of ATP-dependent chromatin remodeling factors (Citterio et al. 1998) but does not display any helicase activity (Selby and Sancar 1997). CSB was originally found to be a key player in the transcription-coupled nucleotide excision repair (TC-NER), a sub pathway of the NER (Nouspikel 2009).

The NER is able to repair damage caused by a large change in the structure of the DNA double helix. It restores the damaged DNA strand by displacing an oligonucleotide containing the lesion and repairing the gap by DNA polymerase and DNA ligase (Lagerwerf et al. 2011). In this way, a large variety of DNA lesions can be repaired by NER, including covalent bindings of chemicals, UV-induced lesions and oxidative damage (Nouspikel 2009). The NER consists of two different pathways, the global genome NER (GG-NER) which is able to repair DNA lesions in the whole genome, and the TC-NER which only repairs DNA lesions in actively transcribed genes (Hanawalt 2002) (Fig. 1.4).

Both pathways, the GG-NER and the TC-NER, vary in the mechanism of lesion recognition but then follow the same repair protocol (Fig. 1.4). GG-NER is initiated by the recruitment of xeroderma pigmentosum (XP)- C, UV excision repair protein RAD23 homolog B (HR23B) and centrin2 or damage-specific DNA binding protein 1 (DDB1) and XPE which form a complex to efficiently sense the damaged DNA region (Chu and Chang 1988, Araki et al. 2001). In case of the TC-NER, a damaged stalled RNA Polymerase II (RNA Pol II) leads to the recruitment of CSB (Hanawalt and Spivak 2008). CSB binds to the DNA while changing their chromatin structure (Beerens et al. 2005) and subsequently, recruits its binding partner CSA and the histone acetyltransferase p300 (Henning et al. 1995). CSA is a component of the E3 ubiquitin-ligase complex and necessary for the recruitment of various additional TC-NER factors, like the high mobility group nucleosome binding domain 1 (HMGN1), the transcription cleavage factor (TF) IIS and XPA binding protein 2 (XABP2) (Lagerwerf et al. 2011).

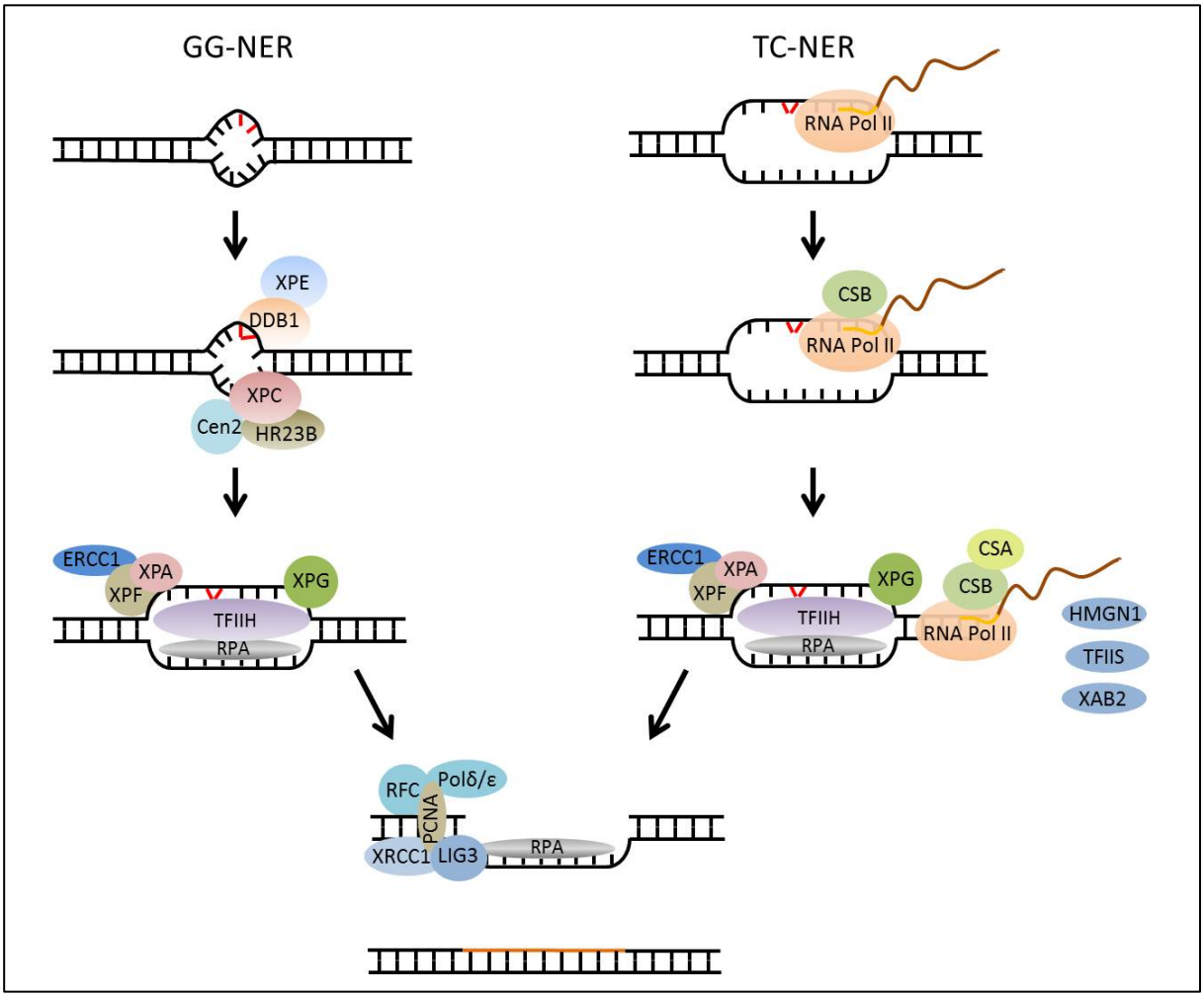

Fig. 1.4: Mechanism of the nucleotide excision repair (NER). The NER consists of two different pathways, the global genome NER (GG-NER) and the transcription-coupled NER (TC-NER). GG-NER detects DNA lesions either by XPC-HR23B-Cen2 complex or DDB1-XPE through the structural distortion of the DNA double helix. TC-NER is needed if the RNA polymerase II (RNA Pol II) is stalled in front of a DNA lesion. In this case CSB recruits various TC-NER-specific proteins, including CSA, HMGN1, TFIIS and XAB2. If the lesion is detected transcription factor TFIIH opens a denaturation bubble around the lesion and ERCC1-XPF and XPG incise the damaged strand and remove an oligonucleotide containing the lesion. The resulting gap is repaired by the DNA Polymerases δ and ε (Pol δ/ε) and the nick is sealed by ligase 3 (Lig3). Modified from (Nouspikel 2009).

After recognizing the damage, the transcription factor TFIIH is required to open a denaturation bubble containing the lesion (Fuss and Tainer 2011). Afterwards, XPG and XPF- DNA excision repair cross-complementing protein 1 (ERCC1) remove a fragment of 25 – 30 nucleotides containing the lesion by cutting it at the 3' and the 5' end, respectively (Fousteri and Mullenders 2008). The resulting gap is filled by the DNA polymerases δ and ε using the complementary DNA strand as a template (Popanda and Thielmann 1992) and the nick is later sealed by ligase 3 together with X-ray repair cross-complementing protein 1 (XRCC1) (Moser et al. 2007).

The loss of CSB or CSA leads to a deficient TC-NER pathway and a hypersensitivity towards UV-induced damage. Consequently after UV-irradiation, CS cells fail to recover their RNA synthesis

and show increased apoptosis (Mayne and Lehmann 1982). This explains the high photosensitivity of CS patients but does not give a proper explanation for the severe neurological defects.

1.3.3 Additional functions of CSB

Besides its role in TC-NER, CSB was found to play a role in various other biological pathways. It has been shown that DNA can be wrapped around the CSB protein depending on ATP binding (Beerens et al. 2005). In this way, CSB has the ability to actively remodel nucleosomes and alter the DNA helix conformation (Citterio et al. 2000). Furthermore, CSB interacts with different subunits of the TFIIH and forms complexes with both, the RNA Pol I and II (Tantin et al. 1997, Tantin 1998, Bradsher et al. 2002) suggesting a function of CSB in transcription elongation or enhancement. Comparative microarray analyses confirmed that CSB deficiency leads to misexpression in several important pathways, such as growth, inflammation and apoptosis (Newman et al. 2006). In the same study CSB has been shown to regulate a similar spectrum of genes also affected by inhibitors of histone deacetylase and DNA methylation. These results taken together strengthen the assumption that loss of CSB function impairs transcription due to epigenetic modulation.

Additionally, CSB plays an important role in p53 ubiquitination and hypoxic response (Filippi et al. 2008). In response to DNA damage, the tumor suppressor p53 is phosphorylated and triggers multiple transcriptional programs, including cell cycle arrest, enhanced DNA repair or apoptosis (Vousden and Lane 2007). In healthy cells, p53 is present in very low doses and quickly polyubiquitinated by the E3 ubiquitin ligase mouse double minute 2 homolog (Mdm2) and becomes phosphorylated exclusively upon genotoxic stress (Fuchs et al. 1998). The finding that CSB and also CSA form a complex together with Mdm2 to enhance polyubiquitination and degradation of p53 led to the hypothesis that increased apoptosis observed in CSB-deficient cells is due to increased p53-dependent transcription (Latini et al. 2011). Consistent with this hypothesis higher basal levels of p53 protein and mRNA could be detected in CSB-deficient cells (Latini et al. 2011, Andrade et al. 2012).

During hypoxic stress, if the tissue is not provided with sufficient oxygen, cells start transcription of several genes to induce vascularization (Rey and Semenza 2010). One of these activated genes is the vascular endothelial growth factor (VEGF) (Majmundar et al. 2010). This transcription program is initiated via the stabilization of the hypoxia inducible factor 1α (HIF1α) which together with p300 binds to the promotor and starts transcription of pro-survival genes (Bertout et al. 2008). However, p300 also represents a binding partner of p53. If p53 is not efficiently degraded, p300 is not available for HIF1α and rather promotes transcription that

leads to apoptosis and cell senescence (Velez-Cruz and Egly 2013). CSB-deficient cells fail to upregulate VEGF during hypoxic stress and therefore are thought to exhibit defective hypoxic response due to the elevated level of p53 (Filippi et al. 2008).

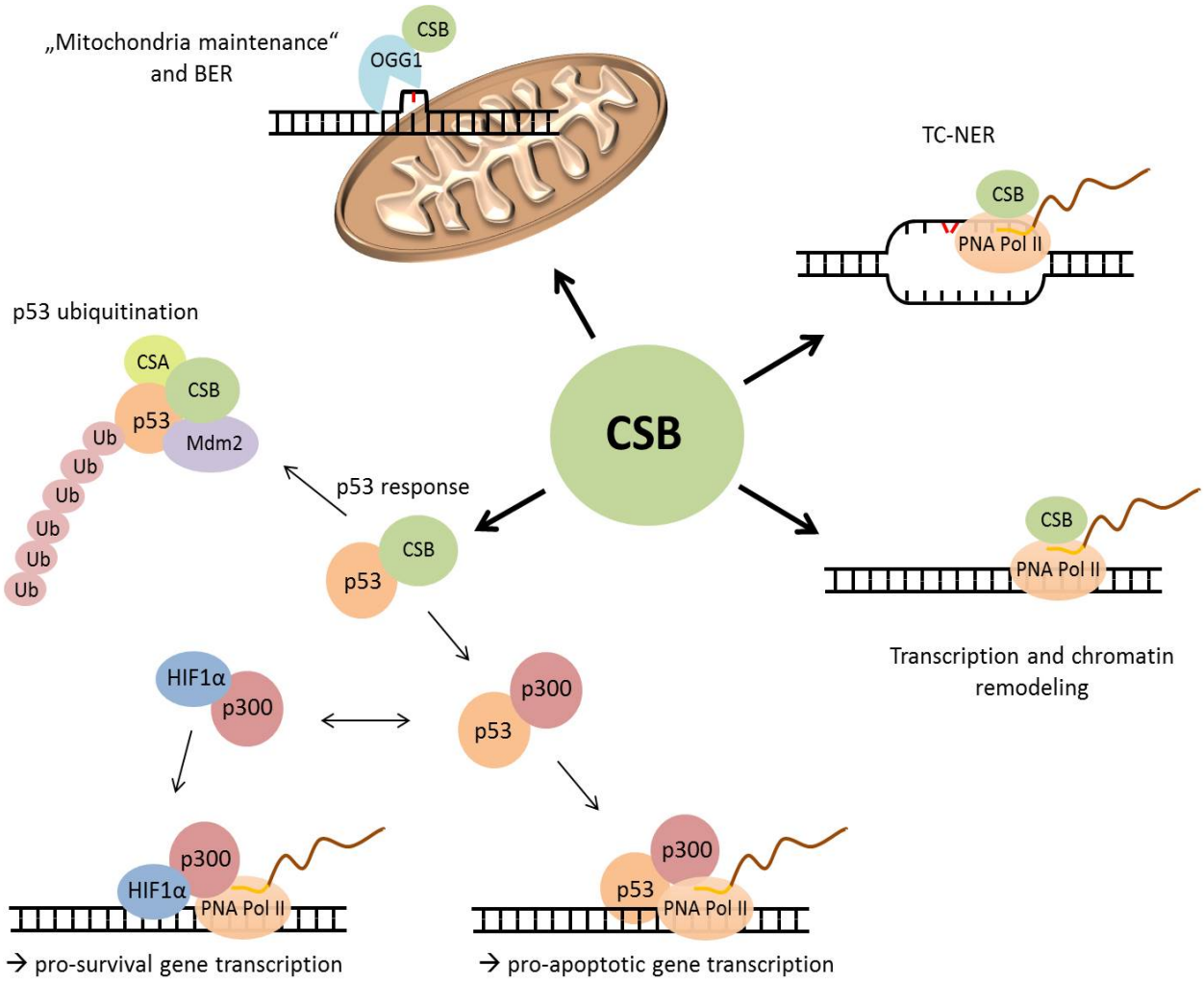

Fig. 1.5: The different pathways of CSB interaction. CSB plays a role in many different signaling pathways in the cell. Besides transcription-coupled nucleotide excision repair (TC-NER) CSB also regulates transcription, chromatin remodeling and p53 ubiquitination. Therefore, CSB function also has an impact on p300-dependent transcription regulation. Moreover, CSB was found to play a role in base excision repair (BER) in mitochondria. Modified from (Frontini and Proietti-De-Santis 2012).

Increased oxidative products, such as nitrotyrosine and 4-hydroxy-2-nonenal-modified protein, were found in autopsied brains of CS patients (Hayashi et al. 2001). Furthermore, CSB-deficient liver cells and fibroblasts exhibited reduced capacity to repair the oxidative product 7,8-hydroxyguanine (8-oxoG) in mitochondria (Stevnsner et al. 2002). The oxidative DNA lesion 8-oxoG is caused by reactive oxygen species (ROS) which are formed during oxidative phosphorylation in mitochondria and may particularly damage mitochondrial DNA (mtDNA).

However, 8-oxoG in mtDNA is normally repaired by the base excision repair (BER) through the 8-oxoG glycosylase OGG1 which recognizes and removes the defective base (Dianov et al. 1998). In addition, OGG1 expression was found to be decreased in CSB-deficient cells and could be increased by transfection of CS cells with the wt *CSB* gene (Dianov et al. 1999). These results suggest a possible role of CSB not only in TC-NER but also BER in mitochondria.

Taken together, all these studies clearly indicate that CSB orchestrates various essential signaling pathways. CS is a highly variable disease what can be explained by the complex function of CSB and probably also CSA. Figure 1.5 summarizes the described pathways in which CSB plays an important role.

1.4 Aim of this study

For studying molecular aspects of human, genetically-driven diseases, transgenic animal models are not always the best model to choose. E.g. in the case of the progeroid syndrome CSB the corresponding mouse model does not display the neurological phenotype that is observed in CSB patients. To understand the molecular mechanisms underlying the so-far unknown disturbed cellular functions during brain development in CSB patients, we intended to use an *in vitro* system that is based on patient-derived hiPSCs. Therefore, the aims of this study were:

1. Establishment and characterization of a hiPSC culture.

2. Generation of a neural induction protocol to differentiate hiPSCs into NPCs cultured as three-dimensional neurospheres and comparative analysis of these cells to primary human fetal neurospheres.

3. Neural induction of hiPSCs obtained from CSB patients and functional comparative analyses of CSB-deficient hiPSC-derived neurospheres to healthy controls.

2. Material and Methods

2.1 Material

2.1.1 Laboratory equipment

Tab. 2.1: List of laboratory equipment

Laboratory equipment	Company
Autoclave	KSG GmbH, Neukirchen-Vluyn, Germany
Water Deionizer	Millipore, Darmstadt, Germany
Binocular Microscope	Olympus, Düsseldorf, Germany
Microscope	Leica, Wetzlar, Germany
FACS Calibur	BDBiosciences, Heidelberg, Germany
Fluorescence microscope	Zeiss, Oberkochen, Germany
Heating cabinet	Memmert GmbH, Schwabach, Germany
Incubators	Heraeus, Cologne, Germany Thermo Fisher Scientific, Carlsbad, USA Sanyo, Moriguchi, Japan
Cell culture sterile bench	Scanlaf, Lynge, Denmark
Light-optical microscope	Olympus, Düsseldorf, Germany
Single-channel pipettes	Eppendorf, Hamburg, Germany
Accurate weighting scale	Sartorius, Göttingen, Germany
Mechanical shakers	Ika, Staufen, Germany LaboTec, Dillenburg-Manderbach, Germany
McIlwain Tissue Chopper	Mickle Laboratory, Guildford, UK
Water bath	Lauda, Lauda-Königshofen, Germany
Weighting scale	Sartorius, Göttingen, Germany
Multimode microplate reader	Tecan, Männedorf, Switzerland
Light microscope camera	Visitron Systems, Puchheim, Germany
Polymerase chain reaction (PCR) cycler	Qiagen, Hilden, Germany
Thermocycler	Biometra GmbH, Göttingen, Germany
Table-top centrifuge	Eppendorf, Hamburg, Germany
Refrigerators/Freezers	Liebherr, Biberach, Germany Thermo Fisher Scientific, Carlsbad, USA
Heating blocks	Thermo Fisher Scientific, Carlsbad, USA Panasonic, Hamburg, Germany
Electrophoresis chamber	Thermo Fisher Scientific, Carlsbad, USA

Gel Imager	INTAS, Göttingen, Germany
Array Scan VTI	Thermo Fisher Scientific, Carlsbad, USA

2.1.2 Consumable supplies

Tab. 2.2: List of consumable supplies

Consumable supplies	Company
Eight-Chamber Slides	BDBiosciences, Heidelberg, Germany
6-Well Plates	Sarstedt, Nümbrecht, Germany
24-Well Plates	Sarstedt, Nümbrecht, Germany
96-Well Plates	Greiner Bio-One, Kremsmünster, Austria
Cover slips	Menzel Gläser, Braunschweig, Germany
Culture Dishes, Ø 100 x 20 mm	BDBiosciences, Heidelberg, Germany
Culture Dishes, Ø 60 x 15 mm	BDBiosciences, Heidelberg, Germany
Disposable Glass Pipettes, 10 mL, 25 mL, 50 mL	Greiner Bio-One, Kremsmünster, Austria
Disposable Pasteur Pipettes, 2.5 mL	Carl Roth GmbH + Co. KG, Karlsruhe, Germany
Tubes, 2 mL, 1.5 mL, 0.5 mL	Eppendorf, Hamburg, Germany
Tubes, 15 mL	Greiner Bio-One, Kremsmünster, Austria
Tubes, 50 mL	Sarstedt, Nümbrecht, Germany
Parafilm	Pechiney, Paris, France
Pipette Tips, 1000 µL, 100 µL, 10 µL	Biozym, Hessisch Oldendorf, Germany
Razor Blades	Wilkinson, Solingen, Germany
PCR tubes, 0.1 mL 4-tubes	Biozym Biotech Trading GmbH
BD Eclipse Needle 0.8 mm x 40 mm	BDBiosciences, Heidelberg, Germany
Ultra-low attachment (ULA) dish, Ø 100 mm	Oehmen, Essen, Germany
Ultra-low attachment (ULA) dish, Ø 60 mm	Oehmen, Essen, Germany

2.1.3 Cell culture media and supplements

Tab. 2.3: Cell culture medium components

Medium component	Company
Dulbecco's Modified Eagle Medium (DMEM) high glucose	Life Technologies, Carlsbad, USA
Ham's F12	Life Technologies, Carlsbad, USA

Fetal calf serum (FCS)	Biochrom, Berlin, Germany
Penicillin/Streptomycin (P/S)	Pan Biotech, Aidenach, Germany
B27 supplement	Life Technologies, Carlsbad, USA
N2 supplement	Life Technologies, Carlsbad, USA
Human basic fibroblast growth factor (bFGF)	R&D Systems, Wiesbaden, Germany
Human epidermal growth factor (EGF)	Biosource, Solingen, Germany
mTeSR1 complete kit	Stemcell Technologies, Cologne, Germany
Knockout DMEM (KoDMEM)	Invitrogen, Carlsbad, USA
Knockout Serum Replacement (KSR)	Invitrogen, Carlsbad, USA
L-Glutamine	PAA Laboratories GmbH, Cölbe, Germany
Non-essential amino acids (NEAA)	Biochrom, Berlin, Germany
β-Mercaptoethanol	Invitrogen, Carlsbad, USA
Noggin	PeproTech, Hamburg, Germany

2.1.3.1 Media composition:

SNL culture medium:
DMEM high glucose
10% FCS (v/v)
1% P/S (v/v)

SNL freezing medium:
DMEM high glucose
20% FCS (v/v)
10% DMSO (v/v)

Unconditional hESC medium (UM):
KoDMEM
20% KSR (v/v)
2 mM L-Glut
$1x10^{-4}$ M NEAA
$1x10^{-4}$ M β-Mercaptoethanol
1% P/S (v/v)
12 ng/mL bFGF

mTeSR1 medium:
mTeSR1 complete kit (mTeSR1 basal medium containing mTeSR1 5X Supplement)
1% P/S (v/v)

hiPSC freezing medium I:
KoDMEM
20% KSR (v/v)

hiPSC freezing medium II:
KoDMEM
20% KSR (v/v)
20% DMSO (v/v)

Noggin medium:
KoDMEM
20% KSR (v/v)
2 mM L-Glut
$1x10^{-4}$ M NEAA
$1x10^{-4}$ M β-Mercaptoethanol
500 ng/mL noggin
1% P/S (v/v)

Neural induction medium (NIM):
DMEM and Ham's F12 (3:1)
1x B27 supplement
1x N2 supplement
20 ng/mL EGF
1% P/S (v/v)
10 ng/mL bFGF

Neural proliferation medium (NPM):
DMEM and Ham's F12 (3:1)
1x B27 supplement
1x N2 supplement
1% P/S (v/v)
20 ng/mL EGF
20 ng/mL bFGF

Neural differentiation medium (NDM):
DMEM and Ham's F12 (3:1)
1x N2 supplement
1x B27 supplement
1% P/S (v/v)

hiPSC-NPC freezing medium:
DMEM and Ham's F12 (3:1)
1x B27 supplement
1x N2 supplement
1% P/S (v/v)
20% KSR (v/v)
10% DMSO (v/v)

Tab. 2.4: Cell culture components

Cell culture component	Company
Poly-D-Lysine-Hydrobromide (PDL)	Sigma Aldrich, Munich, Germany
Laminin	Sigma Aldrich, Munich, Germany
Matrigel	BDBiosciences, Heidelberg, Germany
Gelatin	Sigma Aldrich, Munich, Germany
Phosphate Buffered Saline (PBS)	Life Technologies, Carlsbad, USA
Dulbecco's Phosphate Buffered Saline (DPBS)	Life Technologies, Carlsbad, USA
Poly-2-hydroxyethyl methacrylate (Poly-HEMA)	Sigma Aldrich, Munich, Germany
Accutase	Invitrogen, Carlsbad, USA
Trypsin/EDTA	Millipore, Darmstadt, Germany

Tab. 2.5: List of chemicals

Chemicals	Company
Src kinase inhibitor PP2	Sigma Aldrich, Munich, Germany
ROCK inhibitor Y-27632	R&D Systems, Wiesbaden, Germany
MeHgCl	Sigma Aldrich, Munich, Germany
Mitomycin-C	Sigma Aldrich, Munich, Germany
Midori Green DNA stain	Nippon Genetics Europe, Düren, Germany
DNA loading buffer (6×)	Peqlab Biotechnologies, Erlangen, Germany
PeqGold 100bp DNA ladder	Peqlab Biotechnologies, Erlangen, Germany
DNA Molecular Weight Marker X 0.07 – 12.2 kbp	Roche, Basel, Switzerland
Agarose	Biozym Scientific, H. Oldendorf, Germany
TAE buffer (10×)	Invitrogen, Karlsruhe, Germany
Water Containing Diethyl Dicarbonate (DEPC)	Carl Roth GmbH + Co. KG, Karlsruhe, Germany
Paraformaldehyde (PFA)	Sigma Aldrich, Munich, Germany
Triton-X 100	Sigma Aldrich, Munich, Germany
Dimethyl sulfoxide (DMSO)	Carl Roth GmbH + Co. KG, Karlsruhe, Germany
Propidium iodide	Sigma Aldrich, Munich, Germany

2.1.4 Computer software

Tab. 2.6: List of used computer software

Computer software	Application
SPOT Advanced 4.6	Photographs of migration and proliferation
AxioVision 4.6.3.0	Photographs of differentiation, fluorescent microscope
ImageJ 1.45	Measurement of migration and proliferation
Microsoft Excel 2010	Calculation of data
GraphPad Prism 6.01	Evaluation of statistics and graphic representation
RotorGene 1.7	Performance and evaluation of qRT-PCR
icontrol 1.9	Evaluation of viability assay and measurement of RNA/DNA content
IntasGDS 2009	Photographs of electrophoresis gel
WinMDI 2.9	Evaluation of FACS data
Serial Cloner 2.6	Primer design for sequencing of hiPSCs

2.1.5 Kits

Tab. 2.7: List of used kits

Kit	Company
Cell Titer-Blue® (CTB) Cell Viability Assay	Promega, Mannheim, Germany
RNeasy Mini Kit	Qiagen, Hilden, Germany
QuantiTec Reverse Transcription Kit	Qiagen, Hilden, Germany
PCR-Purification Kit	Qiagen, Hilden, Germany
QuantiFast SYBR Green PCR Kit	Qiagen, Hilden, Germany
Cell Proliferation ELISA BrdU Kit	Roche, Basel, Switzerland
Activin A Quantikine ELISA kit	R&D Systems, Wiesbaden, Germany

2.2 Methods

2.2.1 Cell culture

2.2.1.1 Feeder cell culture and mitotic inactivation using mitomycin C

The mouse cell line SNL76/7 (BioCat GmbH, Heidelberg, Germany) was used as feeder cells for hiPSC culture. This particular cell line is derived from a mouse fibroblast STO (Sandos inbred mice, embryo-derived with thioguanine and ouabain resistance) cell line transformed with neomycin resistance and murine leukemia inhibitory factor (LIF) genes (McMahon and Bradley 1990). The abbreviation SNL is composed of STO, neomycin and LIF. SNL76/7 cells were cultured in 175 cm2 cell culture flasks in SNL medium containing DMEM high glucose medium (Life Technologies, Carlsbad, USA), 10% FCS (v/v) (Biochrom, Berlin, Germany) and 1% P/S (v/v) (Pan Biotech, Aidenach, Germany). SNL76/7 cells were cultured at 37°C and 5% CO_2. To use SNL76/7 cells as feeder cells for hiPSC culture, cells had to be mitotically inactivated. To mitotically inactivate SNL feeders, cells were grown in SNL medium until they reached 80 – 90% confluence. Subsequently, they were treated with 12 µg/mL mitomycin C resolved in SNL medium for 2 h 15 min. Thereafter, 1.5 x 10^6 inactivated SNL feeder cells were either plated on 0.1% gelatin-coated 6-well plates (2.5 x 10^5 cells per well) for direct use or frozen in freezing medium and stored in liquid nitrogen for later use.

2.2.1.2 Bromodeoxyuridine (BrdU) Assay of SNL cells

To test if the mitotic inactivation with mitomycin-c worked for SNL feeder cells, cells were plated on 0.1% gelatin-coated 96-well plates in two different densities (2.5 x 10^4 and 1.25 x 10^4) either treated with mitomycin-c or not. BrdU assay was performed with Cell Proliferation ELISA BrdU (chemiluminescence) kit (Roche, Basel, Switzerland) following the manufacturer's constructions. Briefly, mitomycin-treated and control SNL cells were plated in 96-well plates and treated with 10 µL BrdU labeling solution (1:100 diluted in PBS) for 2 or 6 h at 37°C and 5% CO_2. Afterwards, cells were fixed with 200 µL FixDenat for 30 min at room temperature (RT). Solution was discarded and cells were treated with 100 µL/well Anti-BrdU-POD working solution for 1 h at RT. After three times washing wells were filled with 100 µL Substrate Solution and incubated for 5 min at RT. Subsequently, chemiluminescence was measured with a multimode microplate reader (Tecan, Männedorf, Switzerland). As a reference cells were also plated in each condition without BrdU (BrdU control/Background). Three wells were plated per condition.

2.2.1.3 Proliferation assay (Nuclei staining) of SNL cells

Mitomycin-treated and control SNL cells were plated on 0.1% gelatin-coated 96-well plates in two different densities (2.5 x 10^4 and 1.25 x 10^4) and cultured at 37°C and 5% CO_2. Cells were fixed with 4% paraformaldehyde (PFA) after 24 h, 48 h, 72 h, 96 h and 120 h and stained with Hoechst33258 (Sigma Aldrich, Munich, Germany) for 30 min (1:5000 diluted in PBS). Nuclei were counted with the Array Scan VTI (Thermo Fisher Scientific, Carlsbad, USA) and the Spot Detector V4 vACS Scan software.

2.2.1.4 Quantification of Activin A in SNL feeder cell-conditioned medium

To quantify the amount of Activin A released from SNL feeder cells, cells were cultured in 2 mL hESC medium in 6-well plates for 24 h. SNL-conditioned medium (SNL-CM) was collected and the amount of released Activin A was determined using an enzyme-linked immunosorbent assay (ELISA). The analysis was done using the Activin A Quantikine ELISA kit (R&D Systems, Wiesbaden, Germany) according to the manufacturer's instructions. The results were compared to primary MEFs cultured in 2 mL hESC medium in 6-well plates for 24 h. MEFs were prepared from NSA-CF1 mice (Jozefczuk et al. 2012) and kindly provided by Prof. Dr. Adjaye (Institute for Stem Cell Research and Regenerative Medicine, Heinrich-Heine University, Düsseldorf, Germany).

2.2.1.5 hiPSC culture

The control hiPSC lines A4 (Wang and Adjaye 2011) and CRL2097 (Kristensen et al. 2013) were kindly provided by Prof. Dr. Adjaye (Heinrich-Heine University, Düsseldorf, Germany) and Prof. Dr. Egly (IGBMC, Strasburg, France), respectively (Tab. 2.8 and 3.2). The CSB-deficient hiPSC lines AS548 (classic; Tab. 2.8 and 3.2) and AS789 (COFS; Tab. 2.8 and 3.2) were kindly provided by Prof. Dr. Egly (IGBMC, Strasburg, France). The respective clinical phenotypes of CSB patients from hiPSC lines AS548 (classic) and AS789 (COFS) are summarized in Table 2.9. hiPSCs were cultured either under feeder-dependent conditions on SNL76/7 feeder cells using hESC medium or under feeder-free conditions on Matrigel (BD Biosciences, Heidelberg, Germany) using mTeSR1 medium (Stemcell Technologies, Cologne, Germany) in 6-well plates (Sarstedt, Nümbrecht, Germany). hiPSCs were cultured at 37°C and 5% CO_2. To culture hiPSCs under feeder-dependent conditions, 6-well plates were coated with 0.1% gelatin (v/v) at least 2 h before SNL feeder cells were seeded on the gelatin-coated 6-well plates (2.5 x 10^5 cells per well). Twenty-four hours after seeding SNL feeder cells, hiPSCs were plated on feeder-cells using hESC medium containing 12 ng/mL bFGF. To culture hiPSCs under feeder-free conditions, Matrigel (BDBiosciences, Heidelberg, Germany) was dissolved 1:30 in KnockOut DMEM (Invitrogen, Carlsbad, USA) and added to a 6-well plate (1 mL per well) at least 1 h before usage. Afterwards,

Matrigel-coated wells were washed once with KnockOut DMEM and hiPSCs were seeded on Matrigel-coated wells containing 2 mL mTeSR1 medium.

Medium was changed every day with the exception of the week-end. During the week-end medium was replaced one day with the double amount of fresh medium to skip one feeding day. hiPSCs were passaged when they reached an appropriate confluence on the plate before single colonies touched each other. Differentiated cells were identified under the microscope and removed if necessary every other day and directly before passaging.

Tab. 2.8: List of used hiPSC lines

hiPSC line	Donor cell type	Reprogramming method	Reprogramming cocktail	Reference
A4	Human fetal foreskin fibroblasts	Retroviral transfer	pMX-OCT4, pMX-SOX2, pMX-KLF4, pMX-cMYC	(Wang and Adjaye 2011)
CRL2097	Neonatal fibroblasts	Episomal plasmids	pCXLE-hUL, pCXLE-hSK, pCXLE-hOCT3/4-shp53-F	(Okita et al. 2011)
AS548	Dermal fibroblasts	Episomal plasmids	pCXLE-hUL, pCXLE-hSK, pCXLE-hOCT3/4-shp53-F	(Okita et al. 2011)
AS789	Dermal fibroblasts	Episomal plasmids	pCXLE-hUL, pCXLE-hSK, pCXLE-hOCT3/4-shp53-F	(Okita et al. 2011)

Tab 2.9: Clinical phenotype of respective CSB patients (Laugel et al. 2010)

	CS548	CS789
Clinical classification	CSI (classic)	COFS
Low birth weight	+	+
Mental retardation	severe	severe
Microcephaly	congenital	congenital
Cataracts	5 months	congenital
Retinal degeneration	+	-
Deafness	+	-
Clinical photosensitivity	+	+
Age at onset	0 years	0 years
Age at death	6 years	10 months
Growth failure	+	+

2.2.1.6 Passaging of hiPSCs

hiPSCs were passaged mechanically either with a special passaging tool called StemPro® EZPassage™ Disposable Stem Cell Passaging Tool (Thermo Fisher Scientific, Carlsbad USA) or a syringe needle (BD Biosciences, Heidelberg, Germany). Using the Stem Cell Passaging Tool, hiPSC colonies of the whole well were cut into equal quadrants (Fig. 3.2 A). Subsequently, attached hiPSC colony pieces were washed once with phosphate-buffered saline (PBS), scratched from the plate and carefully transferred with a pipette tip into a new well containing fresh medium. Using the syringe needle, hiPSCs were first screened for colonies with pluripotent morphology (Fig. 3.2). Subsequently, only the hiPSC colonies with pluripotent morphology were cut into little pieces (Fig. 3.2 B), washed once with PBS, scratched from the plate and transferred with a pipette tip into a new well containing fresh medium. To standardize the passaging method, three colonies with equal size were cut and transferred into one new well of a 6-well plate.

For passaging hiPSCs as single cells, hiPSCs were treated with 10 µM of the ROCK inhibitor Y-27632 (R&D Systems, Wiesbaden, Germany) at least 1 h before passaging. Subsequently, hiPSCs were washed once with PBS and treated with 350 µL Accutase per well at 37°C and 5% CO_2 for about 15 min or until cells started to detach from the plate bottom. Afterwards, 1 mL medium was added to each well and singularized hiPSCs were collected into a 15 mL falcon tube. Cells were centrifuged at 1000 rpm for 5 min and either transferred to a new 6-well containing 2 ml fresh medium or prepared for further experiments. If hiPSCs were transferred into a new 6-well for cell culture, cells were treated with 10 µM of the ROCK inhibitor for another 24 h.

2.2.1.7 Cyropreservation of hiPSCs

For cryopreservation hiPSC colonies with hESC morphology (Fig. 3.2) were washed once with PBS and scratched from the plates with a cell scratcher. Colonies from 1 – 2 wells were collected in 2 mL tubes and centrifuged at 1000 rpm for 5 minutes. Supernatant was discarded and hiPSC colonies were gently resuspended in 500 µL freezing medium I containing KoDMEM (Invitrogen, Carlsbad, USA) and 20% KSR (v/v) (Invitrogen, Carlsbad, USA) and transferred into cryo tubes. Subsequently, 500 µL of freezing medium II containing KoDMEM (Invtirogen, Carlsbad, USA), 20% KSR (v/v) (Invitrogen, Carlsbad, USA) and 20% DMSO (v/v) (Carl Roth GmbH + Co. KG, Karlsruhe, Germany) was added drop wise to the cryo tubes containing hiPSC colonies. Cells were frozen at -80°C for 24h and afterwards stored in liquid nitrogen for longer time periods. hiPSCc were thawed at 37°C until only a small piece of ice was present in the cryo tube. Subsequently, hiPSCs were drop wise transferred into a 15 mL falcon tube containing 10 mL NPM and centrifuged at 1000 rpm for 5 minutes. Afterwards, supernatant was discarded and

hiPSCs were transferred into a 6-well plate containing 2 mL mTeSR. After thawing hiPSCs were treated with 10 µM ROCK inhibitor Y-27632 for the first 24 h to inhibit apoptosis.

2.2.1.8 Spontaneous differentiation of hiPSCs

To analyze the pluripotent potential of cultured hiPSCs, cells were treated with 10 µM of the ROCK inhibitor at least 1 h before dissociation. Subsequently, hiPSC colonies were dissociated using 350 µL Accutase per well at 37°C and 5% CO_2 for about 15 min or until cells started to detach from the plate bottom. Afterwards, 1 mL medium was added to each well and singularized hiPSCs were collected into a 15 mL falcon tube. Cells were counted using a Neubauer chamber and centrifuged at 1000 rpm for 5 min. Three-dimensional EBs were generated using the hanging drop (HD) method (Wang and Yang 2008). Therefore, hiPSCs were resuspended in UM without bFGF and 20 µL drops (4 x 10^4 cells per drop) were pipetted at the lid of a 10 cm culture dish. The bottom of the 10 cm2 culture dish was filled with 10 mL PBS to circumvent evaporation and HD-EBs were grown for 3 days at 37°C and 5% CO_2. After the 3 days, drops containing the EBs were washed up using a 5 mL pipette and were cultured in UM without bFGF in 0.1% gelatin-coated 24-well plates for either 5 (for RNA isolation) or 23 (for morphological analyses) additional days. After a total culture time of 10 days, EBs were screened for beating cardiomyocytes.

2.2.1.9 Cytogenetic analysis of hiPSCs

Cytogenetic analyses were performed by the Institute of human genetics and anthropology at the Heinrich-Heine University Düsseldorf. Cytogenetic analyses were done using GTG-banding of chromosomes. After treatment with trypsin fixed metaphase chromosomes were stained with Giemsa which generates a black and white banding pattern (Thalhammer et al. 2001). Subsequently, chromosomes can be identified under the microscope.

2.2.1.10 Neural induction of hiPSCs

Noggin Protocol

The Noggin protocol was performed as previously described (Denham and Dottori 2011) with small modifications. Therefore, hiPSC colonies with pluripotent morphology were treated with induction medium consisting of KoDMEM, 20% Knockout Serum Replacement (KSR), 2 mM L-Glutamine, 1x10^{-4} M non-essential amino acids (NEAA), 1x10^{-4} M β-Mercaptoethanol, 1% P/S (v/v) without growth factors but with 500 ng/mL noggin (PeproTech, Hamburg, Germany) for 14 days. Medium was changed every 2 – 3 days. Afterwards, colonies were cut into pieces and cultured in 10 cm ultra-low-attachment (ULA) plates in 15 mL neural proliferation medium (NPM) consisting of DMEM and Hams F12 (3:1) supplemented with B27 (Invitrogen GmBH,

Karlsruhe, Germany), 20 ng/mL epidermal growth factor (EGF; Biosource, Karlsruhe, Germany) and 20 ng/mL FGF (R&D Systems). Medium was changed every 2 – 3 days.

NIM Protocol

The NIM protocol was performed as previously described (Hibaoui et al. 2014) with small modifications. Therefore, hiPSC colonies with pluripotent morphology were cut into pieces using the StemPro® EZPassage™ Disposable Stem Cell Passaging Tool (Thermo Fisher Scientific, Carlsbad USA). hiPSC clumps were cultured in 6 cm ULA plates in 6 mL neural induction medium (NIM) consisting of DMEM and Hams F12 (3:1) supplemented with B27 (Invitrogen GmBH, Karlsruhe, Germany), 20 ng/mL EGF (Biosource, Karlsruhe, Germany) and N2 supplement (Invitrogen) for 7 days as EBs. After this period of 7 days, EBs were transferred into new 10 cm ULA plates with 15 mL NIM containing 10 ng/mL bFGF for another 14 days. Afterwards, EBs were referred to as hiPSC-NPCs and were transferred into new ULA plates in NPM containing 20 ng/mL EGF and 20 ng/mL bFGF. hiPSC-NPC were cultured under these conditions for at least another 28 days before starting experiments. Medium was changed every 2 – 3 days.

2.2.1.11 hiPSC-derived neurosphere and primary human neurosphere culture

Primary hNPCs were purchased from Lonza Verviers SPRL (Verviers, Belgium). hNPCs 988 and 692 are primary fetal neurospheres obtained from chirurgical and spontaneous aborts from gestational weeks 16 and 18, respectively. Primary hNPCs and hiPSC-NPCs were cultured in suspension culture as neurospheres in un-coated and ULA 10 cm petri dishes, respectively, in NPM containing 20 ng/mL EGF and 20 ng/mL bFGF. Medium was changed every 2 – 3 days. Neurospheres were cultured at 37°C and 5% CO_2. Proliferating neurospheres were passaged using a McIlwaine tissue chopper. Neurospheres were then cut into smaller spheres with a diameter of 200 µm.

2.2.1.12 Preparation of ULA petri dishes

ULA petri dishes were either ordered (Oehmen, Essen, Germany) or prepared using poly-2-hydroxyethyl methacrylate (Poly-HEMA; Sigma Aldrich, Munich, Germany). Therefore, 1.2 g poly-HEMA was solved in 39.5 mL 96% ethanol (EtOH) and 0.5 mL dH_2O in a 50 mL falcon tube (Sarstedt, Nümbrecht, Germany). The poly-HEMA solution was solved using a plate rotator for 5 – 6 h at room temperature (RT). Poly-HEMA stock solution was stored at 4°C protected from light for up to 2 months. To prepare ULA dishes, an appropriate volume of poly-HEMA solution was applied to each dish or well in the tissue culture hood. Subsequently, the lid of the dishes or wells was left opened until the poly-HEMA solution was completely dried out (~ 1 h). The poly-HEMA dishes were closed with Parafilm and stored in the dark at RT for up to 3 months. For 10

cm^2, 6 cm^2 culture dishes and 96-well plates, 3 mL, 1 mL and 250 µL of poly-HEMA solution was used, respectively.

2.2.1.13 Cryopreservation of hiPSC-derived neurospheres

For cryopreservation hiPSC-NPCs were cut into spheres with a diameter of 200 µm using the tissue chopper. Two days later hiPSC-NPCs were again cut into spheres with a diameter of 100 µm and cultured for an additional 5 h at 37°C and 5% CO_2. Afterwards, 100 µm neurospheres were collected in freezing medium containing DMEM and Hams F12 (3:1) supplemented with B27 (Invitrogen GmBH, Karlsruhe, Germany), 20 ng/mL EGF (Biosource, Karlsruhe, Germany), 20% KSR (v/v) (Invitrogen, Carlsbad, USA) and 10% DMSO (v/v) (Carl Roth GmbH + Co. KG, Karlsruhe, Germany). Cells were frozen at -80°C for 24 h and afterwards stored in liquid nitrogen for longer time periods. hiPSC-NPCs were thawed at 37°C until only a small piece of ice was present in the cryo tube. Subsequently, hiPSC-NPCs were transferred into a 15 mL falcon tube containing 10 mL NPM and centrifuged at 1000 rpm for 5 minutes. Afterwards, supernatant was discarded and hiPSC-NPCs were transferred into a 6 cm ULA dish containing 6 mL NPM. After thawing hiPSC-NPCs were treated with 10 µM ROCK inhibitor Y-27632 for the first 24 h to inhibit apoptosis. Two weeks after thawing hiPSC-NPCs were cut using a McIlwaine tissue chopper and transferred into 10 cm ULA dishes containing 15 mL NPM. Medium was changed every 2 – 3 days.

2.2.1.14 Coating of eight-chamber slides for migration and differentiation assay

To perform the migration and differentiation assay on a Poly-D-Lysine (PDL)/Laminin matrix eigth-chamber slides (BDBiosciences, Heidelberg, Germany) had to be coated with both substances. Therefore, eight-chamber slides were filled with 250 µL of 0.1 mg/mL PDL for at least 1 h at 37°C. Subsequently, slides were washed twice with 500 µL dH_2O and filled with 250 µL of 0.01 mg/mL Laminin for at least 1 h at 37°C. Afterwards, slides were washed again twice with 500 µL dH_2O and filled with 500 µL DPBS. Slides can be stored for 1 week at 4°C.

2.2.1.15 The Neurosphere assay

Proliferation assay

hiPSC-derived neuropsheres were cut into 200 µm spheres using a McIlwaine tissue chopper 2 – 3 days before the experiment was started. Six neuropsheres per condition with a diameter of 300 µm were placed into round bottom 96-well plates and cultured either in 100 µL NPM containing 20 ng/mL EGF and 20 ng/mL bFGF or in 100 µL NPM without growth factors for 14 days. Neuropsheres were photographed every 3 – 4 days and diameter was measured using ImageJ. Medium was changed every 2 – 3 days during this assay.

Migration assay

hiPSC-derived neuropsheres were cut into 200 µm spheres using a McIlwaine tissue chopper 2 – 3 days before the experiment was started. Migration analyses were performed after 24 h and 72 h. Therefore, five neurospheres per condition with a diameter of 300 µm were plated on a PDL/Laminin matrix in eight-chamber slides (BDBiosciences, Heidelberg, Germany) in 500 µL neural differentiation medium (NDM) containing B27 supplement. After the corresponding time points, single neurospheres were photographed and migration distance was assessed by measuring the length at four distinct locations between the edge of the sphere and the furthest migrated cells.

Differentiation assay

hiPSC-derived neuropsheres were cut into 200 µm spheres using a McIlwaine tissue chopper 2 – 3 days before the experiment was started. Five neurospheres per condition with a diameter of 300 µm were plated on a PDL/Laminin matrix in eight-chamber slides (BDBiosciences, Heidelberg, Germany) in 500 µL NDM containing B27 supplement for the indicated time points. Medium was changed once a week during this assay. Afterwards, cells were fixed with 4% PFA for 30 min at 37°C and washed with PBS. Neurons and astrocytes were then identified by ICC staining with mouse-anti-βIII-Tubulin (Sigma Aldrich, Munich, Germany) and rabbit-anti-GFAP (Sigma Aldrich, Munich, Germany), respectively.

Viability assay

Viability was determined using the CellTiter Blue (CTB) cell viability assay (Promega, Mannheim, Germany). Therefore, CTB stock solution was diluted 1:3 in the respective cell culture medium and was added to the cells in another 1:4 dilution. Primary human neurospheres were incubated with the CTB solution for 2 h before fluorescence (579Ex/585Em) was measured at a multimode microplate reader (Tecan, Männedorf, Switzerland). In contrast, hiPSC-derived neurospheres CRL2097 and A4 were incubated with the CTB solution for 3.5 and 4.5 h, respectively, before fluorescence was measured at a multimode microplate reader (Tecan, Männedorf, Switzerland).

2.2.1.16 DNT testing for MeHgCl on neurosphere migration and viability

hiPSC-derived neuropsheres were cut into 200 µm spheres using a McIlwaine tissue chopper 2 – 3 days before the experiment was started. For the DNT testing for MeHgCl on neurosphere migration and viability, five neurospheres of either primary human neurospheres (692 and 988) or hiPSC-derived neurospheres (A4 and CRL2097) were plated on a PDL/Laminin matrix in eight-chamber slides (BDBiosciences, Heidelberg, Germany) in NDM for 24 h. Primary human neurospheres were cultured in 500 µL NDM without B27 supplement whereas hiPSC-derived

neurospheres were cultured in 500 µL NDM containing B27 supplement. Neurospheres were treated with different concentrations of MeHgCl (3 µM, 1 µM, 0.3 µM, 0.1 µM and 0.03 µM) solved in 0.15% DMSO. As end point specific controls, neurospheres were treated either with 20 ng/mL EGF (positive control for migration) or with 10 µM of the src kinase inhibitor PP2 (negative control for migration). The used solvent control was NDM containing 0.15% DMSO. After 24 h, single neurospheres were photographed and migration distance was measured using ImageJ. Viability assay was performed according to chapter 2.2.1.15 viability assay.

2.2.2 Fluorescent activated cell sorting (FACS) analysis

For flow cytometry analysis of hiPSC-derived neurospheres 30 spheres of hiPSC-NPCs and primary hNPCs with a diameter of 300 µm were collected in a 2 mL tube. hiPSC-NPCs were centrifuged at 2000 rpm for 5 minutes and supernatant was discarded. Cells were singularized by incubating them in 50 µL Accutase for 20 min at 37°C and 5% CO_2. Afterwards, cells were fixed with 50 µL 4% PFA for 30 min at 37°C and then washed once with 1 mL PBS. Furthermore, cells were permeabilized with 50 µL 0.1% PBS-T at room temperature for 15 min. Finally, cells were stained with anti-Nestin-Alexa647 (BDBioscience, Heidelberg, Germany) and anti-Sox2-PE (BDBioscience, Heidelberg, Germany) in 0.1% PBS-T (Tab. 2.10) in the dark at 4°C for 30 min. Samples were analyzed using FACS Calibur and the software WinMDI.

For flow cytometry analysis of undifferentiated hiPSCs, colonies were treated with 10 µM ROCK inhibitor at least 1 h before dissociation. hiPSC colonies were dissociated with 350 µL Accutase per well and incubated at 37°C and 5% CO_2 for about 15 min or until cells started to detach from the plate bottom. Afterwards, 1 mL medium was added to each well and singularized hiPSCs were collected into a 15 mL falcon tube. Cells were counted and centrifuged at 1000 rpm for 5 min. Furthermore, cells were stained with anti-TRA-1-60-PE (Miltenyi, Cologne, Germany), anti-SSEA-4-APC (Miltenyi, Cologne, Germany) and propidium iodide (Sigma Aldrich, Munich, Germany) to detect dead cells. Antibodies were dissolved in PBS (Tab. 2.10) and hiPSCs were incubated in the dark at 4°C for 30 min. Samples were analyzed using FACS Calibur and the software WinMDI.

Tab. 2.10: List of antibodies for flow cytometry

Antibody	Dilution/concentration	Company
Anti- Nestin-Alexa647	1:50 in PBS-T	BDBioscience, Heidelberg, Germany
Anti-Sox2-PE	1:50 in PBS-T	BDBioscience, Heidelberg, Germany
Anti-Tra-1-60-PE	1:11 in PBS	Miltenyi, Cologne, Germany
Anti-SSEA-4-APC	1:11 in PBS	Miltenyi, Cologne, Germany
Propidium iodide	0.2 µg/mL in PBS	Sigma Aldrich, Munich, Germany

2.2.3 Immunocytochemical staining

For immunocytochemical (ICC) staining cells were fixed with 4% PFA for 30 min at 37°C. Afterwards, cells were washed twice with PBS and stained with the primary antibody dissolved either in PBS or PBS-T for 1 h at 37°C or overnight at 4°C together with 10% normal goat serum (NGS). Concentration and incubation time was depending on the respective primary antibody (Tab. 2.11). After incubation time, cells were washed three times with PBS and stained with the secondary antibody together with Hoechst33258 dissolved in PBS for 30 min at 37°C together with 2% NGS. Concentration was depending on the respective secondary antibody (Tab. 2.12). Cells were analyzed using a fluorescent microscope (Zeiss, Oberkochen, Germany) and the software Axio Vision.

Tab. 2.11: List of primary antibodies

Primary antibody	Dilution	Company
Mouse-anti-βIII-Tubulin (IgG)	1:100 in PBS-T	Sigma Aldrich, Munich, Germany
Rabbit-anti-GFAP (IgG)	1:200 in PBS-T	Sigma Aldrich, Munich, Germany
Mouse-anti-TRA-1-60 (IgM)	1:250 in PBS	BDBiosciences, Heidelberg, Germany

Tab. 2.12: List of secondary antibodies

Secondary antibody	Dilution	Company
Anti-mouse-IgG-Alexa548	1:250 in PBS	Invitrogen, Carlsbad, USA
Anit-rabbit-IgG-Alexa488	1:250 in PBS	Invitrogen, Carlsbad, USA
Anti-mouse-IgM-Alexa488	1:250 in PBS	Life Technologies, Carlsbad, USA

Tab. 2.13: Additional components for ICC staining

Component	Dilution	Company
Normal goat serum (NGS)	10% (1st antibody solution) 2% (2nd antibody solution)	Life Technologies, Carlsbad, USA
Hoechst33258	1:100	Sigma Aldrich, Munich, Germany
Triton-X in PBS (PBS-T)	1:1000 (0.1%) Triton-X in PBS	Sigma Aldrich, Munich, Germany

Tab. 2.14: Additional material for ICC staining

Material	Company
Aqua Poly/Mount	Polysciences Inc., Eppelheim, Germany
Cover slips	Menzel Gläser, Braunschweig, Germany
Staining Chamber	-

2.2.4 Live staining of hiPSCs for TRA-1-60

For the live staining of hiPSCs, mouse-anti-TRA-1-60 antibody (BDBiosciences, Heidelberg, Germany) was diluted 1:250 in mTeSR1 medium (Stemcell Technologies, Cologne, Germany). hiPSCs were incubated with 1 mL of the antibody solution without NGS for 1 h at 37°C and 5% CO_2. Afterwards, hiPSCs were washed twice with PBS and the secondary antibody anti-mouse-IgM-Alexa488 (Chemicon, Limburg, Germany) was diluted 1:250 in 1 mL fresh mTeSR1 medium and cells were incubated for 30 min at 37°C and 5% CO_2. Subsequently, cells were analyzed using a fluorescent microscope (Zeiss, Oberkochen, Germany) and the software Axio Vision. After the live staining, hiPSCs were cultured as usually and antibody staining was lost over culture time.

2.2.5 DNA isolation

DNA of hiPSCs was isolated using QIAamp DNA Mini and Blood Mini Kit (Qiagen, Hilden, Germany). Briefly: hiPSC colonies of one well were scraped off the dishes and collected in 1.5 mL Eppendorf tubes. Subsequently, DNA was isolated following the manufacturer's instructions. DNA concentration was determined using a multimode microplate reader (Tecan, Männedorf, Switzerland).

2.2.6 Polymerase chain reaction (PCR) analysis and Sanger sequencing

PCR was performed using a Thermocycler (Biometra GmbH, Göttingen, Germany) and the following oligonucleotides with the respective PCR mix and programs. Oligonucleotides were designed using Serial Cloner 2.6 and Primer3web version 4.0.0. Designed oligonucleotides were ordered at Eurofins MWG GmbH, Ebersberg, Germany. Before sequencing, resulting PCR products were analyzed using gel electrophoresis. Subsequently, the PCR product was purified using the Qiaquick PCR purification kit (Qiagen, Hilden, Germany) following the manufacturer's constructions. Afterwards, PCR products were dissolved in dH_2O in the respective concentration dependent on the product size according to the service provider's constructions (BMFZ, Heinrich-Heine University, Düsseldorf, Germany). Sanger sequencing (Sanger et al. 1977) was performed by the BMFZ, Heinrich-Heine University, Düsseldorf, Germany.

Oligonucleotides used for sequencing of the classical CSB-deficient hiPSC line (AS548):

hCSB548_FW1: GAAGAAAGGGAAGACAGAGCC

hCSB548_RV1: ACTGCCTGGATCTGATGTCG

PCR mix and program used before sequencing of the classical CSB-deficient hiPSC line (AS548):

Tab. 2.15: PCR mix for the classical CSB-deficient hiPSC line (AS548)

Reagent	1x 50 µL reaction mix	Company
10 x Coral Load Buffer	5 µL	Qiagen, Hilden, Germany
dNTPs (10 mM)	1 µL	Peqlab Biotechnologies, Erlangen, Germany
DMSO (100%)	1.25 µL	Carl Roth GmbH + Co. KG, Karlsruhe, Germany
dH_2O	34.75 µL	-
FW primer (4 µM)	2.5 µL	Eurofins MWG, Ebersberg, Germany
RV primer (4 µM)	2.5 µL	Eurofins MWG, Ebersberg, Germany
Taq Polymerase (5 U)	0.5 µL	Qiagen, Hilden, Germany
Genomic DNA (gDNA)	2.5 µL	-

Tab. 2.16: PCR program for the classical CSB-deficient hiPSC line (AS548)

Process	Temperature	Time	Cycles
T1 Denaturation	94°C	4 min	1x
T2 Denaturation	94°C	45 sec	35x
T3 Annealing	55°C	45 sec	
T4 Elongation	72°C	60 sec	
T5 Elongation	72°C	4 min	1x
T6 Cooling	4°C	∞	-

Oligonucleotides used for sequencing of the COFS hiPSC line (AS789):

hCSB789_FW1: GGAGAGTACCAAAATGATGCAAG

hCSB789_RV1: GAGCCTGGCCATCTTTCTCAC

PCR mix and program used before sequencing of the COFS hiPSC line (AS789):

Tab. 2.17: PCR mix for COFS hiPSC line (AS789)

Reagent	1x 50 µL reaction mix	Company
10 x Coral Load Buffer	5 µL	Qiagen, Hilden, Germany
dNTPs (10 mM)	1 µL	Peqlab Biotechnologies, Erlangen, Germany
DMSO (100%)	1.25 µL	Carl Roth GmbH + Co. KG, Karlsruhe, Germany
dH_2O	34.75 µL	-
FW primer (4 µM)	2.5 µL	Eurofins MWG GmbH, Ebersberg, Germany
RV primer (4 µM)	2.5 µL	Eurofins MWG GmbH, Ebersberg, Germany
Taq Polymerase (5 U)	0.5 µL	Qiagen, Hilden, Germany
gDNA	2.5 µL	-

Tab. 2.18: PCR program for the COFS hiPSC line (AS789)

Process	Temperature	Time	Cycles
T1 Denaturation	94°C	4 min	1x
T2 Denaturation	94°C	45 sec	35x
T3 Annealing	54°C	30 sec	
T4 Elongation	72°C	60 sec	
T5 Elongation	72°C	4 min	1x
T6 Cooling	4°C	∞	-

2.2.7 RNA isolation

RNA was isolated using the RNeasy Mini Kit (Qiagen, Hilden, Germany) according to the manufacturer's description. RNA concentration was determined using a multimode microplate reader (Tecan, Männedorf, Switzerland).

2.2.8 Reverse transcription of RNA into cDNA

To transcribe RNA into cDNA 300 ng RNA was used. cDNA was transcribed using the QuantiTect Rev Transcription Kit (Qiagen, Hilden, Germany) according to the manufacturer's description. Briefly: genomic DNA was eliminated by mixing 12 µL of the template RNA (dissolved in H_2O) and 2 µL of 7x gDNA wipeout buffer (Qiagen, Hilden, Germany) and gDNA was removed incubating the reaction components for 2 min at 42°C. Subsequently 1 µL of reverse transcriptase (RT)-Primer mix, 4 µL of 5x Quantiscript RT and 1 µL of Quantiscript RT (Qiagen,

Hilden, Germany) was added to reaction mix. cDNA was synthesized for 30 min at 42°C. End reaction was performed for 3 min at 95°C.

Tab. 2.19: RT-PCR program

Process	Temperature	Time
Removal of gDNA	42°C	2 min
Synthesis of cDNA	42°C	30 min
End reaction	95°C	3 min
Cooling	4°C	∞

2.2.9 Quantitative real-time PCR

Quantitative real-time PCR (qRT-PCR) was performed using the Rotor Gene Q Cycler (Qiagen, Hilden, Germany) with QuantiFast SYBR green PCR Master Mix (Qiagen, Hilden, Germany) following the manufacturer's instructions. The C_t value is calculated from the fluorescence measurement chart. This value corresponds to the number of cycles where the fluorescence reaches a defined threshold. The higher the amount of the target product the lower is the C_t value. To calculate the relative expression of the target gene the C_t value has to be referred to the C_t value of a housekeeping gene which is constitutively expressed. This reference enables a compensation of irregularities between cDNA quantities. In this study, β-Actin was used as housekeeping gene. To calculate the relative expression of each target gene the ddC_t values are determined:

$$ddC_t = dC_{t,control} - dC_{t,sample}$$

$$dC_t = C_{t,target\ gene} - dC_{t,housekeeping\ gene}$$

The calculations were performed using Microsoft Excel 2010. Oligonucleotide primers were designed with NCBI Primer-BLAST.

Tab. 2.20: SYBR Fast program

Process	Temperature	Time	Cycles
Denaturation	95°C	7 min	1x
Denaturation	95°C	10 sec	47x
Annealing	60°C	35 sec	
Elongation	72°C	20 sec	
Melting	75°C – 99°C		1x

2.2.10 Oligonucleotides for qRT-PCR

Tab. 2.21: List of oligonucleotide primers

Oligonucleotide primers	Sequence
hβ-Actin	FW: 5' CAGGAAGTCCCTTGCCATCC 3' RV: 5' ACCAAAAGCCTTCATACATCTCA 3'
hOct4	FW: 5' CGAGAAGGATGTGGTCCGAG 3' RV: 5' AGCCTGGGGTACCAAAATGG 3'
hNanog	FW: 5' CAATGGTGTGACGCAGAAGG 3' RV: 5' TGCACCAGGTCTGAGTGTTC 3'
hSox2	FW: 5' GGGAAAGTAGTTTGCTGCCTC 3' RV: 5' AGAGAGGCAAACTGGAATCAGG3'
hNestin	FW: 5' CAGCTGGCGCACCTCAAGATG 3' RV: 5' AGGGAAGTTGGGCTCAGGACTGG 3'
hPax6	FW: 5' ACACCGGTTTCCTCCTTCAC 3' RV: 5' GGCAGCATGCAGGAGTATGA 3'
hMAP2	FW: 5' TGCGCTGATTCTTCAGCTTG 3' RV: 5' TGTGTCGTGTTCTCAAAGGGT 3'
hPDGFRα	FW: 5' ATTAAGCCGGTCCCAACCTG 3' RV: 5' AGCTCCGTGTGCTTTCATCA 3'
hNG2	FW: 5' CCCATCCTCACTACAAACACA 3' RV: 5' TGTAGACCAGATCCTCAGACC 3'
hGFAP	FW: 5' GATCAACTCACCGCCAACAGC3' RV: 5' CTCCTCCTCCAGCGACTCAATCT 3'
hAFP	FW: 5' GCGGCCTCTTCCAGAAACTA 3' RV: 5' ATAATGTCAGCCGCTCCCTC 3'
hMSX1	FW: 5' CCACTCGGTGTCAAAGTGGA 3' RV: 5' GAAGGGGACACTTTGGGCTT 3'
hCSB	FW: 5' TAAGCAGCGGTTAAGGAGATGG 3' RV: 5' AACCTGGCACTTTAAAACCTTCG 3'
hEGFR	FW: 5' ATCACCTGCACAGGACGGGGA 3' RV: 5' GGACGGGATCTTAGGCCCATTCG 3'
hFGFR2	FW: 5' CGGCCCTCCTTCAGTTTAGTT 3' RV: 5' GGTCCAGTATGGTGCTCTCTTGT 3'
hALDH1L1	FW: 5' TGATGAGTTCGTGCGGAGAG 3' RV: 5' TCAAAGAAGAACCCTGGCCG 3'

2.2.11 Statistical analyses

Statistical analysis was performed using the GraphPad Prism 6.01 software. For the comparison of different groups a one-way ANOVA was performed for one independent variable whereas a two-way ANOVA was performed for two independent variables.

3. Results

3.1 Establishment of a hiPSC culture

hiPSCs are defined by their self-renewal and pluripotent nature (Fukusumi et al. 2013). They usually grow in multi-layered colonies and are characterized by their small and round cell morphology with a high nucleus-to-cytoplasm ratio (Smith et al. 2009, Courtot et al. 2014). Moreover, hiPSCs require special culture conditions supporting their pluripotent character, including feeder cells (Dravid et al. 2005) or specific matrices and medium to replace the feeder cell layer (Valamehr et al. 2012). In general, maintenance of pluripotent stem cells including hiPSCs is challenging due to their high sensitivity and tendency to spontaneously differentiate (Sathananthan and Trounson 2005, Ohtsuka and Dalton 2008). Therefore, medium has to be changed every day including mechanical removal of differentiated cells. Every change in the culture conditions might result in different cell morphology and behavior what makes it necessary to carefully define highly standardized culture conditions to maintain the pluripotent character of the cells and therefore guarantee reproducibility of the obtained results.

3.1.1 Preparation of feeder cells

The first hESCs, pluripotent stem cells derived from blastocysts, which share the same characteristics than hiPSCs, were cultured using mitotically inactivated MEFs as feeder cells (Thomson et al. 1998). Meanwhile, instead of MEFs, there is also the possibility to use the SNL76/7 cell line for culturing pluripotent stem cells (Takahashi et al. 2007). This particular cell line is derived from a mouse fibroblast STO cell line transformed with neomycin resistance and murine leukemia inhibitory factor (LIF) genes (McMahon and Bradley 1990). SNL cells are commercially available and circumvent the necessity to isolate fibroblasts from mouse embryos. In order to use MEFs or SNL cells for the cultivation of hiPSCs they have to be mitotically inactivated. This can be either done by treatment of the cells with mitomycin C, an antibiotic produced by Streptomyces caespitosus also used in cancer therapy (Saif et al. 2013), or by γ-irradiation (Ponchio et al. 2000, Roy et al. 2001, Llames et al. 2015). Mitomycin C inhibits cell proliferation by covalently reacting with the DNA, forming crosslinks and therefore inhibiting DNA synthesis (Tomasz et al., 1988). Treatment is an easy procedure and does not require special safety precautions or special equipment like a γ-source for irradiation. Therefore, within this thesis, SNL76/7 cells were mitotically inactivated using 12 µg/mL mitomycin C in SNL medium for 2 h 15 min. Thereafter, inactivated feeder cells were either plated on gelatin-coated plates or frozen and stored in liquid nitrogen for later use.

To test if the mitotic inactivation of the SNL cells was successful, i.e. mitomycin-treated cells stopped to proliferate, a BrdU assay was performed. BrdU is a pyrimidine analogue which when

added to the cell culture is - in place of thymidine - incorporated into the DNA of proliferating cells. The experiment was done using two different cell densities (2.5 x 10^4 and 1.25 x 10^4 cells). After 2 h of incubation mitomycin-treated SNL cells seeded in the higher cell density revealed a mitotic reduction of about 70%, whereas at the lower cell density of mitomycin-treated cells the mitotic reduction reached 99% compared to mitotically active SNL cells (Fig. 3.1 A).

To verify if the remaining observed proliferative activity of 30% in the BrdU assay was actually caused by active cell division, mitomycin-treated SNL cells and the respective untreated controls were plated on gelatin-coated plates using the same cell densities. Cells were cultured for 0, 24, 48, 72, 96 or 120 h to observe the proliferative capacity. Afterwards, the cells were fixed with 4% PFA and the nuclei were stained with Hoechst. Subsequently, Hoechst-positive nuclei were counted (Fig. 3.1 B). This experiment revealed that mitomycin-treated cells of both seeding densities did not show an increase in the nuclei number, whereas the control cells almost doubled their number of nuclei after 24 h and continued to proliferate until they reached a steady state after 48 and 72 h, respectively, caused by a natural proliferation stop due to contact inhibition after the cells reached confluence. These results clearly indicated that mitomycin C treatment for 2 h 15 min was sufficient to mitotically inactivate SNL cells independent of cell density. Therefore, SNL cells were cultured until they reached confluence, treated with 12 µg/mL mitomycin C for 2 h 15 min and stored as frozen stocks before usage.

Feeder cells secrete several substances which support the pluripotency of stem cells (Lim and Bodnar 2002). While overall little is known about these substances, Activin A is known to be a crucial component of MEF-conditioned medium inducing the expression of the pluripotent markers *OCT4*, *SOX2* and *NANOG* (Greber et al. 2007) and is therefore an indicator for the quality of used feeder cells. After 24 h in culture the supernatant of inactivated SNL cells was collected and the level of Activin A was determined by enzyme-linked immunosorbent assay (ELISA). The analysis revealed that SNL feeder cells released 2.5 ng/mL Activin A (Fig. 3.1 C). Additionally, Activin A release from primary isolated MEFs was measured and compared to SNL feeder cells. According to the literature supportive MEFs should release approximately 15 – 20 ng/mL Activin A (Greber et al. 2007). Both, SNL feeder cells and primary MEFs, released less Activin A (2.5 ng/mL and 8 ng/mL, respectively) as described in the literature. Because SNL 76/7 cells were previously used for the first generated hiPSCs (Takahashi et al. 2007) they seem to represent supportive feeder cells for hiPSC culture despite their low production of Activin A.

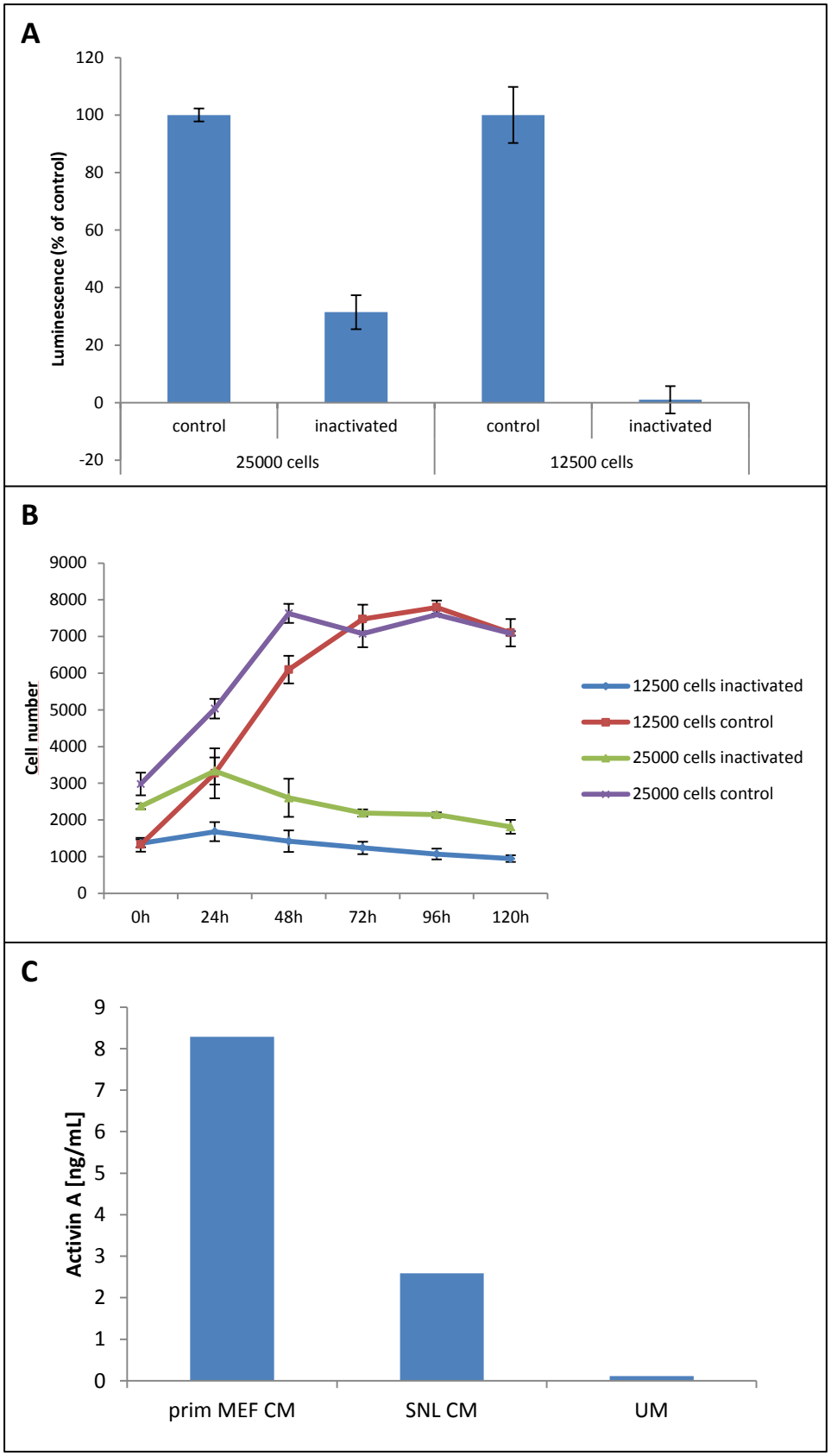

Figure 3.1: Mitotic inactivation of SNL76/7 cells. A) BrdU incorporation was measured for mitomycin-treated and control cells in two different cell densities. Values are presented as mean +/- standard deviation (SD), n = 1 **B)** Increase of cell number was measured for mitomycin-treated and control cells in two different cell densities over the time, values are presented as mean + SD, n = 1 **C)** Activin A concentration was measured either in primary mouse embryonic fibroblast (MEF)-conditional medium (CM), SNL-CM or unconditional medium (UM), n = 1.

3.1.2 Comparison of different culture media and matrices to maintain hiPSCs

Although the culture conditions of human pluripotent stem cells were first described using MEFs (Thomson et al. 1998) there have been various other feeder-free culture conditions published so far (Valamehr et al. 2012, Fukusumi et al. 2013). The advantages of feeder-free cultures are an easier handling, a higher reproducibility due to less batch-to-batch variations and a reduction or complete absence of non-human animal material in the hiPSC culture. To establish feeder-free hiPSC culture conditions MEFs can be replaced by special extracellular matrices, which resemble the basement membrane, e.g. Matrigel or laminin (Crocco et al. 2013, Nakagawa et al. 2014). Supportive factors of MEF co-culture can be compensated either by MEF-conditioned medium (CM), commercially available feeder-independent medium or a combination of both.

To compare the efficiencies of different hiPSC culture methods, hiPSC (A4) (Wang and Adjaye 2011) cultures were established both under feeder-dependent conditions using SNL feeder cells and hESC medium (also referred to as unconditioned medium, UM), as well as under feeder-free conditions using the commercially available Matrigel (BDBioscience, Heidelberg, Germany) and feeder-independent medium mTeSR1 (Stemcell Technologies, Cologne, Germany) rather alone or in combination with CM.

hiPSCs were cultured under these conditions in parallel for several months. The direct morphological comparison by phase-contrast microscopy revealed that hiPSC colonies exhibited defined colony edges either cultured on SNL feeder cells or cultured on Matrigel (Fig. 3.2 A-B). However, a closer look at the cell morphology demonstrated a more regular and defined cell shape for the hiPSCs cultured on Matrigel under feeder-free conditions (Fig. 3.2 C-D). Whereas the hiPSCs showed a more undefined cell structure if cultured on feeder cells (Fig. 3.2 C), hiPSCs cultured on Matrigel exhibited a small and round cell shape with a big nucleus and a high nucleus-to-cytoplasm ratio (Fig. 3.2 D) as described for undifferentiated hiPSCs in the literature (Courtot et al. 2014). Another advantage of feeder-free hiPSC culture was the easier handling and the saving of time: Culture dishes were covered with Matrigel at least 1 h before usage whereas SNL feeder cells had to be thawed on gelatin-coated culture dishes first, the whole process taking about more than one day before hiPSCs could be seeded (see 2.2.1.5). Furthermore, the passaging rhythm of hiPSCs was more flexible on Matrigel-coated culture dishes compared to feeder-dependent conditions. Even though mitotically inactivated feeder cells are still viable they only survive for approximately 7 days. If hiPSCs need to be maintained for longer time periods on the same culture dish new feeder cells were needed to guarantee sufficient culture conditions. In contrast, there was no observed impairment of Matrigel quality depending on the culture time period.

Concerning the comparison between hiPSCs cultured either only with mTeSR1 medium or with a combination of CM and mTeSR1 no striking differences were observed in the morphology of hiPSC colonies (Fig. 3.2 E-F).

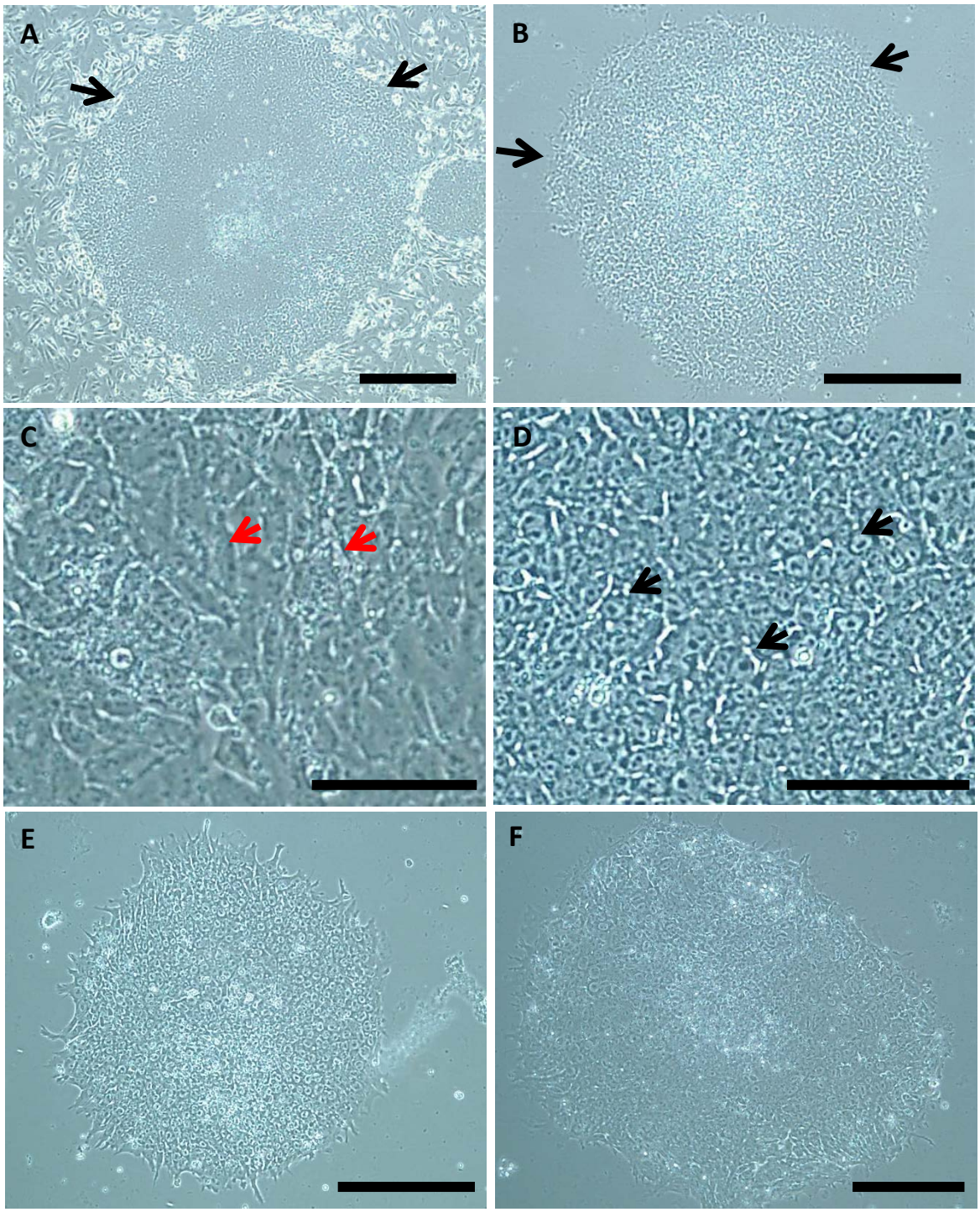

Figure 3.2: Morphological comparison of hiPSCs cultured under different culture conditions. hiPSC colonies cultured either on feeder cells **(A)** or Matrigel **(B)** showed clear borders (black arrows). hiPSCs exhibited more undefined cell morphology (red arrows) if cultured on feeder cells **(C)** compared to small and round cells with high nucleus-to-cytoplasm ratio (black arrows) if cultured on Matrigel **(D)**. Newly passaged hiPSC colonies showed a similar morphology if cultured on Matrigel with mTeSR1 medium alone **(E)** or a combination of mTeSR1 and CM **(F)**. A, B, E, F) Scale bars = 500 µm; C, D) Scale bars = 100 µm.

3.1.3 Comparison of different passaging methods

Besides the careful choice for the most efficient cell culture conditions, passaging also represents one of the most critical points concerning the maintenance of pluripotent stem cells. hiPSCs are very sensitive to any treatment and need their cell-cell interactions to survive (Kurosawa 2012). Therefore, hiPSCs are often passaged as small colony pieces rather than as single cells (Beers et al. 2012). This passaging is either done mechanically using special material, e.g. small syringe needles, or enzymatically (Rajala et al. 2010, Zhang et al. 2010). For the passaging as colony pieces it is important to cut the colonies into almost equal pieces of suitable size. If the passaged colony pieces are too big cells will start to differentiate, on the other hand, in colony pieces that are too small cells might undergo apoptosis (Amit and Itskovitz-Eldor 2012). However, the exact size of passaged colony pieces is not clearly defined.

In this thesis, hiPSCs (A4) were mechanically passaged using two different tools. First, hiPSC colonies from the whole dish were passaged using a commercially available passaging tool called StemPro® EZPassage™ Disposable Stem Cell Passaging Tool (Thermo Fisher Scientific, USA) that cuts hiPSC colonies into equal quadrants (Fig. 3.3 A). Even though this passaging tool represents the easiest way to get equal colony pieces it turned out to result in a culture with a high number of differentiated cells. This might result from contaminations with already differentiated cells present in the dish which were also passaged to the new one. To obtain a more pure cell culture of undifferentiated hiPSCs and to reduce the costs, colonies with cells that showed the typical hiPSC morphology were first identified under the microscope, and then only these colonies were cut into pieces using a small syringe needle (Fig. 3.3 B). Although the colony pieces were not as equal and small as they were using the passaging tool, a high number of colonies with undifferentiated hiPSC morphology was observed after passaging.

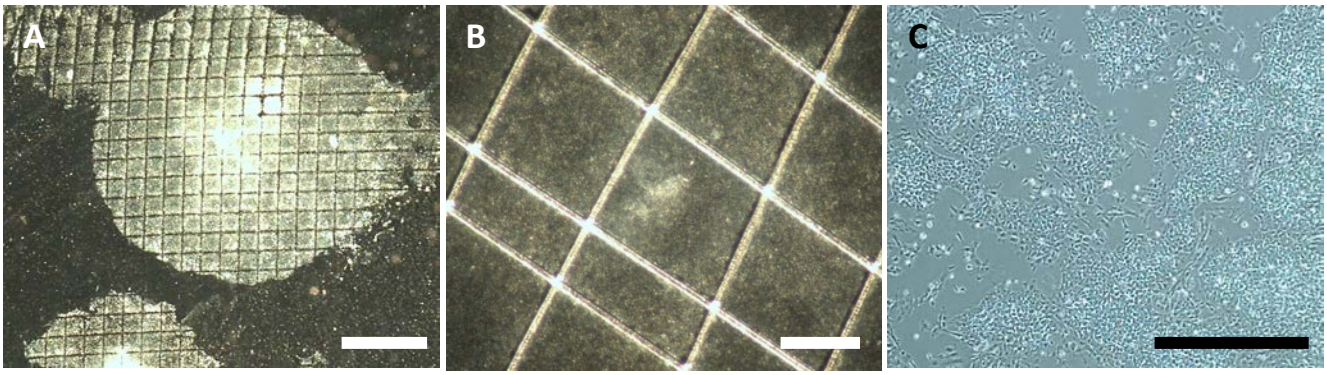

Figure 3.3: **Comparison of different passaging methods.** hiPSCs were mechanically passaged either **A)** with the StemPro® EZPassage™ Disposable Stem Cell Passaging Tool; Scale bar = 500 µm or **B)** a small syringe needle; Scale bar = 100 µm. **C**) hiPSCs are shown 3 days after single cell splitting using Accutase. Scale bar = 500 µm.

Another passaging method that further facilitates hiPSC handling under feeder-free conditions is to singularize hiPSC colonies with the aim to receive a single cell culture of pluripotent stem cells (Fig. 3.3 C). To prevent cells from undergoing apoptosis in single cell culture, hiPSCs were treated with the Rho-associated coiled coil forming protein serine/threonine kinase (ROCK) inhibitor Y-27632 for at least 1 h before and for 24 h after passaging (Watanabe et al. 2007). In contrast to hiPSCs cultured as colonies, single cells can be analyzed via flow cytometry to evaluate the quality of the running hiPSC culture. Another advantage of this method is that single cells are easier to expand than colonies and that they give the possibility to use a specific cell number of pluripotent cells for further experiments.

After comparison of the different culture and passaging methods, the decision was made for feeder-free culturing of hiPSCs with mechanical passaging. Although the single-cell splitting technique was also successfully performed, due to the higher costs of the ROCK inhibitor this technique was only used if necessary, e.g. for flow cytometry analyses of hiPSCs (see below).

3.1.4 Pluripotency characterization of hiPSCs cultured with feeder cells or under feeder-free conditions

hiPSCs are derived from somatic cells and have to undergo several steps to become fully reprogrammed (Li and Wang 2013). As pluripotent stem cells are defined by their potential to differentiate into any cell type of the three germ layers (endoderm, mesoderm, ectoderm) it is important to control and characterize hiPSCs regarding their pluripotency.

A widely-used pluripotency marker is alkaline phosphatase, a hydrolase enzyme. However, alkaline phosphatase is not a sufficient marker to detect fully reprogrammed stem cells (Nguyen et al. 2011, Tiscornia et al. 2011) and therefore, was not used in this study. More reliable pluripotency markers for hiPSCs are the cell surface antigens SSEA-4, TRA-1-60 and TRA-1-81 or the gene expression markers OCT4, SOX2 and NANOG (Gonzalez et al. 2011).

TRA-1-60 is rapidly down-regulated if pluripotent stem cells start to differentiate and is therefore a good indicator for the pluripotent potential of hiPSC cultures (Chan et al. 2009, Tanabe et al. 2013). To evaluate if hiPSCs (A4) expressed the pluripotency marker TRA-1-60, hiPSCs cultured under feeder-dependent and feeder-free conditions were fixed and stained using an anti-TRA-1-60 antibody. Both hiPSC cultures exhibited TRA-1-60 positive cells inside the colonies (Fig. 3.4 A-F). In contrast, feeder cells were not positive for TRA-1-60 indicating a specific staining for the antibody (Fig. 3.4 D-F).

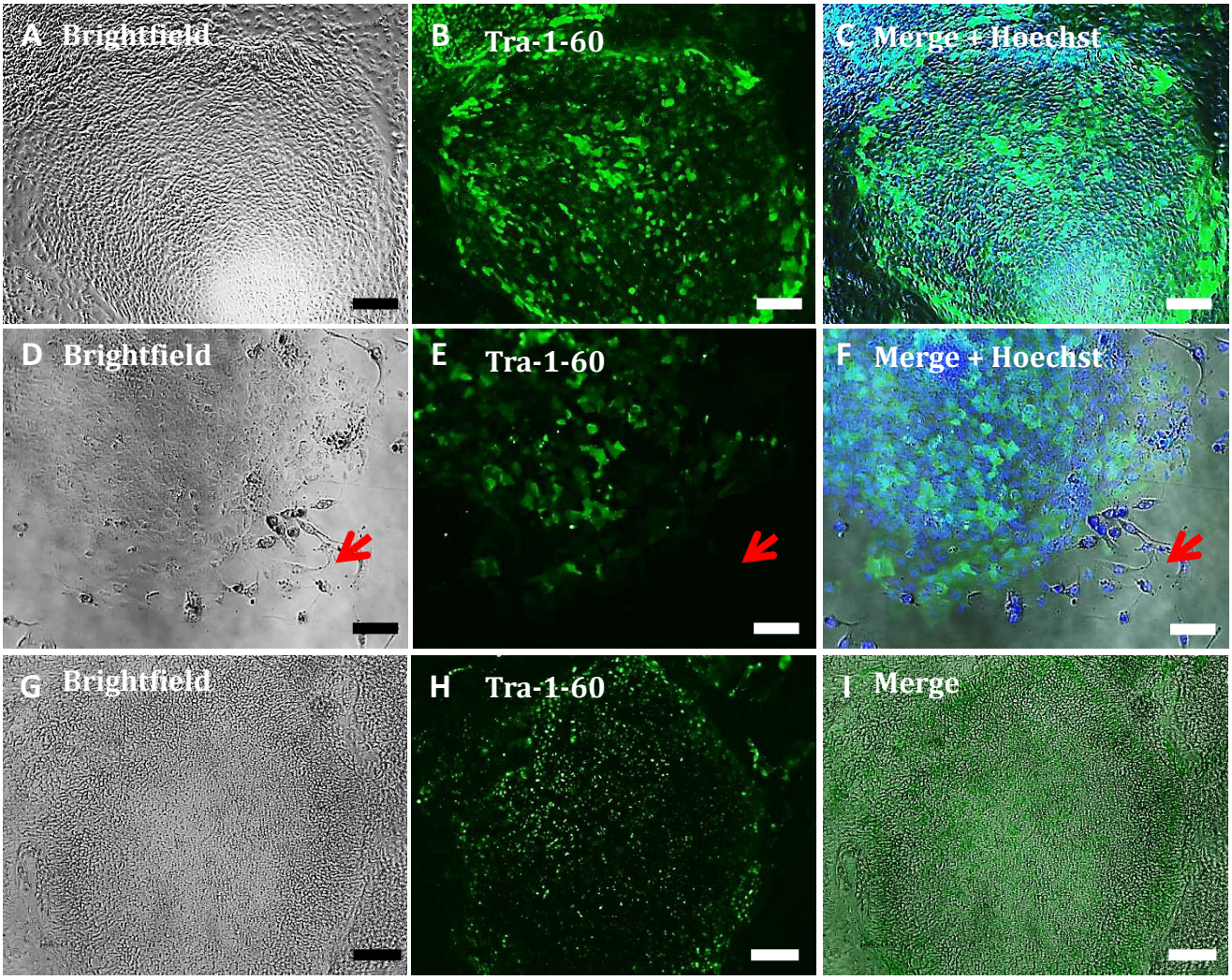

Figure 3.4: Tra-1-60 staining of hiPSCs. hiPSC colonies cultured under feeder-free **(A-C)** or feeder-dependent **(D-F)** conditions were fixed and stained for Tra-1-60 (green) and nuclei were stained with Hoechst (blue). Whereas hiPSC colonies show Tra-1-60 staining, feeder cells are negative for Tra-1-60 (red arrows, **D-F**). Living hiPSCs cultured under feeder-free conditions **(G-I)** were stained for Tra-1-60 (green). Scale bars= 100 µm.

TRA-1-60 can also be stained in living cells making it possible to detect viable pluripotent cells in the running cell culture. To test if pluripotent stem cells can be detected by live staining hiPSCs (A4) were only stained with anti-TRA-1-60 in mTeSR1 medium for 1 h (see 2.2.4). Subsequently, the second antibody was used for 30 min in fresh mTeSR1 medium. Living hiPSCs also exhibited TRA-1-60 staining (Fig. 3.4 G-I) that rapidly disappeared during continuous culture time and did not seem to influence the viability of hiPSCs, making it a valid tool to control for pluripotency in the running culture.

Additionally, TRA-1-60-staining of hiPSCs cultured either as colonies or as single cells revealed that both cultures contained TRA-1-60 positive cells (Fig. 3.5).

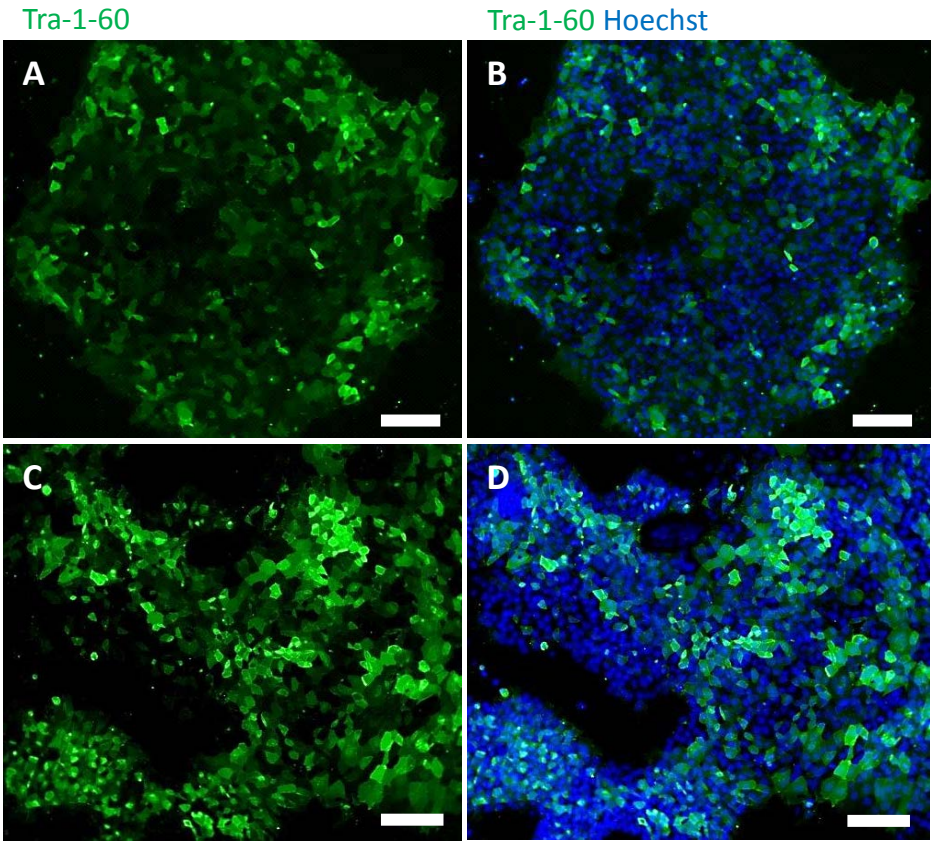

Figure 3.5: Tra-1-60 staining of hiPSCs passaged as colonies and single cells. hiPSCs passaged either as colonies **(A-B)** or as single cells **(C-D)** were stained for Tra-1-60 (green). Nuclei were stained with Hoechst (blue). Scale bars = 100 µm.

These results indicate that hiPSCs either cultured under feeder-dependent or feeder-free conditions as well as either passaged as colonies or single cells express the pluripotency marker TRA-1-60. Nevertheless, to choose suitable cell culture conditions to preserve the pluripotent character for a long time in culture but at the same time keep the expenditure of time within a limit, hiPSCs in this thesis were all cultured with pure mTeSR1 medium on Matrigel.

To get a more quantitative analysis of the distribution of pluripotency markers expressed in hiPSCs, cells were co-stained for TRA-1-60 and SSEA-4 and analyzed via fluorescent activated cell sorting (FACS). Fig. 3.6 represents two different FACS analyses of the two different hiPSC lines A4 (Wang and Adjaye 2011) and CRL2097 (Kristensen et al. 2013) cultured under feeder-free conditions. Due to the highly dynamic character of hiPSCs it is difficult to define a standard value for TRA-1-60$^+$ or SSEA-4$^+$ cells. However, the analyzed hiPSC populations consisted of 76.55% (A4) and 59.51% (CRL2097) TRA-1-60$^+$/SSEA-4$^+$ cells and 95.48% (A4) and 89.04% (CRL2097) SSEA-4$^+$ cells. These data indicate that the distribution of cells expressing pluripotency markers is highly variable due to the tendency of spontaneous differentiation and therefore, hiPSC cultures should be analyzed on a regular basis.

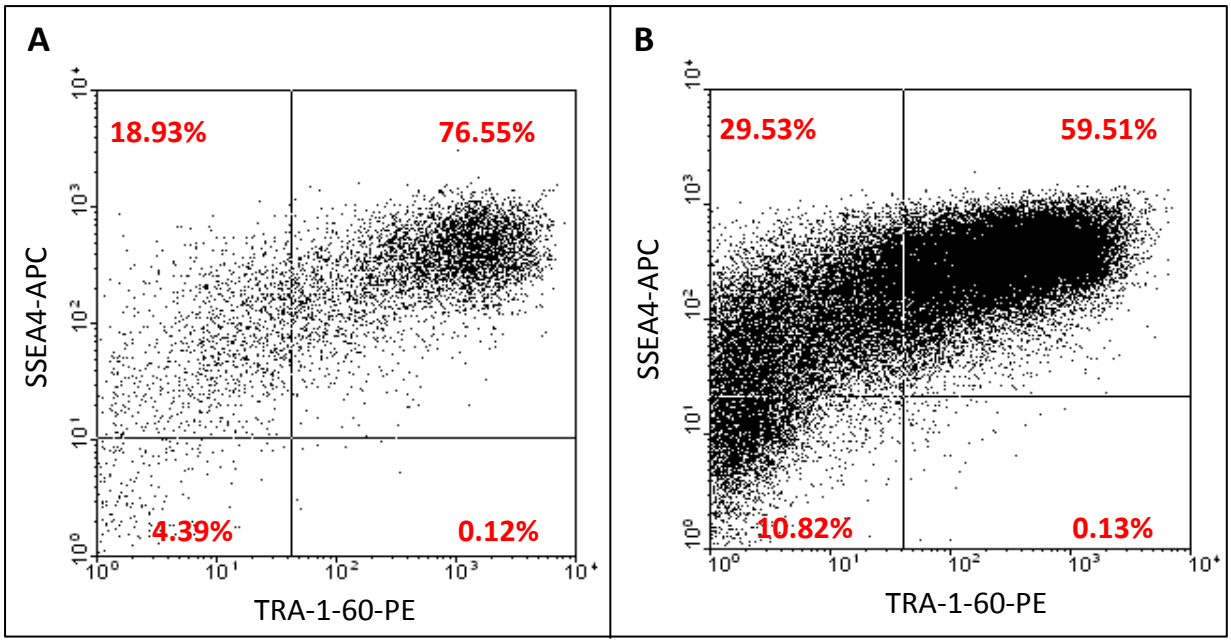

Figure 3.6: Flow cytometry analysis of hiPSCs. Two hiPSC lines A4 **(A)** and CRL2097 **(B)** cultured under feeder-free conditions were stained for TRA-1-60-PE and SSEA-4-APC and analyzed via fluorescent activated cell sorting (FACS).

Another method to demonstrate hiPSC pluripotency is the spontaneous differentiation of so-called hiPSC-derived EBs into cells of the three different germ layers (Itskovitz-Eldor et al. 2000). Thus, EBs were generated from hiPSCs grown as colonies under feeder-free conditions by using the hanging-drop method (Wang and Yang 2008). EBs were differentiated for either 8 or 26 days. Therefore, hiPSCs were resuspended in UM without basic fibroblast growth factor (bFGF) and 20 µL drops (4 x 10^4 cells per drop) were pipetted at the lid of a 10 cm culture dish. After 3 days, drops containing the EBs were rinsed using a 5 mL pipette and were cultured in UM without bFGF in 0.1% gelatin-coated 24-well plates for either 5 (in total 8 days for RNA isolation) or 23 (in total 26 days for morphological analyses) additional days.

RNA was isolated from undifferentiated hiPSCs and from 8 days old EBs and the expression levels of pluripotent stem cell markers (*OCT4*, *NANOG* and *SOX2*) and early markers for endodermal (*alpha-fetoprotein*, *AFP*), mesodermal (*Msh homeobox 1*, *MSX1*) and ectodermal (*microtubule-associated protein 2*, *MAP2* and *paired-box protein 6*, *PAX6*) cell lineages were analyzed using qRT-PCR (Takahashi et al. 2007). Whereas the pluripotency markers *OCT4*, *NANOG* and *SOX2* were downregulated during the undirected differentiation process resulting in EBs, the endodermal marker *AFP*, the mesodermal marker *MSX1* and the ectodermal markers *MAP2* and *Pax6* were all upregulated after spontaneous differentiation (Fig. 3.7).

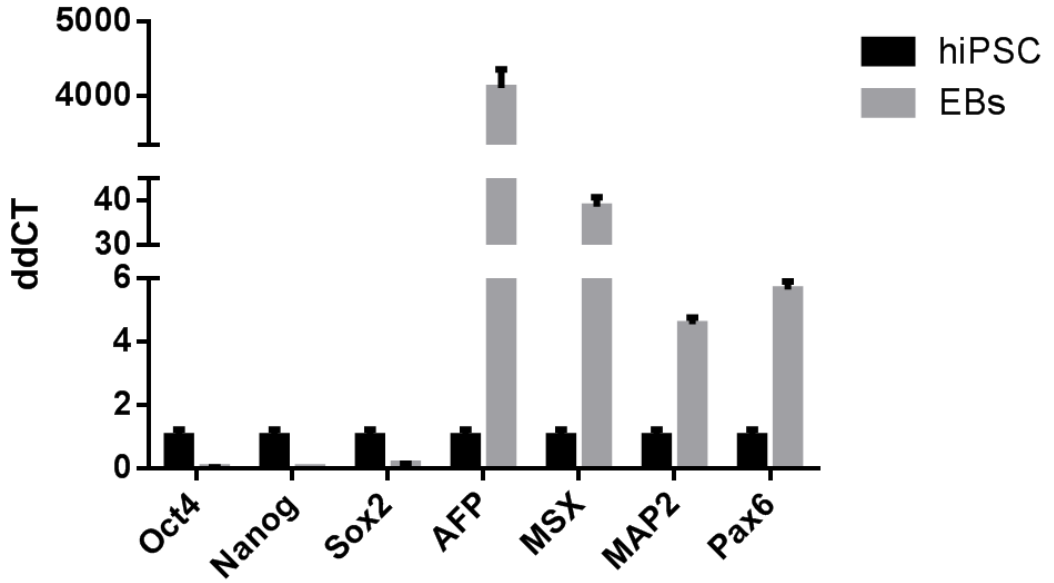

Figure 3.7: qRT-PCR analysis of hiPSC and hiPSC-derived Embryoid bodies (EBs). EBs were cultured for 8 days and compared to undifferentiated hiPSCs. Values are presented as mean +/- standard error of mean (SEM), n = 1.

In addition, EBs differentiated for 26 days resulted in cells with different morphologies, including fibroblast- or neural-like cells (Fig. 3.8). EBs were also able to differentiate into beating cardiomyocytes showing their potential to spontaneously differentiate into mesodermal tissue (Fig. 3.8 C).

These results indicate that hiPSCs cultured under feeder-free conditions are able to spontaneously differentiate into cell types from endodermal, mesodermal and ectodermal origin.

3.1.5 Cytogenetic analysis of hiPSCs

Genomic instability and chromosomal abnormality are serious problems for long-term culture of pluripotent stem cells (Maitra et al. 2005, Ludwig et al. 2006, Catalina et al. 2007) due to their high proliferative potential. To guarantee a physiological hiPSC culture, cells have to be tested for chromosomal aberrations on a regular basis. Therefore, two different passages, an earlier (P47) and a later (P74) passage number of the hiPSC line A4 were analyzed (Fig. 3.9). The karyotype analysis revealed no structural or numerical abnormalities in chromosomes for both passages. Cytogenetic analyses were performed by the Institute of human genetics and anthropology at the Heinrich-Heine University Düsseldorf.

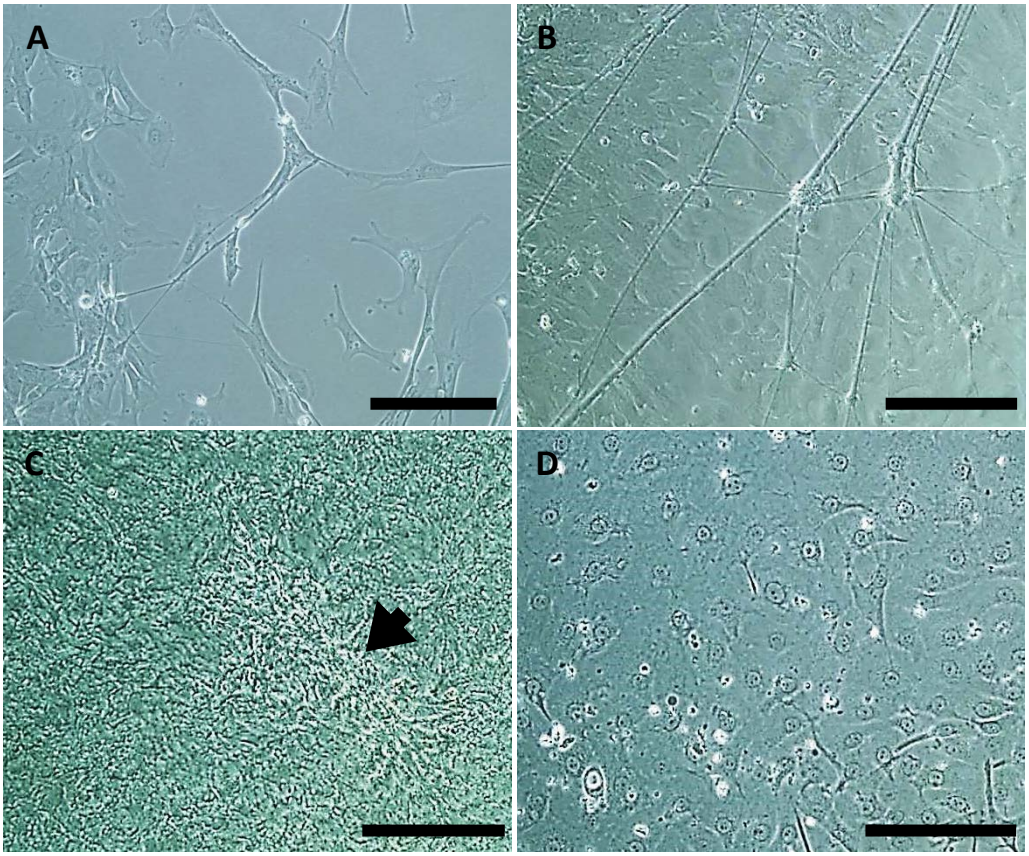

Figure 3.8: Representative pictures of embryoid bodies (EBs) derived from hiPSCs. After 26 days EBs showed diverse cell morphologies, like fibrblast-like (A), neuronal-like (B) and chondrocyte-like (D) morphology, as well as beating cardiomyocytes (C, black arrow). Scale bars = 100 µm.

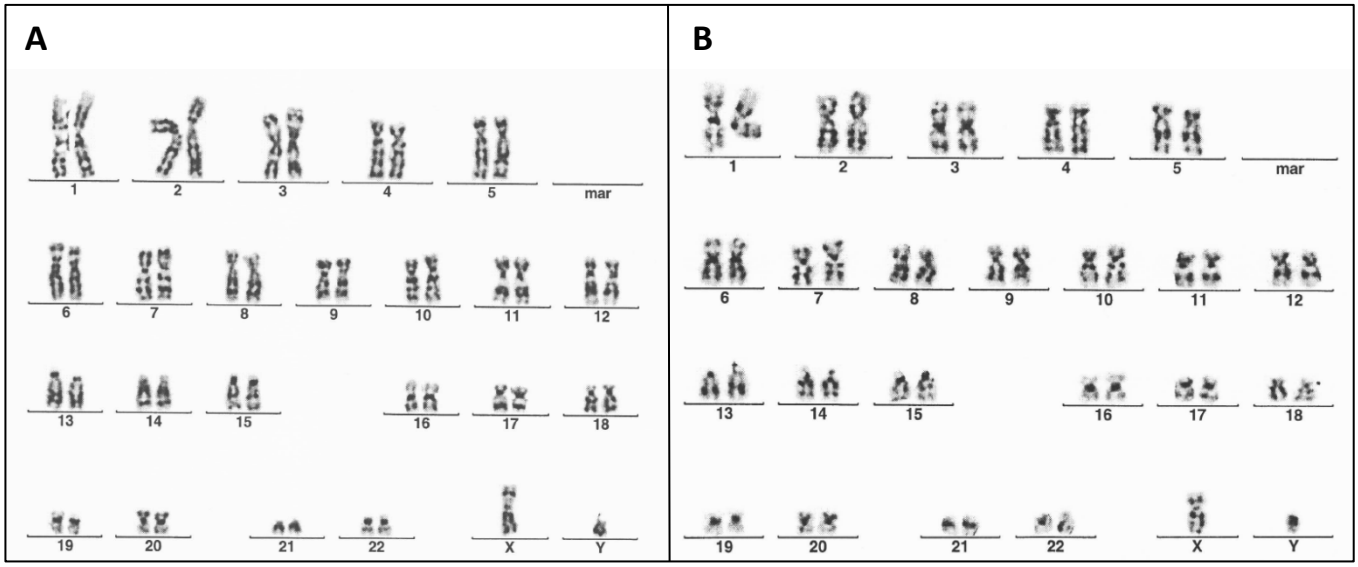

Figure 3.9: Karyotype analysis. Two different passage numbers (P), early (P47) **(A)** and late (P74) **(B)**, of hiPSC line A4 were analyzed for chromosomal aberrations. Karyotype analysis revealed no structural or numerical abnormalities. (In cooperation with the Institute for Human Genetics and Anthropology of the Heinrich-Heine University Düsseldorf)

3.2 Establishment of a hiPSC-derived neurosphere culture

Human neural progenitor cells (hNPCs) cultured as three-dimensional (3D) free-floating neurospheres represent a good model to study human neurodevelopmental processes *in vitro* (Moors et al. 2009, Lai et al. 2011, Alepee et al. 2014). Primary hNPCs can be directly obtained from embryonic or fetal neuronal tissue. However, these sources are rather restricted and bear ethical problems (Dunnett and Rosser 2014). Substituting human material with animal tissue, on the other hand, might lead to differences in study results due to species differences (Uhl and Warner 2015). To overcome the ethical concerns but still use human cells for mimicking physiological processes of neurodevelopment, one goal of this thesis was to establish a neurosphere culture derived from hiPSCs. To evaluate possible differences between the hiPSC-derived neurospheres and primary human neurospheres both cultures were compared with each other concerning their expression pattern of different markers and their functional performance regarding different processes of neurodevelopment: NPC proliferation, migration and differentiation.

3.2.1 Establishment of two different neural induction protocols to differentiate hiPSCs into neurospheres

Since Yamanaka and Takahashi reported the possibility to reprogram somatic cells backwards into a pluripotent state mimicking an ESC-like character (Takahashi and Yamanaka 2006, Takahashi et al. 2007) the interest of hiPSCs and their usage for various applications has been continuously increasing, especially for the investigation of neuronal diseases. Thus, the publication list of possible ways to differentiate iPSCs into NPCs quickly reached an enormous level. If induced via SMAD inhibition (Du et al. 2012, Shofuda et al. 2013) or rather via spontaneous differentiation using a neural-supporting medium (Brennand et al. 2011, Lancaster et al. 2013, Hibaoui et al. 2014), if differentiated as two-dimensional (2D) layer to support equal distribution of substances (Shi et al. 2012, Espuny-Camacho et al. 2013, Hick et al. 2013) or rather as 3D EBs to create a more physiological environment with strong cell-cell contact (Karumbayaram et al. 2009, Uemura et al. 2012, Mohamad et al. 2013) – studies are numerous posing an effort to determine the most efficient protocol. Without comparison of hiPSC-derived NPCs to primary hNPCs one does not know if a protocol produces cells that resemble the characteristics of primary cells. Therefore, in this thesis, hiPSC-derived NPCs were compared with an already established primary hNPC culture (Fig. 3.10 A) to better predict the relevance of the hiPSC-based neural culture.

Two different neural induction protocols based on two different differentiation strategies were compared with each other. For the first protocol hiPSCs were treated with 500 ng/mL noggin

(referred to as Noggin protocol; Fig. 3.10 B) which is known to play a crucial role in neurodevelopment due to the inhibition of bone morphogenic proteins (BMPs) (Lamb et al. 1993, Moreau and Leclerc 2004). The second protocol was based on a 'neural-supporting' serum-free neural induction medium (referred to as NIM protocol; Fig. 3.10 C) containing B27 and N2 supplements without additional SMAD inhibitors. Both protocols were tested for the hiPSC lines A4 (Wang and Adjaye 2011) and CRL2097 (Kristensen et al. 2013) and resulted in free-floating aggregates with spheroid morphology comparable to primary fetal human neurospheres (Lonza Verviers SPRL, Belgium; Fig. 3.10, right).

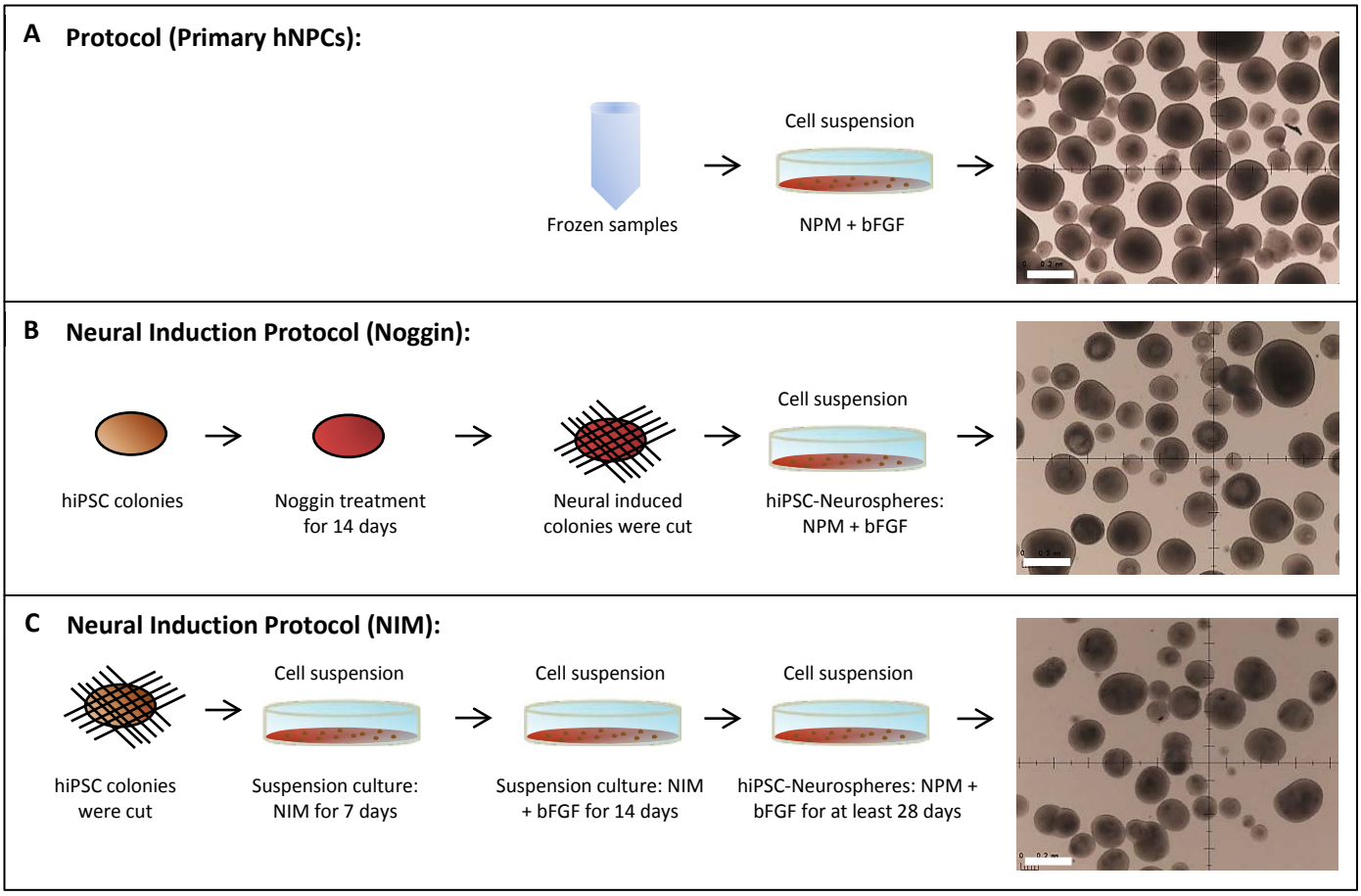

Fig. 3.10: Neural Induction Protocols. hiPSCs were differentiated into neurospheres resembling primary human fetal neurospheres **(A)** using two different protocols. **B)** For the Noggin protocol hiPSCs were treated with 500 ng/mL noggin for 14 days. Afterwards they were cut into pieces and cultured as cell suspension culture in neural proliferation medium (NPM) containing basic fibroblast growth factor (bFGF). **C)** For the NIM protocol hiPSCs were cut into pieces and directly cultured as suspension culture in neural induction medium (NIM). After 7 days, bFGF was added to the culture for an additional 14 days. Finally hiPSC-derived neurospheres were cultured in NPM containing bFGF for at least 28 days. Scale bars = 500 µm.

3.2.2 Comparative analyses of the gene expression pattern of hiPSC-derived neurospheres with primary human neurospheres

To ensure that the neurospheres obtained from both protocols consisted of NPCs, proliferating neurospheres were singularized and analyzed for their expression of the neural stem/progenitor cell markers Nestin and SOX2 using flow cytometry analyses (Fig. 3.11). Almost 100% of primary hNPCs were double-positive for both markers and the hiPSC-derived NPCs (hiPSC-NPCs) obtained with the different protocols (Noggin and NIM) also consisted of 92.97% (Noggin) and 84.91% of Nestin$^+$/SOX2$^+$ cells, respectively.

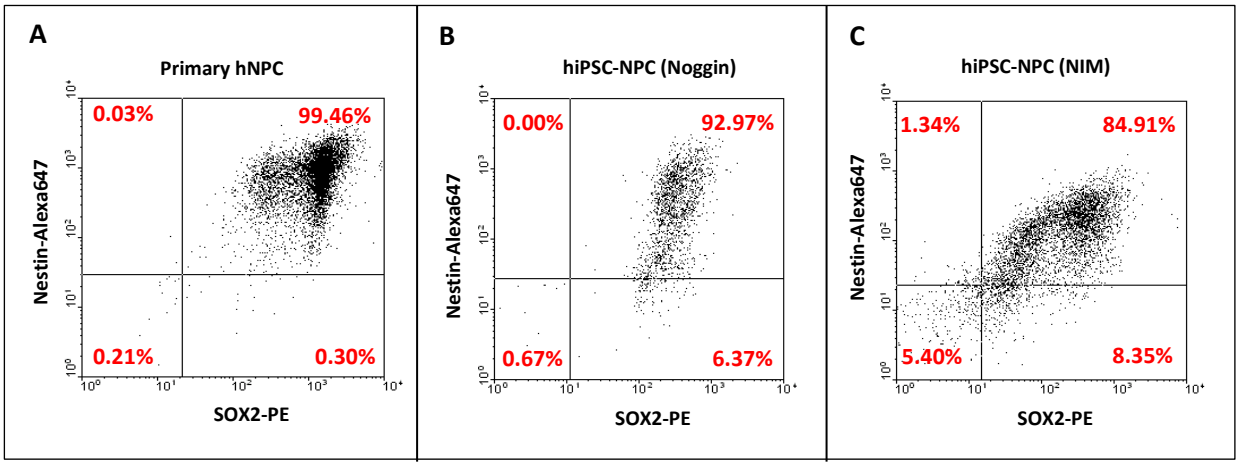

Fig. 3.11: FACS analysis of hiPSC-derived neural progenitor cells (NPCs). hiPSC-derived neurospheres consisting of NPCs from both protocols (Noggin, **B** and NIM, **C**) were analyzed for their expression of the neural stem/progenitor markers Nestin and SOX2 via FACS analysis and compared to primary human NPCs (**A**).

To further characterize the resulting proliferating hiPSC-NPCs and to compare them with the primary hNPCs their mRNA expression profile regarding pluripotency, neural/neuronal as well as glial markers was investigated using qRT-PCR analyses (Fig. 3.12). *OCT4*, *NANOG* and *SOX2*, which are known to be highly expressed in hiPSCs (Takahashi et al. 2007, Warren et al. 2010) were analyzed as pluripotency markers. This revealed that primary hNPCs expressed significantly less *OCT4* compared to undifferentiated hiPSCs (Fig. 3.12 A). hiPSC-NPCs from the NIM but not from the Noggin protocol expressed significantly higher levels of this pluripotency marker when compared to primary hNPCs yet 10-fold lower levels than the undifferentiated hiPSCs. *NANOG* expression was significantly down-regulated in both hiPSC-NPCs, even reaching expression levels similarly low to the one of primary hNPCs, which were at the detection limit (<0.0001/β-actin) and thus probably without any biological function (Fig. 3.12 A). In contrast expression of *SOX2*, which is expressed in both pluripotent stem cells and multipotent neural

stem cells (Breier et al. 2010, Zhang and Cui 2014), was not altered between undifferentiated hiPSCs and hiPSC-NPCs (Fig. 3.12 A). Primary hNPCs expressed significantly more *SOX2* compared to undifferentiated hiPSCs and hiPSC-NPCs, however, expression was in the same order of magnitude suggesting no biological relevance of this statistical significance.

For the characterization of proliferating hiPSC-derived or primary neurospheres regarding neural/neuronal markers, the expression of the NPC marker *Nestin* as well as at the early neuroectodermal marker *PAX6* and the neuronal marker *MAP2* was analyzed (Fig. 3.12 B). *Nestin* was only slightly expressed in undifferentiated hiPSCs but was 10-fold induced after neural induction in both hiPSC-NPCs reaching an expression level similar to the one of primary hNPCs. Furthermore, a similar expression pattern was detected for the neuroectodermal marker *PAX6*, which was not detectable in undifferentiated hiPSCs but upregulated in hiPSC-NPCs derived from both protocols comparable to the expression in primary hNPCs. *MAP2* expression was also not detectable in undifferentiated hiPSCs whereas it was slightly induced in both hiPSC-NPCs also reaching an expression level comparable to the one of primary hNPCs. These results indicate an analog state of maturity in hiPSC-NPCs and primary hNPCs regarding the expression of neural/neuronal markers.

The analysis of the expression profile of glial markers in the different analyzed cell types revealed that all analyzed markers (*glial fibrillary acidic protein* (*GFAP*), *platelet-derived growth factor receptor alpha* (*PDGFRα*) and *chrondritin sulfate proteoglycan 4* (*CSPG4*), also called *NG2*) were expressed at very low levels in general (<0.0001/β-actin, <0.01/β-actin, <0.0003/β-actin, respectively). However, markers for oligodendrocyte progenitor cells (OPCs), *PDGFRα* and *NG2*, were higher expressed in hiPSC-NPCs generated with both protocols compared to undifferentiated hiPSCs and reached an expression level similar to the one of primary hNPCs. Noteworthy, hiPSC-NPCs derived from the NIM protocol were statistically different from primary hNPCs, but as the overall expression of glial markers was extremely low this, again, will probably not be of biological relevance. Analysis of the astrocyte marker *GFAP* revealed a significantly higher expression in primary hNPCs, compared to undifferentiated hiPSCs, where it was not detectable. Both hiPSC-NPCs expressed extremely low and significantly less *GFAP* compared to primary hNPCs. These results suggest that hiPSC-NPCs of both protocols may represent a cell stage that correlates with the neuronal character of primary fetal hNPCs but differs with regard to glial marker expression, especially for the astrocyte marker *GFAP* (Fig. 3.12 C). It is of note, that these expression profiles were generated from proliferating neurospheres. Because these neural marker expression analyses do not reveal satisfying results in differentiating NPCs, differentiation stage has to be assessed by alternative methods.

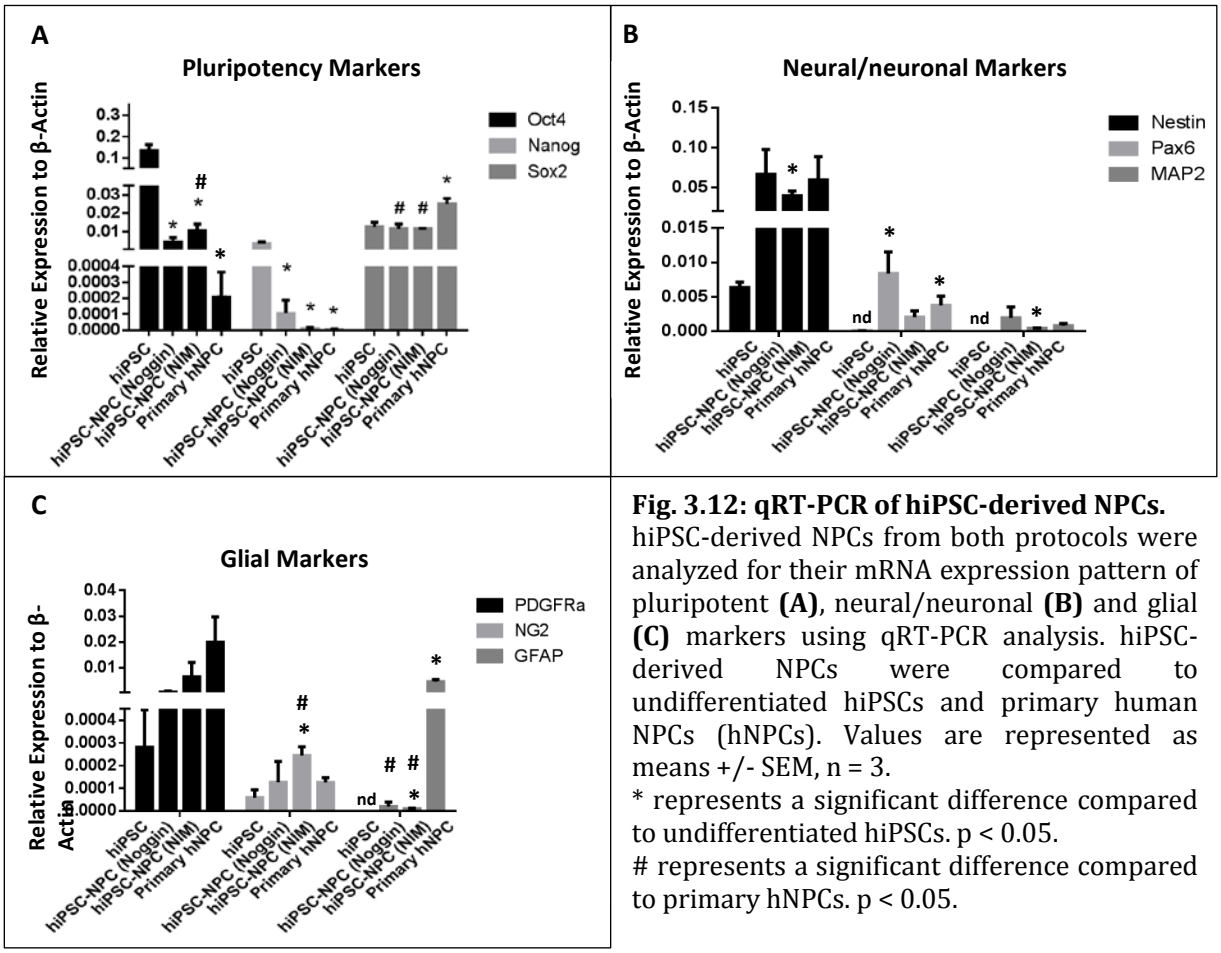

Fig. 3.12: qRT-PCR of hiPSC-derived NPCs. hiPSC-derived NPCs from both protocols were analyzed for their mRNA expression pattern of pluripotent **(A)**, neural/neuronal **(B)** and glial **(C)** markers using qRT-PCR analysis. hiPSC-derived NPCs were compared to undifferentiated hiPSCs and primary human NPCs (hNPCs). Values are represented as means +/- SEM, n = 3.
* represents a significant difference compared to undifferentiated hiPSCs. $p < 0.05$.
# represents a significant difference compared to primary hNPCs. $p < 0.05$.

3.2.3 Functional analyses of hiPSC-derived neurospheres compared to primary human neuropsheres using the Neurosphere assay

The Neurosphere assay represents a method to analyze the main neurodevelopmental processes proliferation, migration, and differentiation *in vitro* (Fig. 1.2 and 2.2.1.15). Moreover, the Neurosphere assay can also be used to study possible interferences of chemical compounds with these processes (Moors et al. 2007, Gassmann et al. 2010, Baumann et al. 2015). One of the goals of this thesis was to establish a corresponding neurosphere culture consisting of hiPSC-NPCs, as hiPSCs, due to their more or less inexhaustible proliferation capacity, bear an almost unlimited pool of material. Subsequently, the Neurosphere assay was performed for hiPSC-derived neurospheres in comparison to primary human neurospheres.

The standardized proliferation assay (Baumann et al. 2014)(2.2.1.15) was performed by selecting neurospheres from hiPSC-NPCs and primary hNPCs with a diameter of 300 µm. The cells were cultured in neural proliferation medium (NPM) containing epidermal growth factor (EGF) and bFGF or as a negative control in NPM without growth factors for 14 days. The

neurospheres of different origin were photographed every 3 to 4 days followed by measurement of the diameter (Fig. 3.13 A). The diameter of primary human neurospheres cultured with growth factors increased to approximately 750 µm after 14 days whereas the diameter of primary human neurospheres cultured without growth factors (negative control) did not change. The diameter of hiPSC-derived neurospheres (Noggin) increased only slightly over the 14 days from 300 to 400 µm and upon withdrawal of growth factors stayed stable at 300 µm. In contrast, hiPSC-derived neurospheres (NIM) reached a final diameter of around 850 µm after 14 days and even when cultured without growth factors, diameter increased to approximately 400 µm. Thus, proliferation behavior of hiPSC-derived neurospheres produced with the NIM protocol showed the highest similarity to primary hNPCs.

Another endpoint which can be assessed with the Neurosphere assay is cell migration (Moors et al. 2007). To evaluate if hiPSC-derived neurospheres cover a similar migration distance as primary human neurospheres, neurospheres of different origin were plated on a PDL/Laminin matrix in the presence of neural differentiation medium (NDM) for 3 days. As indicated by the representative images (Fig. 3.13 B) all neurospheres, either from primary human neurospheres or from hiPSC-derived neurospheres from both protocols, covered a similar migration distance of approximately 800 µm after 3 days in NDM.

Not only migration but also differentiation is essential to form the different brain regions during brain development and this endpoint is also addressed in the Neurosphere assay. To assess the neuronal differentiation potential of hiPSC-NPCs compared to primary hNPCs, neurospheres were again plated on a PDL/Laminin matrix in NDM. After seven days cells were fixed with 4% PFA and immunocytochemically stained for the neuronal marker βIII-Tubulin. This analysis revealed that all neurospheres were able to differentiate into βIII-Tubulin positive neurons, although they differed in their neuronal morphology (representative images shown in Fig. 3.13 C). Primary human neurospheres differentiated into βIII-Tubulin-positive neurons with short processes and only few branches (Harrill et al. 2011). Neurons differentiated from neurospheres obtained with the Noggin protocol displayed a very weak βIII-Tubulin staining indicative of a less mature differentiation stage in these cells. In contrast, neurons differentiated from hiPSC-derived neurospheres by using the NIM protocol exhibited βIII-Tubulin positive neurons with long, branched, overlapping neurites suggesting a more mature neuronal network.

The above results taken together indicate that the NIM protocol results in hiPSC-derived neurospheres that better resemble the gold standard of primary human neurospheres than neurospheres derived with the Noggin protocol. The neurospheres generated with this protocol not only proliferated faster but also seemed to form more sophisticated neuronal networks than

the ones generated with the Noggin protocol. Therefore, all following experiments were performed using hiPSC-derived neurospheres generated with the NIM protocol.

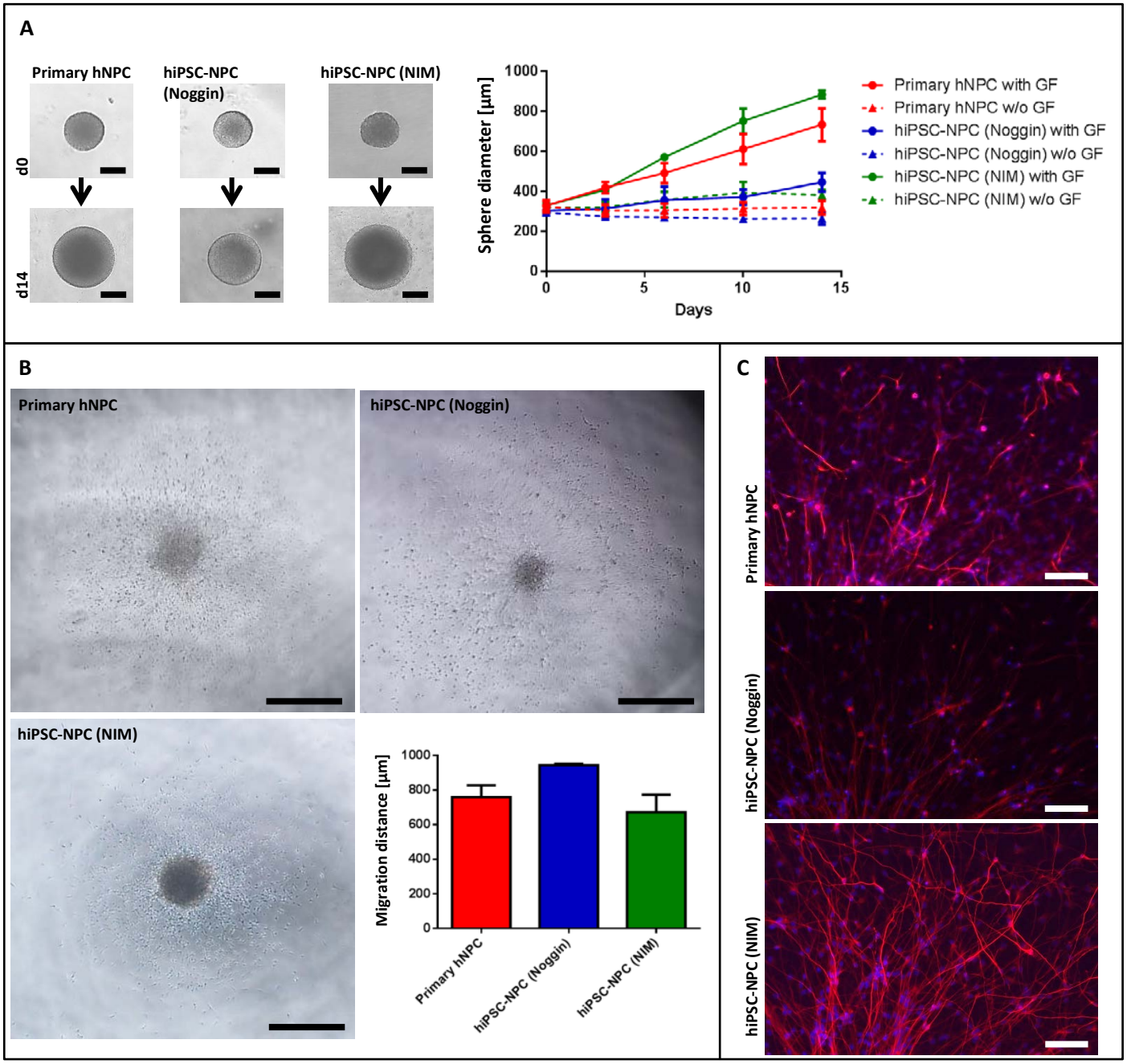

Fig. 3.13: Comparative analyses of hiPSC-derived neurospheres and primary human neurospheres using the Neurosphere Assay. A) Proliferation was measured for 14 days either in neural proliferation medium (NPM) containing growth factors (GF; continuous line) or without GF (dotted line). Values represent the mean +/- SD, n = 3. Scale bars = 200 µm. **B)** Migration distance was measured on Poly-D-Lysin (PDL)/Laminin coated plates for 3 days in neural differentiation medium (NDM). Values represent the mean +/- SEM, n = 3. Scale bars = 500 µm. **C)** Representative images of hiPSC-derived neurospheres. Neurospheres were cultured on PDL/Laminin coated plates in NDM for 7 days and stained for the neuronal marker βIII-Tubulin (red). Nuclei were stained with Hoechst (blue). Scale bars = 100 µm.

Even though the neuronal network of βIII-Tubulin positive neurons seemed more mature in hiPSC-derived neurospheres (NIM) compared to primary human neurospheres after 7 days (Fig. 3.13 C), qRT-PCR analyses revealed that differentiating primary human neurospheres expressed significantly more astrocyte markers, like *GFAP* and *aldehyde dehydrogenase 1 family member L1* (*ALDH1L1*) during a differentiation time of 14 days (Fig. 3.14 A+B). Additionally, differentiating primary human neurospheres expressed significantly more OPC marker *PDGFRα* compared to hiPSC-derived neurospheres (Fig. 3.14 C). All these markers were expressed at very low levels in hiPSC-derived neurospheres (<0.002-0.0005/β-actin) suggesting almost no differentiation of glia cells in these cultures at this time point. These results further support the hypothesis that hiPSC-derived neurospheres represent an earlier maturation stage compared to primary human neurospheres resembling the neuronal but not glial stage. For hiPSC-derived neurospheres expression of glial markers is slightly induced after 14 days, however, this increase is not significant and still in the same low order of magnitude. Later differentiation time points might be necessary to see a significant increase of glial markers in hiPSC-derived neurospheres.

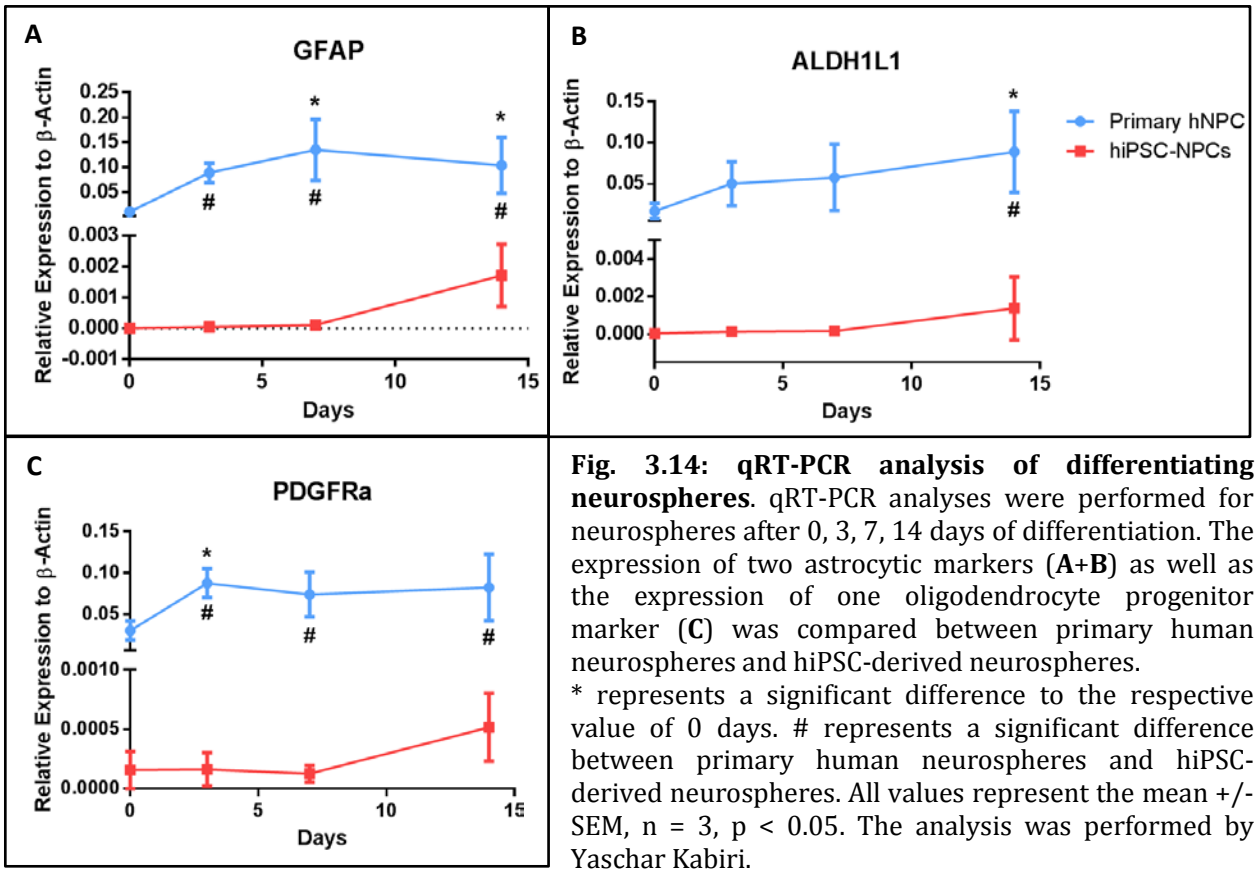

Fig. 3.14: qRT-PCR analysis of differentiating neurospheres. qRT-PCR analyses were performed for neurospheres after 0, 3, 7, 14 days of differentiation. The expression of two astrocytic markers (**A**+**B**) as well as the expression of one oligodendrocyte progenitor marker (**C**) was compared between primary human neurospheres and hiPSC-derived neurospheres.
* represents a significant difference to the respective value of 0 days. # represents a significant difference between primary human neurospheres and hiPSC-derived neurospheres. All values represent the mean +/- SEM, n = 3, $p < 0.05$. The analysis was performed by Yaschar Kabiri.

3.2.4 Comparative analyses of methylmercury toxicity in hiPSC-derived and primary human neurospheres

Another way of determining similarities or differences between *in vitro* systems is to compare their sensitivities towards toxins. The best-studied compound toxic to the developing nervous system is methylmercury (MeHgCl) (Clarkson 2002). MeHgCl reduces migration in developing human brains *in vivo* (Schettler 2001) possibly by interfering with SH-groups of proteins (Bal-Price et al. 2015b). Previous work of our group showed that MeHgCl also interferes with neural migration in the Neurosphere assay *in vitro* (Moors et al. 2007, Baumann et al. 2015). Therefore, this compound is well-suited to compare hiPSC-derived and primary human neurospheres with each other.

To analyze if hiPSC-derived neurospheres also respond with impairment of neural migration towards MeHgCl exposure, primary human and hiPSC-derived neurospheres were treated with different concentrations of MeHgCl (0 µM, 0.03 µM, 0.1 µM, 0.3 µM, 1 µM and 3 µM) for 24 h. Subsequently, migration distance and viability were measured (see 2.2.1.15 and 2.2.1.16).

Primary human neurospheres as well as hiPSC-derived neurospheres (A4 and CRL2097) exhibited a concentration-dependent decrease of migration distance and loss of viability after treatment with MeHgCl for 24 h (Fig. 3.15). However, in both cultures migration distance was more susceptible towards MeHgCl exposure than viability (Fig. 3.15 A+B). Whereas migration distance was significantly reduced to 70% and 60% of control conditions at a concentration of 0.3 µM MeHgCl in primary human and hiPSC-derived neurospheres, respectively, the minimal concentration with a significant decrease of viability was 1 µM for primary human neurospheres (60% of control conditions) and 3 µM for hiPSC-derived neurospheres (50% of control conditions; Fig. 3.15 A). Additionally, results are illustrated as sigmoidal dose-response curve fits to calculate the EC_{50} value and corresponding 95% confidence intervals of MeHgCl on migration and viability (Fig. 3.15 B; Tab. 3.1). The EC_{50} value is defined as the concentration associated with 50% response (Neubig et al. 2003). In this study, the calculated EC_{50} value for migration distance in hiPSC-derived neurospheres was 0.39 µM MeHgCl compared to the EC_{50} value of 0.77 µM in primary human neurospheres, which are both in the same order of magnitude (Tab. 3.1). In contrast, the calculated EC_{50} value for viability was the same for both (2.35 µM for primary human neurospheres and 2.74 µM for hiPSC-derived neurospheres; Tab. 3.1). Moreover, the effect of MeHgCl on migration seems to be specific for both, primary human and hiPSC-derived neurospheres, due to the non-overlapping 95% confidence intervals of migration and viability (Tab. 3.1). Even though hiPSC-derived neurospheres revealed a lower EC_{50} value for migration in response to MeHgCl treatment, neither migration nor viability decrease exhibited any significant difference between primary human and hiPSC-derived neurospheres (Fig. 3.15 C).

These data support the similarity of hiPSC-derived and primary human neurospheres here in response to a well-studied developmental neurotoxin. In addition, hiPSC-derived neurospheres might also be a valuable *in vitro* test system for DNT testing as there is no ethical concern for usage of such cells and the material is rather unlimited.

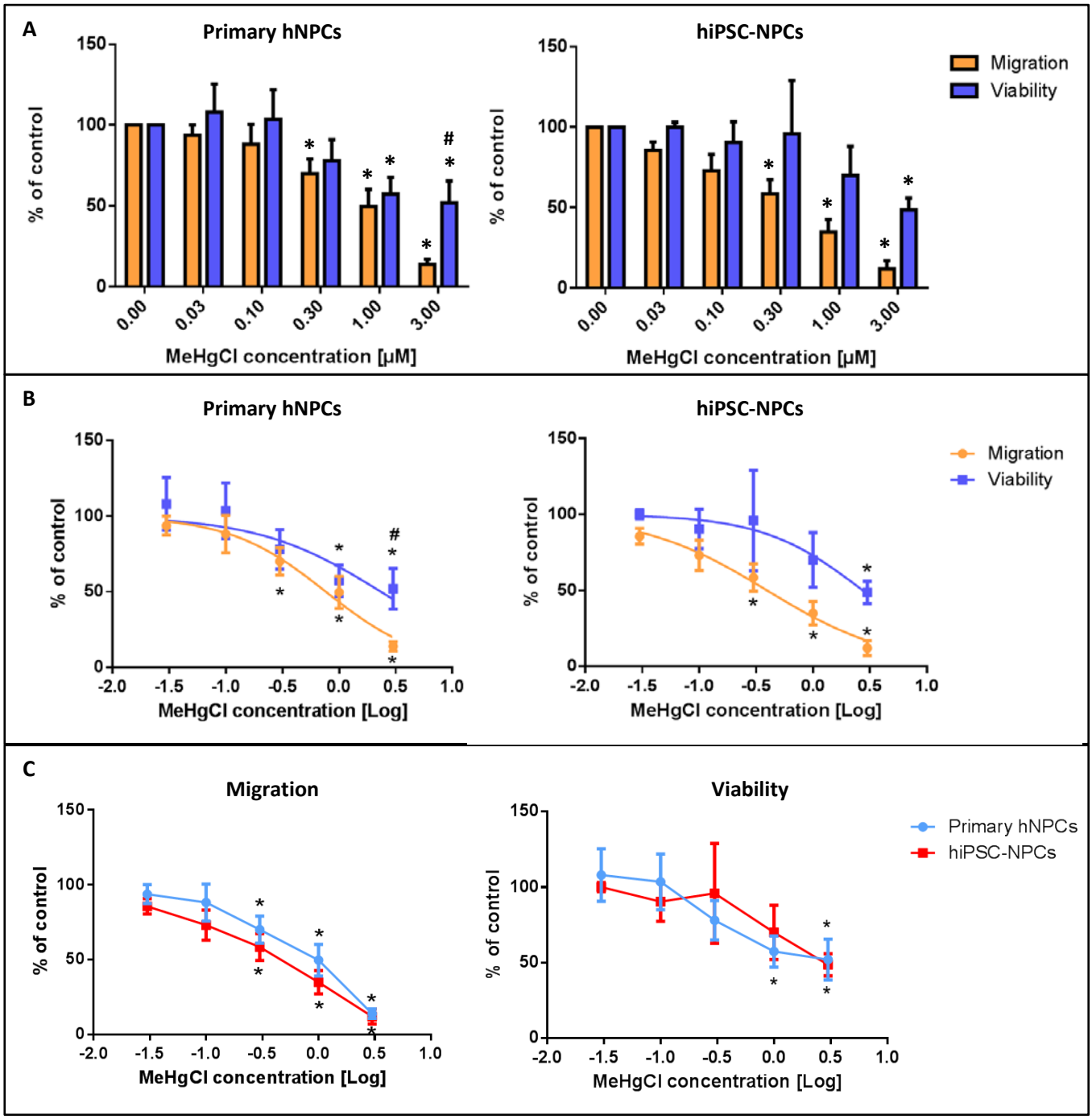

Fig. 3.15: Effect of MeHgCl on neurosphere migration and viability. Primary hNPCs and hiPSC-NPCs were treated with different concentrations of MeHgCl for 24 h and the effect on migration distance and viability was measured. **A)** The effect on migration and viablity was compared in either primary hNPCs (left graph) or hiPSC-NPCs (right graph). **B)** Data was presented as dose-response cruve fit. **C)** The effect of MeHgCl on migration (left graph) and viability (right graph) from A was compared between primary hNPCs and hiPSC-NPCs. * represents a significant difference compared to the respective control. # represents a significant difference between the two measured variables. All values represent the mean +/- SD, n = 3, $p < 0.05$.

Tab. 3.1: Calculated EC50 values for migration and viability.

EC50 Values	Primary hNPCs	hiPSC-NPCs
Migration	0.77 µM	0.39 µM
95% Confidence Interval (Migration)	0.59 - 0.99 µM	0.30 – 0.53 µM
Viability	2.35 µM	2.74 µM
95% Confidence Interval (Viability)	1.17 – 4.73 µM	1.29 – 5.81 µM

3.3 hiPSC-derived neurospheres as a model to study the human genetic disease Cockayne syndrome B

CS is a rare genetic disease which is caused by a deficiency in the NER (Jaspers 1996). The majority of the mutations which lead to CS are mutations in the *CSB* gene (Laugel 2013). Besides its role in the NER, CSB fulfills important functions in various other biological processes as transcription, chromatin maintenance and remodeling, and hypoxic response (Newman et al. 2006, Proietti-De-Santis et al. 2006, Filippi et al. 2008, Velez-Cruz and Egly 2013). Patients who suffer from CSB exhibit a photosensitivity, a progeroid phenotype as well as developmental and neurological defects (Nance and Berry 1992, Kamenisch and Berneburg 2009, Jeppesen et al. 2011). Especially the neurological defects are difficult to study, because the CSB mouse model shows a significantly milder brain phenotype compared to the CSB patients (van der Horst et al. 1997). To study the neurodevelopmental defects of CSB, in this thesis, hiPSCs obtained from CSB patients were differentiated into neurospheres using the NIM protocol and compared to control hiPSC-derived neurospheres as well as the primary hNPCs culture.

3.3.1 Characterization of CSB-deficient hiPSCs

In this thesis, two different CSB-deficient hiPSC lines (AS548 and AS789) were compared with two different control hiPSC lines (A4 and CRL2097) as well as with primary human neurospheres (individuals 692 and 988). The two CSB-deficient hiPSC lines used in this thesis, both carried different mutations in the *CSB* gene which led to different clinical classifications of the patients (Table 3.2). Whereas the AS548 hiPSC line was obtained from a patient who exhibited the classical CSB phenotype (CSB I, referred to as classic), the AS789 hiPSC line was obtained from a patient who exhibited the very severe form COFS (referred to as COFS). Both patients were characterized to have a congenital microcephaly and an extreme mental

retardation. However, the patient with the classical CSB phenotype (AS548) died with 6 years of age whereas the patient with COFS (AS789) died with only 10 months of age (for a more detailed clinical picture of the CSB patients see Tab. 2.8).

Tab. 3.2: hiPSC lines used in this thesis.

hiPSC line ID (provider)	Original Cell Type (provider)	Clinical classification	Mutated gene	Mutation type
A4 (wt) (Prof. Adjaye, University Düsseldorf, Germany)	Neonatal fibroblast (ATCC)	Healthy control	_	_
CRL2097 (wt) (Prof. Egly, IGBMC, Strasburg, France)	Neonatal fibroblast (ATCC)	Healthy control	_	_
AS548 (classic) (Prof. Egly, IGBMC, Strasburg, France)	Fibroblast from CSB patient CS548VI (Dr. Laugel, University of Strasburg, France)	CSB I	CSB	Deletion in genomic DNA, no detectable CSB protein (p.0)
AS789 (COFS) (Prof. Egly, IGBMC, Strasburg, France)	Fibroblast from CSB patient CS789VI (Dr. Laugel, University of Strasburg, France)	COFS (Cerebro-Oculo-Facio-Skeletal Syndrome)	CSB	Non-sense mutation, truncated CSB protein (pArg683x)

The classical CSB phenotype has been described to carry a large deletion in the promoter region of the *CSB* gene resulting in an undetectable *CSB* mRNA using PCR analysis (Fig. 3.16 A) and the total lack of a CSB protein (Laugel et al. 2008a). However, the exact location of the deletion in the classical CSB cells had not been investigated yet (Laugel et al. 2008a, Laugel et al. 2010). In contrast, the COFS phenotype was previously described to have a point mutation in exon 10 of the *CSB* gene, which causes a nonsense mutation and leads to an irregular stop codon and thus a predicted truncated CSB protein (Laugel et al. 2008b). Whereas the mRNA in the COFS hiPSC line was detected earlier, the presence of the predicted irregular truncated protein has not been identified yet (Laugel et al. 2008b, Laugel et al. 2010). PCR analyses in this thesis revealed a much lower amount of *CSB* mRNA in the COFS hiPSCs compared to the control hiPSCs (Fig. 3.16 A) indicating a possible degradation or impaired transcription of *CSB* mRNA in the COFS hiPSCs. Degradation or impaired transcription of *CSB* mRNA might explain why the predicted truncated protein has not been detected yet (Laugel et al. 2008b).

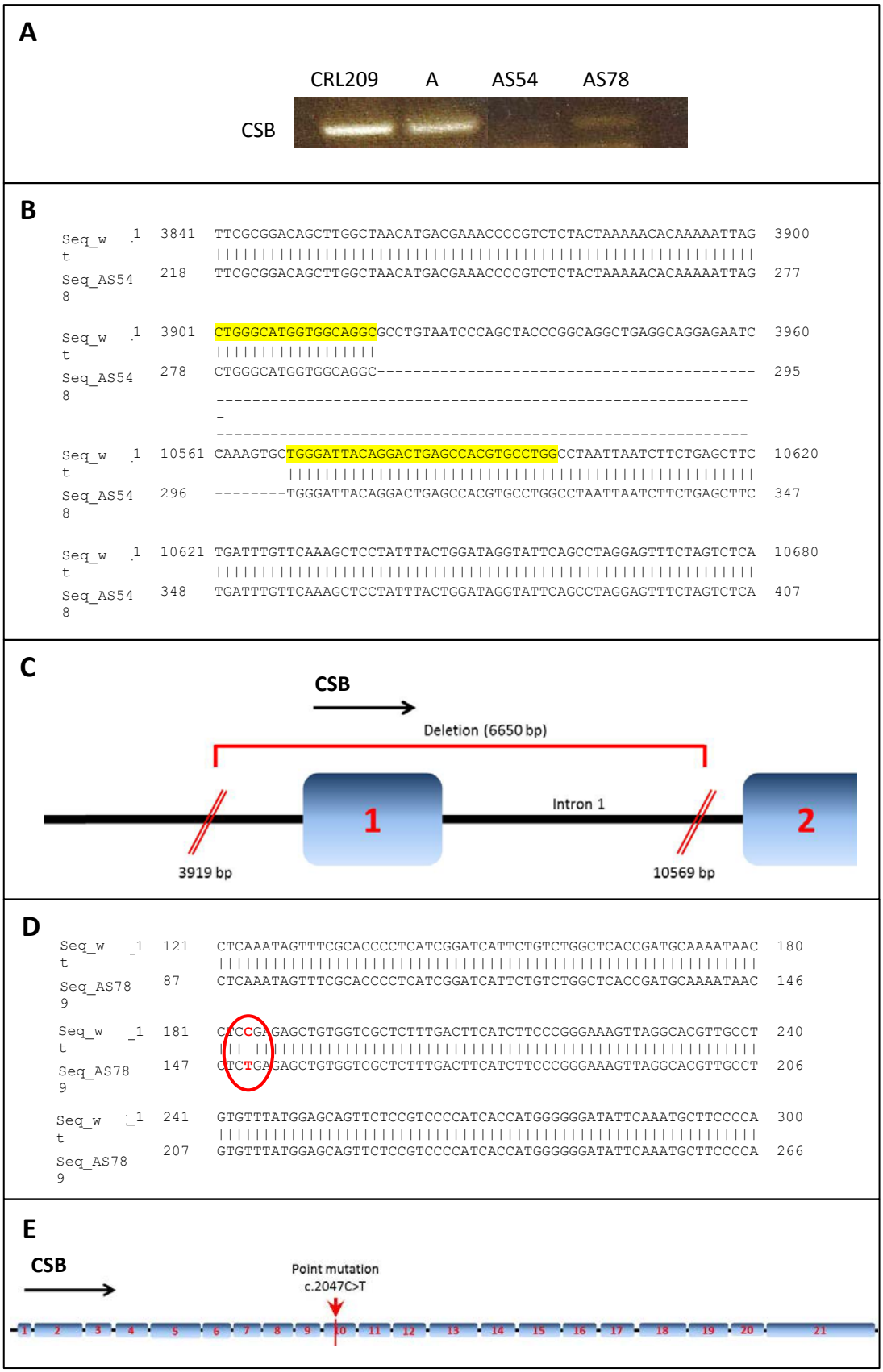

Fig. 3.16: Characterization of CSB-deficient hiPSC lines. A) Gelelectophoresis analysis of the expression of *CSB* mRNA. **B)** Sequencing analysis of classical CSB-deficient hiPSC line (AS548) compared to wild-type (wt) *CSB* DNA sequence. **C)** Illustration of the sequenced location for the DNA deletion in classical CSB-deficient hiPSCs. **D)** Sequencing analysis of COFS CSB-deficient hiPSC line (AS789) compared to wt *CSB* DNA sequence. **E)** Illustration of the location and kind of the point mutation in COFS CSB-deficient hiPSCs.

To verify that the cultivated CSB-deficient hiPSC lines used in this thesis really contain the mutations described in the literature and to identify the exact size and location of the deletion in the classical CSB-deficient hiPSC line, PCR products of the DNA regions containing the expected mutations were sequenced with the Sanger sequencing method (in cooperation with the BMFZ, Heinrich-Heine University, Düsseldorf) and compared to the wt DNA sequence of the *CSB* gene (taken from NCBI). The comparison of the sequenced PCR product of the classical CSB-deficient hiPSC line with the wt DNA sequence (accession number: NG_009442.1) revealed that the deletion started at 3919 bp and finished at 10569 bp of the *CSB* gene resulting in a deletion size of 6650 bp including the whole first exon of the *CSB* gene (Fig. 3.16 B+C). Specifically, the deletion starts 1156 bp in front of Exon 1 and finishes 554 bp in front of Exon 2. The sequencing of the PCR product of the COFS hiPSC line confirmed the C>T transition in exon 10 at position 2047 of the *CSB* gene (Fig. 3.16 D+E) (Laugel et al. 2008b, Laugel et al. 2010).

3.3.2 Comparison of CSB-deficient hiPSCs with control hiPSCs

Both CBS-deficient and both control hiPSC lines were cultured under feeder-free conditions using Matrigel and mTeSR1 medium. First differences between control and disease cultures were already observed during the culturing period. Whereas both control hiPSC lines had to be passaged every 5 to 10 days, the classical CSB-deficient hiPSC line proliferated faster compared to the control and had to be passaged every 4 to 7 days. In contrast, the COFS hiPSC line proliferated slower compared to the control and had to be passaged every 7 to 14 days. Furthermore, whereas both control hiPSC lines and the COFS hiPSC line exhibited the typical hiPSC morphology (Fig. 3.17 A, B, D), cells from the classical CSB-deficient hiPSC line exhibited a more diffuse morphology with a decreased nucleus-to-cytoplasm ratio (Fig. 3.17 C). Moreover, it is noteworthy that control hiPSCs were more prone to spontaneous differentiation compared to the COFS hiPSC lines presumably due to their higher proliferation rate. In contrast, spontaneously differentiated cells were not detected in the classical CSB-deficient hiPSC line due to their already diverse cell morphology.

To get a better picture of their pluripotent character, classical CSB-deficient hiPSCs and COFS hiPSCs were stained for TRA-1-60 and SSEA-4 and analyzed using FACS analysis (Fig. 3.18). The control hiPSCs A4 and CRL2097 consisted of 76.55% and 59.51% TRA-1-60$^+$/SSEA-4$^+$ and 95.48% and 89.04% SSEA-4$^+$ cells, respectively (Fig. 3.18 A+B). In contrast, classical CSB-deficient hiPSCs consisted of only 13.90% TRA-1-60$^+$/SSEA-4$^+$ but 98.63% SSEA-4$^+$ cells (Fig. 3.18 C). COFS hiPSCs were composed of 78.65% TRA-1-60$^+$/SSEA-4$^+$ cells and 95.4% SSEA-4$^+$ cells (Fig. 3.18 D). These analyses revealed that all hiPSC lines consisted of a comparable SSEA-4$^+$ cell population. However, whereas the majority of control and COFS hiPSCs are double positive for the pluripotency markers TRA-1-60 and SSEA-4, the classical CSB-deficient hiPSCs only

consisted of 13.90% TRA-1-60$^+$/SSEA-4$^+$ cells and revealed an altered morphology during cell culture. These analyses thus revealed not only a difference in cell morphology but also in their expression profile of pluripotent cell markers. However, the observation that the classical CSB-deficient hiPSCs did not lose their SSEA-4$^+$ character but consisted of only few TRA-1-60$^+$/SSEA-4$^+$ cells might indicate an impaired quality of pluripotent stem cells. It is noteworthy that this analysis was only performed once and further analyses are necessary to confirm a difference between hiPSC cultures.

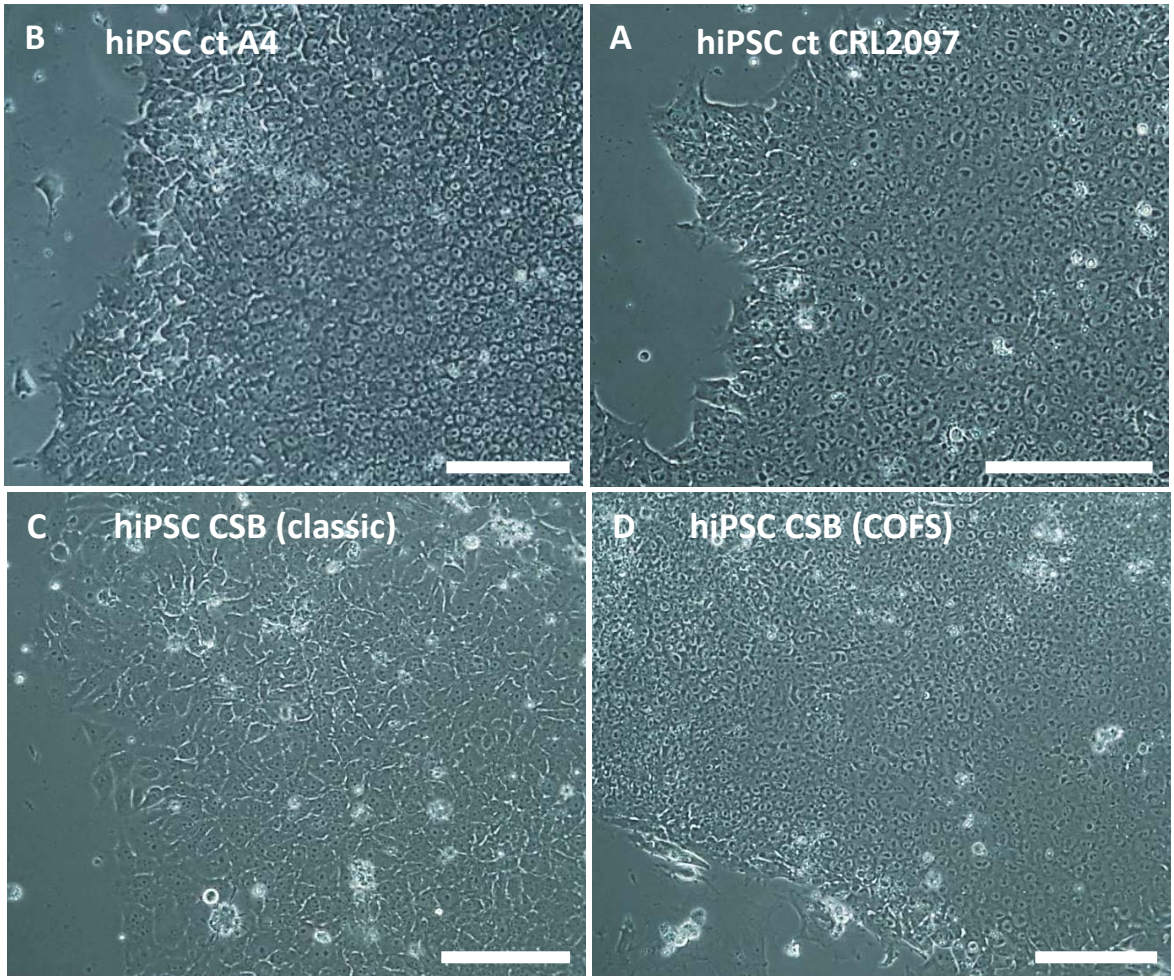

Fig. 3.17: Representative pictures of morphological comparison of hiPSC lines. Control (ct; **A-B**) and CSB-deficent hiPSC lines (**C-D**) were compared under the microscope with regard to their cell morphology. Scale bars = 100 µm.

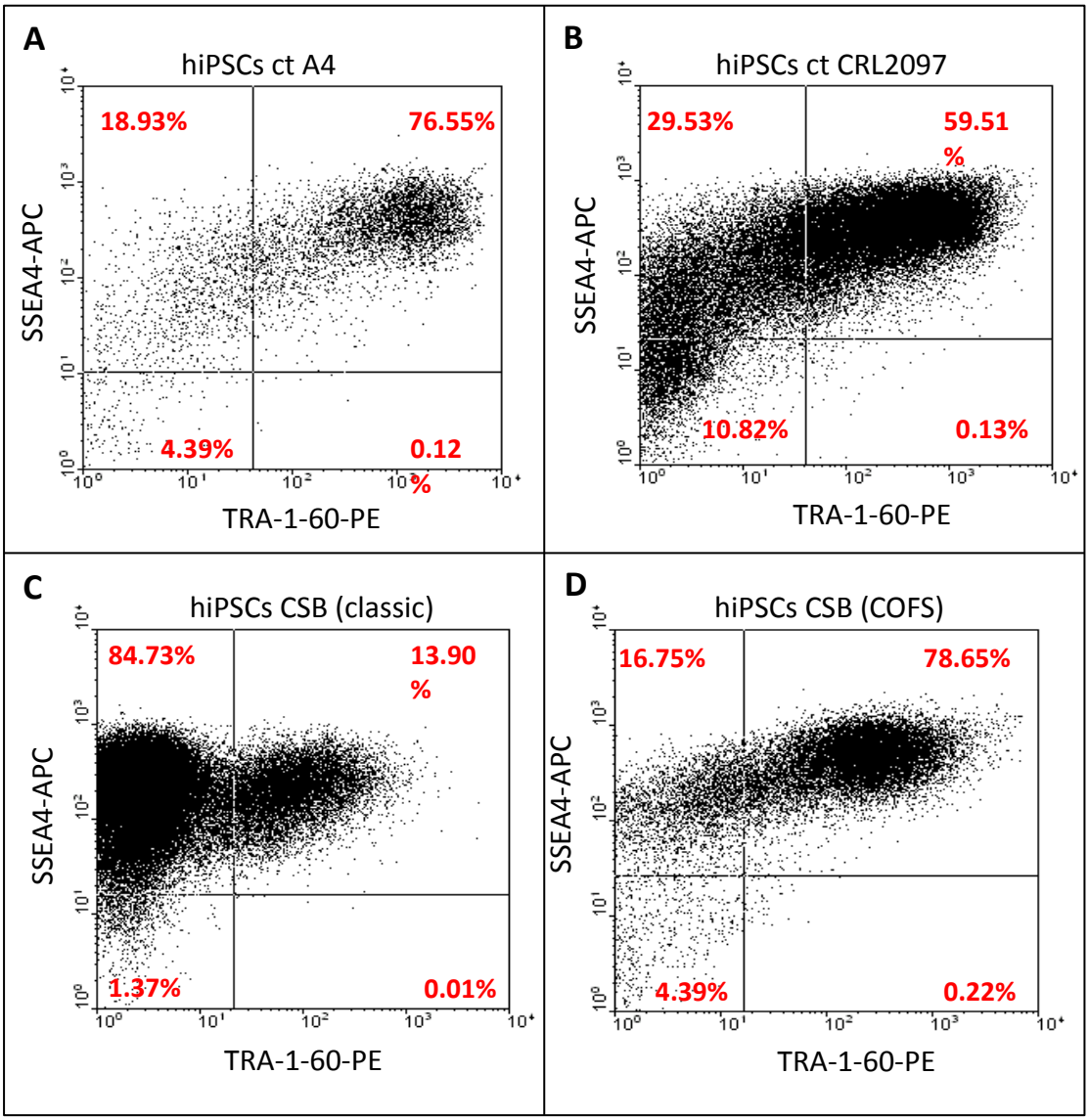

Fig. 3.18: Representative images of FACS analysis of hiPSC lines. Control (ct) hiPSCs (**A-B**) and CSB-deficient hiPSCs (**C-D**) were analyzed for their expression profile of the pluripotency markers TRA-1-60 and SSEA-4 using FACS analysis.

3.3.3 Neural induction of CSB-deficient hiPSCs

To evaluate if CSB-deficient hiPSC-derived neurospheres differ from control hiPSC-derived neurospheres in their neurodevelopmental potential, both CSB-deficient hiPSC lines were differentiated into NPCs using the NIM protocol (see Fig. 3.10 C and 2.2.1.10). After neural induction both CSB-deficient hiPSC-derived NPCs exhibited a spherical morphology comparable to the control hiPSC-derived neurospheres and primary human neurospheres (Fig. 3.19). However, whereas the classical CSB-deficient hiPSC-derived NPCs showed numerous neurospheres of various sizes (Fig. 3.19 C) COFS hiPSC-derived neurospheres still showed the same impaired proliferation as in the undifferentiated pluripotent state indicated here by less

neurospheres with decreased diameter (Fig. 3.19 D). To analyze the expression pattern of the two neural stem/progenitor markers Nestin and SOX2, proliferating classical CSB-deficient as well as COFS hiPSC-derived neurospheres were singularized and stained with Nestin and SOX2 antibodies. The percentage of positive cells was measured using FACS analysis (Fig. 3.20). Both CSB-deficient hiPSC-derived neurosphere cultures consisted of more than 90% $Nestin^{+}/SOX2^{+}$ cells suggesting that both CSB-deficient hiPSC lines were able to differentiate into NPCs (Fig. 3.20 C+D).

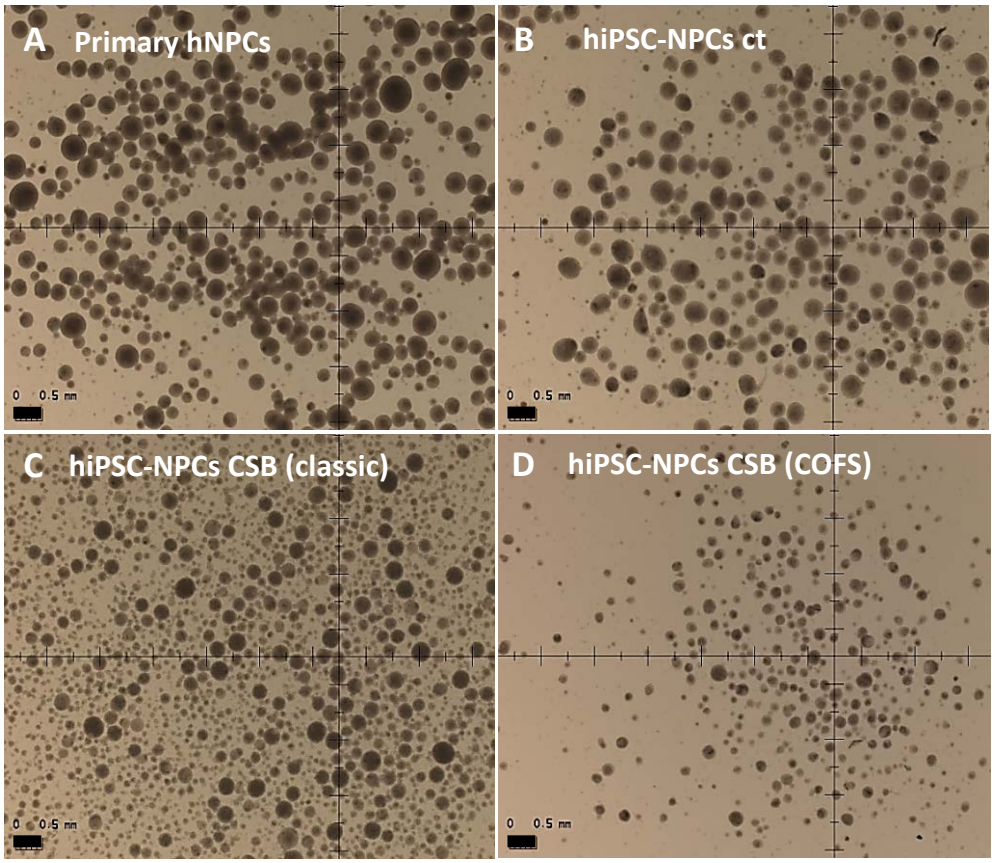

Fig. 3.19: Representative images of morphological comparison of hiPSC-derived neurospheres. Morphology of control (ct; **B**) and CSB-deficient (**C-D**) hiPSC-derived neurospheres was compared to primary human neurospheres (**A**). Scale bars = 500 µm.

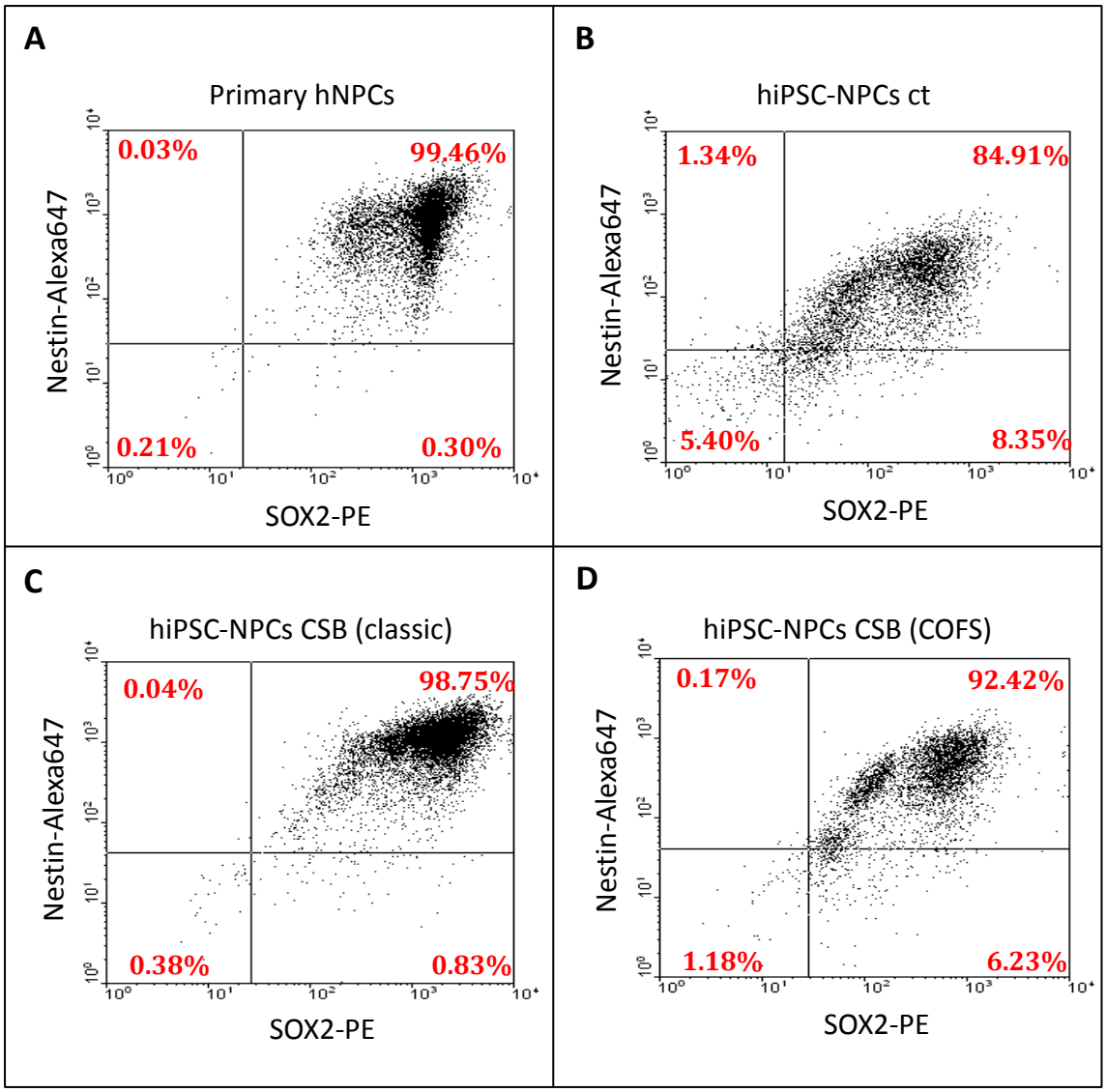

Fig. 3.20: FACS analysis of hiPSC-derived neural progenitor cells (NPCs). Control (ct; **B**) and CSB-deficient (**C-D**) hiPSC-derived NPCs were analyzed for their expression of the neural stem/progenitor markers Nestin and SOX2 via FACS analysis and compared to primary human NPCs (**A**).

3.3.4 Comparative analyses of CSB-deficient hiPSC-derived neurospheres with control hiPSC-derived neurospheres

CSB patients exhibit various severe neurological defects, including microcephaly and neurodegeneration (Kraemer et al. 2007). Therefore, the last aim of this thesis was to examine if CSB-deficient hiPSC-derived neurospheres display impaired function in neurodevelopmental processes *in vitro*. To answer this question, the neurodevelopmental processes proliferation, migration and differentiation were analyzed using the hiPSC-Neurosphere assay. For the proliferation assay development of neurosphere size over time was determined photographically in control (CRL2097) and CSB-deficient hiPSC-derived neurospheres (classic and COFS) as well as primary human neurospheres. Therefore, neurospheres were cultured either in NPM containing EGF and bFGF or in NPM without growth factors over 14 days (Fig. 3.21 A). As already observed in the hiPSC but also in the neurosphere culture, COFS hiPSC-derived neurospheres exhibited an impaired proliferative capacity compared to control hiPSC-derived neurospheres and primary human neurospheres. They only reached a final diameter of 530 µm after 14 days whereas the diameter of control hiPSC-derived neurospheres increased to approximately 900 µm. In contrast, classical CSB-deficient hiPSC-derived neurospheres displayed a significantly increased proliferation, with an increase of diameter up to 1160 µm after 14 days, compared to the controls (primary hNPCs and hiPSC-NPCs control). Noteworthy, whereas the sphere diameter of primary human neurospheres and COFS hiPSC-derived neurospheres cultured without growth factors slightly decreased over the time, control hiPSC-derived neurospheres (CRL2097) and classical CSB-deficient hiPSC-derived neurospheres continued to proliferate (Fig. 3.22). However, classical CSB-deficient hiPSC-derived neurospheres proliferated significantly more (final diameter of 760 µm) compared to control hiPSC-derived neurospheres (final diameter of 500 µm) if cultured without growth factors.

To analyze if the CSB-deficient hiPSC-derived neurospheres also display an altered migration potential, neurospheres were plated on PDL/laminin matrix and cultured in NDM for 3 days either under control conditions or together with EGF or the src kinase inhibitor PP2 (Fig. 3.21 B left), the two endpoint specific controls. EGF is known to increase migration of primary human neurospheres after 3 days whereas PP2 inhibits migration (Moors et al. 2007). Comparable to primary human neurospheres EGF significantly increased (from 600 µm up to 890 µm) and PP2 significantly reduced (from 600 µm down to 200 µm) migration of control hiPSC-derived neurospheres. In contrast to primary neurospheres, migration distance was significantly shorter in control hiPSC-derived neurospheres for all conditions. Interestingly, both CSB-deficient hiPSC-derived neurospheres migrated significantly less (classical CSB about 400 µm and COFS about 350 µm) compared to control hiPSC-derived neurospheres with 600 µm migration

distance if cultured under control conditions. If EGF was added COFS hiPSC-derived neurospheres reached a significantly increased migration distance (from 350 µm up to 960 µm) compared to control conditions. Moreover, the migration distance of COFS hiPSC-derived neurospheres cultured with EGF resembled the same migration distance of control hiPSC-derived neurospheres cultured with EGF. However, if cultured with PP2 COFS hiPSC-derived neurospheres migrated less with a migration distance of 180 µm compared to control conditions but this decreased migration distance was not significantly different. In contrast to the COFS hiPSC-derived neurospheres, classical CSB-deficient hiPSC-derived neurospheres did not increase their migration distance if cultured with EGF (both around 400 µm). This suggests a possible insensitivity of classical CSB-deficient hiPSC-derived neurospheres towards EGF. In presence of PP2, migration distance of classical CSB-deficient hiPSC-derived neurospheres was significantly decreased compared to control conditions with a migration distance of only 100 µm.

Not only EGF but also bFGF increases migration *in vit*ro of primary human neurospheres after 3 days under differentiating culture conditions (Marta Barenys, unpublished observations). To study the selectivity of the missing EGF-effects on CSB neurosphere migration, the migratory responses towards bFGF of control and CSB-deficient neurospheres were analyzed (Fig. 3.21 B right). Compared to the bFGF responses of primary neurospheres (from 800 µm up to 1100 µm), hiPSC-derived control (from 600 µm up to 1050 µm) and COFS neurospheres (from 400 µm up to 1000 µm), classical CSB neurospheres migration responses towards bFGF were significantly less (from 260 µm up to 590 µm). However, in contrast to the total lack of EGF-induced migration, bFGF was still able to induce some migration.

For the differentiation assay, control hiPSC-derived neurospheres and CSB-deficient hiPSC-derived as well as primary human neurospheres were differentiated on a PDL/laminin matrix with NDM for 28 days. Afterwards, differentiated cells were stained for neuron-specific βIII-Tubulin and astrocyte-specific GFAP (Fig. 3.21 C). Whereas primary human neurospheres and control hiPSC-derived neurospheres differentiated into βIII-Tubulin positive neurons and GFAP positive astrocytes, classical CSB-deficient hiPSC-derived neurospheres failed to differentiate into GFAP positive astrocytes. COFS hiPSC-derived neurospheres, on the other hand, were able to differentiate into both, βIII-Tubulin positive neurons and GFAP positive astrocytes. However, astrocytes exhibited an altered morphology compared to control hiPSC-derived neurospheres possibly indicating a less mature stage of astrocytes in differentiated COFS hiPSC-derived neurospheres.

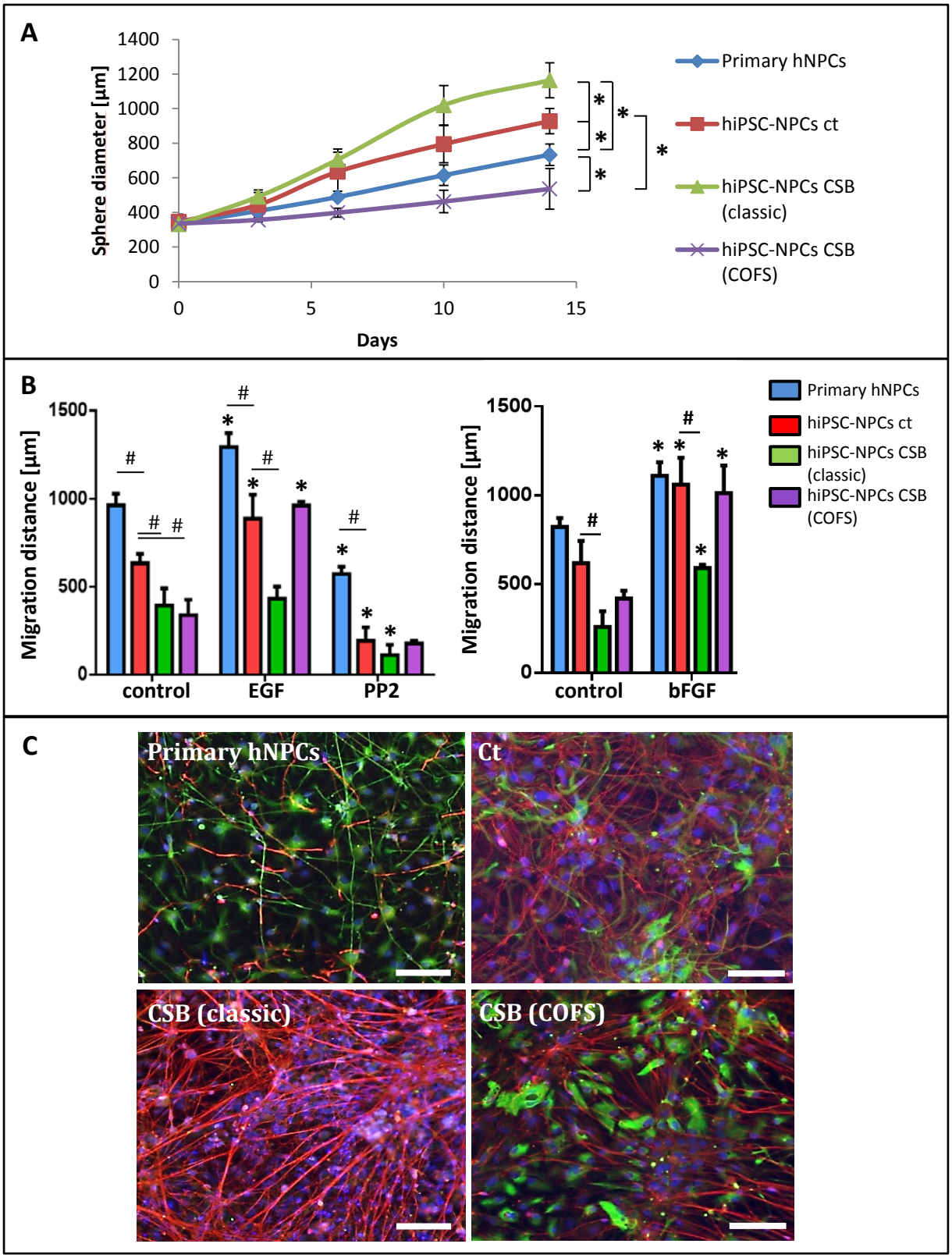

Fig. 3.21: Comparative analyses of control (ct) and CSB-deficient hiPSC-derived neurospheres using the Neurosphere assay. A) Proliferation was measured for 14 day in neural proliferation medium (NPM) containing growth factors (GF). Values represent mean + SD, n = 3, $p < 0.05$. **B)** Migration distance was measured for 3 days in neural differentiation medium (NDM) either under control conditions or in the presence of epidermal growth factor (EGF) or the src kinase inhibitor PP2, or the basic fibroblast growth factor (bFGF). * represents significant difference to respective control, n = 3, $p < 0.05$. **C)** Representative images of differentiated neurospheres. Neurospheres were differentiated for 28 days in NDM and stained for the neuronal marker βIII-Tubulin (red) and the astrocyte marker GFAP (green). Nuclei were stained with Hoechst (blue). Scale bars = 100 µm.

Moreover, whereas primary human neurospheres, control hiPSC-derived neurospheres and classical CSB-deficient hiPSC-derived neuropsheres migrated in the dish over the whole 28 days of differentiation, COFS hiPSC-derived neurospheres hardly migrated over the time.

Growth factors are important key players in neural proliferation, migration and differentiation (Fortin et al. 2005). To further analyze the altered growth factor signaling of classical CSB-deficient hiPSC-derived neurospheres (Fig. 3.21 A+B), proliferating neurospheres were analyzed for their expression profile of *EGF receptor* (*EGFR*) and *FGF receptor 2* (*FGFR2*) using qRT-PCR (Fig. 3.23). Whereas the expression of *EGFR* did not differ between control or CSB-deficient hiPSC-derived neurospheres, *FGFR2* was significantly increased in classical CSB-deficient hiPSC-derived neurospheres compared to all other neurosphere cultures studied.

This up-regulation of the *FGFR2* suggests a possible counter-regulation of a malfunctioning signaling pathway in this CSB genotype.

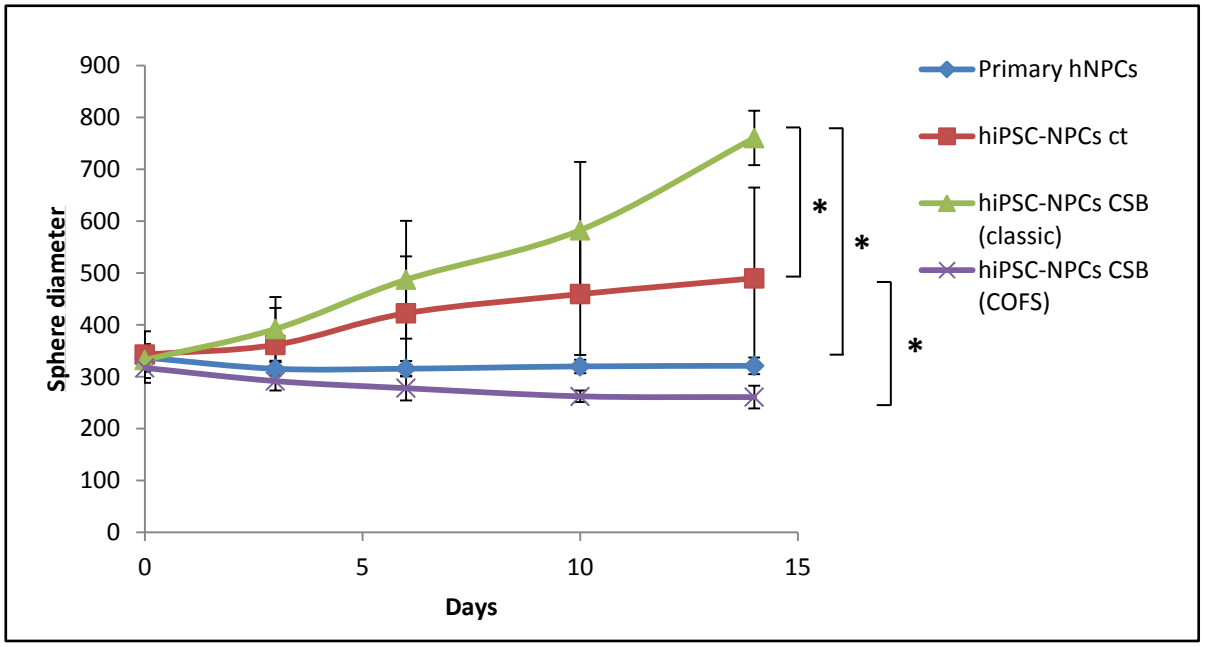

Fig. 3.22: Proliferation assay of neurospheres cultured without growth factors (GF). Proliferation of primary human neurospheres (hNPCs), control (ct) and CSB-deficient hiPSC-derived NPCs was measured for 14 days in neural proliferation medium (NPM) without GF. Values are represented as means +/- SD, n = 3, $p < 0.05$.

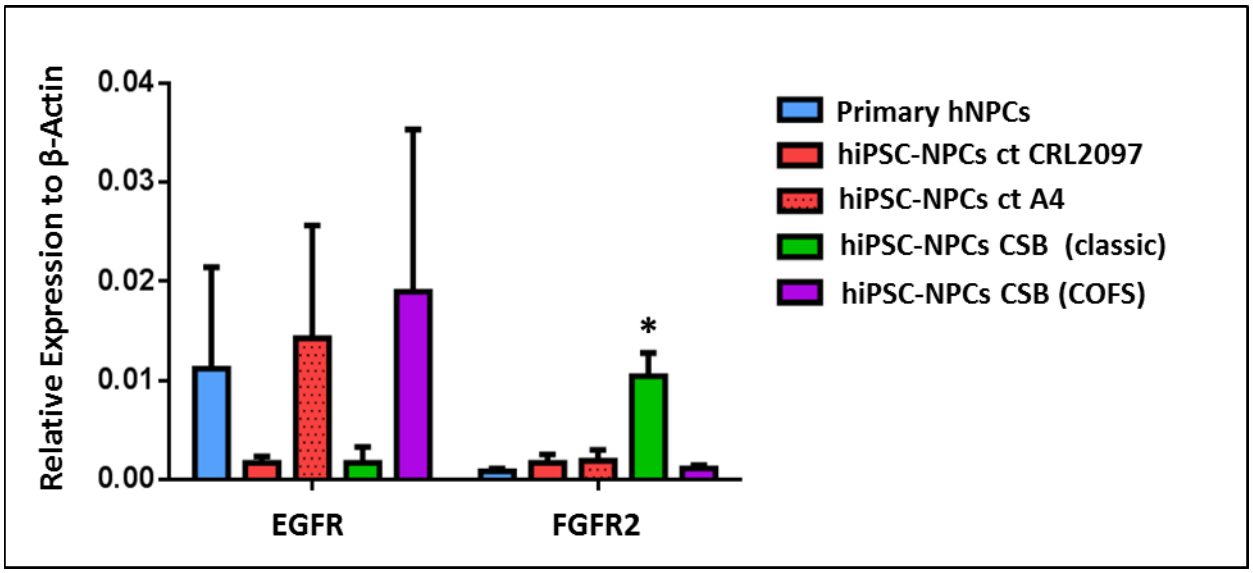

Fig. 3.23: Comparative analyses of control (ct) and CSB-deficient hiPSC-derived neurospheres. Expression of epidermal growth factor receptor (EGFR) and basic fibroblast growth factor receptor 2 (FGFR2) were analyzed in proliferating primary human neural progenitor cells (hNPCs), ct and CSB-deficient hiPSC-derived NPCs usig qRT-PCR analysis. Values are represented as means + SEM, $n = 3$, $p < 0.05$.

4. Discussion

The major aim of this thesis was to establish a hiPSC-derived neuropshere culture for studying neurodevelopmental disorders *in vitro*. Two different hiPSC neural induction protocols were tested for neurosphere generation. hiPSC-derived neurospheres from both protocols were compared to primary human neurospheres regarding their expression profile of different markers and functional performance by using the Neurosphere assay. Moreover, first analyses were performed using patient-specific hiPSC-derived neurospheres as a new *in vitro* tool for studying neurodevelopmental defects observed in CSB patients.

4.1 Establishment of a hiPSC culture

The prerequisite for developing a hiPSC-based neurosphere culture was the establishment of a hiPSC culture. hiPSCs are defined by their self-renewal capacity and their ability to differentiate into any cell type of the three germ layers endoderm, mesoderm and ectoderm (Fukusumi et al. 2013). Besides their potential to differentiate into any cell type, hiPSCs are highly sensitive and tend to spontaneously differentiate (Ohtsuka and Dalton 2008) Therefore, it is necessary to provide them with special culture conditions supporting their undifferentiated pluripotent character.

4.1.1 Comparison between feeder-dependent and feeder-free hiPSC culture

Even though the first generated hiPSCs were cultured on feeder cells (Takahashi et al. 2007), ongoing research made it possible to substitute feeder cells for special extracellular matrices which resemble the basement membrane, e.g. Matrigel and laminin (Crocco et al. 2013, Nakagawa et al. 2014). Advantages of feeder-free matrices are the easier and quicker handling but also the reduction of animal material used in human cell culture (Tamm et al. 2013, Lu et al. 2014). Nevertheless, it is noteworthy to mention that Matrigel is extracted from mouse Engelbreth-Holm-Swarm sarcoma consisting of laminin, collagen IV, heparan sulfate proteoglycans and entactin (Kleinman and Martin 2005). Moreover, Matrigel also contains several growth factors supportive for hiPSC culture but also variable in concentration (Kleinman and Martin 2005). Therefore, the standardization of the hiPSC culture using Matrigel also remains restricted due to possible batch to batch variations of Matrigel production (Hughes et al. 2010).

To identify the most supportive culture conditions, hiPSCs were either cultured under feeder-dependent conditions using SNL feeder cells and hESC medium (also referred to as UM) or under feeder-free culture conditions using Matrigel and mTeSR1 medium alone or in combination with CM (Fig. 3.2). The first observation of different culture conditions revealed diverse cell

morphology in hiPSCs cultured either under feeder-dependent or feeder-free conditions (Fig. 3.2 A-D). hiPSCs cultured under feeder-free conditions on Matrigel exhibited the typical hESC morphology with small and round shaped cells with a big nucleus and a high nucleus to cytoplasm ratio (Fig. 3.2 A + C) (Courtot et al. 2014). Furthermore, there was no obvious difference between feeder-free hiPSCs cultured either with mTeSR1 alone or with a combination of mTeSR1 and CM (Fig. 3.2 E + F). In contrast, hiPSCs cultured on feeder cells showed more undefined cell morphology (Fig. 3.2 C).

Feeder cells secrete several substances supportive for undifferentiated pluripotent stem cells (Greber et al. 2007). One of these substances is Activin A (Beattie et al. 2005). The amount of secreted Activin A can be measured in the culture medium using an ELISA. The analysis of the supernatant of SNL feeder cells revealed 2.5 ng/mL Activin A which was less than the amount measured in the supernatant of primary MEFs and according to the literature (Fig. 3.1 C) (Greber et al. 2007). However, even primary MEFs only released 8 ng/mL Activin A which is also less than the 15 – 20 ng/ml indicated in the literature (Greber et al. 2007). This low amount of secreted Activin A from SNL feeder cells used in this thesis might be an explanation for the variable cell morphology of hiPSCs on feeder cells (Figure 3.2 C). Nevertheless, Activin A only represents one of the known secreted substances and there are various other compounds secreted by feeder cells, which are discussed to be supportive for pluripotency (Lim and Bodnar 2002). Despite the low amount of Activin A produced in the cultures, SNL feeder cells were already reported to be supportive feeder cells for the culture of hiPSCs with unknown Activin A concentrations in these cultures (Takahashi et al. 2007).

Pluripotent stem cells also express several surface markers including TRA-1-60 and SSEA-4 (Gonzalez et al. 2011). Especially TRA-1-60 is rapidly down-regulated if pluripotent stem cells start to differentiate and therefore, is a reliable indicator for the pluripotent potential of the running hiPSC culture (Chan et al. 2009, Tanabe et al. 2013). Despite the different morphologies, both hiPSC cultures, either cultured under feeder-dependent or under feeder-free conditions, exhibited TRA-1-60 positive cells inside the colonies indicating a pluripotent character for both cell cultures (Fig. 3.4 A-F). However, the feeder-free hiPSC culture clearly exhibited advantages concerning simplicity and expenditure of time but no disadvantages compared to the feeder-dependent culture. Therefore, hiPSCs used for further experiments of this thesis were only cultured on Matrigel with mTeSR1 medium alone.

4.1.2 Comparison between different passaging methods

Not only the choice of optimal culture conditions but also passaging is a very important factor in the maintenance of hiPSCs. They are highly sensitive to any treatment and need cell-cell-contact to survive (Beers et al. 2012). This is why hiPSCs in this thesis were passaged mechanically, unless stated otherwise. Therefore, hiPSC colonies were cut into little pieces using two different tools, a small syringe needle or a special passaging tool called StemPro® EZPassage™ Disposable Stem Cell Passaging Tool (Thermo Fisher Scientific, USA). The special passaging tool cuts hiPSC colonies into equal quadrants whereas the passaging with the syringe needle resulted in small colony pieces of variable size (Fig. 3.3 A + B). According to the literature it is highly important to cut the colonies into mostly equal pieces of specific size (Amit and Itskovitz-Eldor 2012). Whereas oversized pieces result in clumps with differentiating cells, undersized pieces easily undergo apoptosis (Amit and Itskovitz-Eldor 2012). However, the appropriate colony piece size is not clearly defined. Even though the special passaging tool represented a good way to obtain small and equal colony pieces, passaged hiPSCs often resulted in more differentiated cells compared to hiPSCs passaged with the small syringe needle. A possible explanation for this could be that the special passaging tool was too big to cut single colonies and therefore colonies of the whole dish were cut and passaged. Hence, differentiated cells already existing in the hiPSC culture might also have been transferred into the new culture dish. Using the small syringe needle, on the other hand, made it possible to only cut hiPSC colonies with pluripotent morphology, which were identified under the microscope, resulting in a purer hiPSC culture in the next passage. One disadvantage of mechanical passaging with the small syringe needle was the inability to standardize the passaging process. Standardization was tried by passaging three colonies of equal size into a new culture dish. However, it was not possible to get equal numbers or equal distributed colonies in the new culture dishes.

Another method that has been described in the literature is single cell splitting (Watanabe et al. 2007). This method enables a more standardized passaging due to the possibility to use a specific cell number for further experiments and, in contrast to mechanically split colonies, single cells can be analyzed via flow cytometry to evaluate the quality of the running hiPSC culture. The drawback however is that in order to circumvent apoptosis hiPSCs need to be treated with the ROCK inhibitor Y-27632 (Watanabe et al. 2007), which makes this method rather expensive. Moreover, single cell splitting has been reported to promote genetic instability in hiPSCs (Thomson et al. 2008, Beers et al. 2012). Therefore, regular karyotype analysis should be performed to guarantee the genetic integrity of hiPSCs. Nevertheless, due to the risk of genetic instability and due to the higher costs of ROCK inhibitor, this thesis revealed that mechanical passaging of hiPSCs with a syringe was still the most useful way of hiPSC splitting.

4.1.3 Feeder-free hiPSCs express pluripotent markers and are able to differentiate into all three germ layers

To get a more quantitative analysis of the hiPSC culture, cells were dissociated and stained for the pluripotency markers TRA-1-60 and SSEA-4. Subsequently, hiPSCs were analyzed using FACS analysis. This analysis revealed that hiPSCs consisted of more than 50% TRA-1-60$^+$/SSEA-4$^+$ cells and about 90% SSEA-4$^+$ cells (Fig. 3.6). hiPSCs represent a highly dynamic system due to their tendency to spontaneously differentiate (Sathananthan and Trounson 2005). This might explain that the percentage of TRA-1-60$^+$/SSEA-4$^+$ cells and SSEA-4$^+$ cells did not reach 100%. It is difficult to define a threshold regarding the percentage of pluripotency markers expressed in hiPSCs due to high variability of different hiPSC lines. This variability not only depends on the original cell type and the reprogramming method but also on specific culture conditions (Gonzalez et al. 2011). Different culture conditions have different impact on hiPSCs what might also result in different expression profiles of pluripotency markers (Newman and Cooper 2010). Therefore, FACS analyses of the hiPSC culture represent a good method to obtain an overview of the pluripotency markers' expression profile of the cells and thus make it possible to monitor hiPSC quality over time.

Another characteristic of hiPSCs is their ability to differentiate into any cell type of the three germ layers endoderm, mesoderm and ectoderm (Zhang et al. 2012). This differentiation capacity can be analyzed either *in vivo* using teratoma analysis (Przyborski 2005, Prokhorova et al. 2009) or *in vitro* using EB formation (Itskovitz-Eldor et al. 2000). Even though teratoma formation still represents the gold standard (Smith et al. 2009) it is a time-consuming method and requires a lot of experience (Prokhorova et al. 2009, Smith et al. 2009). Therefore, only EB formation was performed in this thesis. EBs were prepared and spontaneously differentiated for 26 days resulting in various cell morphologies (Fig. 3.8). These cell morphologies included neuronal- as well as fibroblast-like morphologies (Fig. 3.8 A + B). Furthermore, EBs were able to differentiate into beating cardiomyocytes indicating their potential to differentiate into the mesodermal cell lineage (Fig. 3.8 C). EBs were also stained with antibodies for AFP for endoderm, smooth-muscle actin (SMA) for mesoderm and βIII-Tubulin for ectoderm but this staining did not reveal any positive cells. A possible explanation for this might be that spontaneous differentiation depends on various parameters and therefore, might vary extensively (Pettinato et al. 2014). As spontaneous differentiation represents an undirected process with unpredictable outcome, it is not possible to efficiently choose proper markers or antibodies for characterization. However, qRT-PCR analysis of 8 days old EBs in comparison to undifferentiated hiPSCs revealed a down regulation of the pluripotency markers *OCT4*, *NANOG* and *SOX2* in 8 days old EBs (Fig. 3.7). No statistical analyses were performed because the

experiment was only performed once. In contrast to the pluripotent markers, early markers for endoderm (*AFP*), mesoderm (*MSX1*) and ectoderm (*MAP2*, *PAX6*) were up-regulated in 8 days old EBs compared to undifferentiated hiPSCs (Fig. 3.7). This result clearly indicates that hiPSCs cultured under feeder-free conditions were able to differentiate into cells of all three germ layers. Noteworthy, the hiPSC line A4 has been already fully characterized including teratoma analysis by Wang and Adjaye (2011).

4.2 Establishment of a hiPSC-derived neurosphere culture

The next aim of this thesis was to establish a hiPSC-derived neurosphere culture because neurospheres are an accepted model for the analyses of neurodevelopmental processes *in vitro* (Suslov et al. 2002, Moors et al. 2007, Breier et al. 2010, Gassmann et al. 2010, Fritsche et al. 2011, Garcia-Parra et al. 2013, Baumann et al. 2014). Whereas fetal hNPCs are rather restricted in material and can generate ethical concerns (Dunnett and Rosser 2014) hiPSCs can be obtained from any somatic cell of the body. Therefore, hiPSCs do not only circumvent ethical concerns but also bear an unlimited pool of material (Kao et al. 2008, Kastenberg and Odorico 2008, Singh et al. 2015). Many protocols already exist to differentiate hiPSCs into NPCs. However, the vast majority of these studies lack an adequate reference to compare their obtained results to physiological controls as primary hNPCs. In this thesis, hiPSCs were differentiated into neurospheres consisting of NPCs using two different protocols, Noggin and NIM (Fig. 3.10), and were compared to primary human neurospheres.

For the first protocol, hiPSC colonies were treated with 500 ng/mL noggin in hESC medium without growth factors (referred to as Noggin protocol; Fig. 3.10 B) for 14 days. Noggin plays a crucial role in neurodevelopment due to the inhibition of BMP4, a member of the SMAD/TGFβ superfamily (Lamb et al. 1993, Moreau and Leclerc 2004). During embryonic development, these signaling pathways induce epidermal or mesodermal cell fate (Qiang et al. 2013). In contrast, inhibition of BMP and Activin/Nodal/TGFβ signaling pathways promotes neural progenitor fate *in vivo* and *in vitro* (Munoz-Sanjuan and Brivanlou 2002). Many protocols are based on SMAD inhibition either with noggin or with additional small proteins inhibiting BMP and TGFβ signaling (Denham and Dottori 2011, Qiang et al. 2013).

For the second protocol, undifferentiated hiPSC colonies were cut into little pieces and cultured in cell suspension in defined differentiation medium (referred to as NIM protocol; Fig. 3.10 C) containing B27 and N2 supplements. In contrast to the Noggin protocol, the NIM protocol does not include any additional SMAD inhibitors. It partly relies on the observation that pluripotent stem cells cultured in low density in a defined medium have the autonomous tendency to differentiate into neural cells (Tropepe et al. 2001). Application of N2 and B27 supplements in

serum-free medium was previously shown to induce neural differentiation in hESCs in adherent culture (Gerrard et al. 2005) and in hiPSCs differentiated as EBs (Hibaoui et al. 2014).

4.2.1 Molecular comparison of hiPSC-derived with primary human neurospheres

Neurospheres consist of multipotent NPCs able to further differentiate into the three main cell types of the brain: neurons, astrocytes and oligodendrocytes (Moors et al. 2007). They also express the neural stem/progenitor markers Nestin and SOX2 (Breier et al. 2010). FACS analyses revealed that hiPSC-derived neurospheres from the Noggin and NIM protocol consisted of 92.91% and 84.91% $Nestin^+/SOX2^+$ cells, respectively indicating that both neural induction protocols resulted in similar cell populations regarding the Nestin and SOX2 expression.

Moreover, qRT-PCR analysis showed that the pluripotency markers *OCT4* and *NANOG* were significantly down regulated in hiPSC-derived neurospheres from both protocols compared to undifferentiated hiPSCs (Fig. 3.12 A). These observations indicate that hiPSC-derived neurospheres, as expected, lost their pluripotent character. OCT4 and NANOG have been shown to be highly expressed in pluripotent stem cells (Takahashi et al. 2007) and to repress the differentiation into the neuroectodermal cell lineage. On the other hand, low expression of OCT4 and NANOG in the absence of BMP4 promotes neuroectodermal differentiation (Wang and Doering 2012). In contrast to OCT4 and NANOG, SOX2 does not only represent a marker for pluripotency but also for NPCs and therefore, is highly expressed in both cell types (Breier et al. 2010, Zhang and Cui 2014). While SOX2 interacts with OCT4 to maintain the pluripotent stem cell character of hiPSCs, in NPCs it interacts with neural transcription factors like PAX6 to induce neural progenitor gene expression (Zhang and Cui 2014). In this study, *SOX2* expression was not changed in hiPSC-derived neurospheres compared to undifferentiated hiPSCs but significantly different to primary human neurospheres (Fig. 3.12 A). However, *SOX2* expression was in the same order of magnitude suggesting no biological relevance between hiPSC-derived and primary human neurospheres. Moreover, these observations are in accordance with previously published data of one of the few studies in which hiPSC-derived neurospheres were compared to primary human neurospheres (Shofuda et al. 2013). Shofuda and colleagues showed that hiPSC-derived neurospheres expressed slightly or significantly lower *SOX2* compared to forebrain and spinal cord neurospheres, respectively.

Furthermore, the mRNA expression pattern of the neural marker *Nestin*, the neuroectodermal marker *PAX6* and the neuronal marker *MAP2* revealed no differences between proliferating hiPSC-derived neurospheres from both protocols and primary human neurospheres (Fig. 3.12 B) indicating a similar maturation stage regarding neural and neuronal markers. In contrast, the astrocyte marker *GFAP* was not detectable in undifferentiated hiPSCs but slightly expressed in

proliferating hiPSC-derived neurospheres. Primary human neurospheres, on the other hand, expressed significantly more *GFAP* compared to hiPSC-derived neurospheres. Further qRT-PCR analysis of differentiating hiPSC-derived neurospheres (NIM) and primary human neurospheres also revealed a significant difference in the expression of the glial markers *GFAP*, *ALDH1L1* and *PDGFRα* during a differentiation period of 14 days (Fig. 3.14). According to these data, hiPSC-derived neurospheres seem to represent an earlier maturation stage as primary human neurospheres regarding glial markers. Previous studies also reported that hiPSC-derived NPCs and so-called EZ spheres, which resemble a very early hiPSC-dervied NSC stage, expressed significantly less glial markers, including *GFAP* and *S100β*, compared to hNPCs (Shofuda et al. 2013, Sareen et al. 2014) supporting the data of this study. Whereas the above mentioned studies compared the hiPSC-derived NS/PCs to hNPCs of gestational week 8 to 10, primary human neurospheres used in this study are derived from 16 to 18 weeks old fetuses. In contrast, hiPSC-derived neurospheres generated in this study were only differentiated from the stem towards the neural progenitor cell lineage for 3 weeks and then cultured as proliferating NPCs. During neurodevelopment neurons are born before glial cells (Kolb and Gibb 2011) providing further evidence towards the hypothesis of different developmental stages. Furthermore, it has been already shown that hESC- and hiPSC-derived neuroepithelial cells are able to differentiate into neurons within one month whereas the differentiation into astrocytes and oligodendrocytes takes 2 - 4 months (Hu et al. 2010). These observations further support the hypothesis of the earlier developmental stage of hiPSC-derived neurospheres generated in this study compared to primary human neurospheres. Taken together, these results show that both protocols, Noggin and NIM, result in similar cell types resembling the neural/neuronal but not the glial expression profile of proliferating primary human neurospheres.

4.2.2 Functional comparison of hiPSC-derived with primary human neurospheres

Besides the expression patterns in hiPSC-NPC, hiPSC-derived neurospheres were analyzed for their functional performance using the Neurosphere assay. The Neurosphere assay represents a method to analyze the main processes of brain development: proliferation, migration, and differentiation *in vitro* (Fig.1.2; chapter 1.1.2 and 2.2.1.15). One of the aims of this thesis was to establish a hiPSC-derived neurosphere culture which is also able to display neurodevelopmental processes *in vitro* and has the advantages to circumvent ethical concerns and material restriction. Therefore, proliferation, migration and neuronal differentiation were analyzed for hiPSC-derived neurospheres from both neural induction protocols (Noggin and NIM) and compared to primary human neurospheres (Fig. 3.13) as the gold standard. These comparative analyses revealed that hiPSC-derived neurospheres from the NIM protocol better resembled the neurodevelopmental processes proliferation and differentiation than spheres generated with

the Noggin protocol when compared to the primary human neurospheres (Fig. 3.13 A+C). Whereas both hiPSC-derived neurospheres (NIM and Noggin) exhibited the same migration distance as primary human neurospheres after 3 days (Fig. 3.13 B), hiPSC-derived neurospheres from the NIM protocol showed a higher proliferative capacity compared to the Noggin protocol (Fig. 3.13 A). Furthermore, hiPSC-derived neurospheres from the NIM protocol resulted in βIII-Tubulin positive neurons with long, branched neurites suggesting a more mature neuronal network compared to hiPSC-derived neurospheres from the Noggin protocol (Fig. 3.13 C). Thus, the NIM protocol was chosen to differentiate hiPSCs into neurospheres for further experiments. Furthermore, hiPSC-derived neurospheres obtained from the NIM protocol are able to differentiate into neuronal networks consisting of βIII-Tubulin positive neurons and GFAP positive astrocytes after 4 weeks of differentiation (Fig. 3.21 C). Immunocytochemical staining for pre- and post-synaptic markers Synapsin-1 and PSD-95 revealed that hiPSC-derived neurospheres (NIM) showed positive staining overlapping with βIII-Tubulin positive neurites after 4 weeks of differentiation (Laura Nimtz, unpublished group data). One possibility to verify the function of cultured neurons is to determine their ability to show electrical activity (Odawara et al. 2014). Beside patch clamp analysis, multielectrode arrays (MEA) represent a good way to measure the spontaneous electrical activity within a neuronal network (Massobrio et al. 2015). Using MEA analysis, spontaneous electrical activity was measured in hiPSC-derived neurospheres (NIM) differentiating for several weeks (Laura Nimtz, unpublished data). Even though MEA analyses have been reported for hESC-derived neurons (Heikkila et al. 2009), it is still challenging to detect electrical activity of hiPSC-derived neurons using the MEA technique. Recently, Odawara and colleagues reported functional networks of hiPSC-derived neurons on MEA chips if co-cultured with rat astrocytes (Odawara et al. 2014) indicating that the multipotent character of the hiPSC-derived neurosphere culture generated in this thesis is supportive for the maturation into functional neuronal networks.

Nevertheless, it is noteworthy to mention that hiPSC-derived neurospheres from the NIM protocol do not behave exactly the same as primary human neurospheres. One observed difference was the proliferative capacity cultured in NPM even without any growth factors (Fig. 3.13 A and Fig. 3.22). Further analyses are needed to understand why hiPSC-derived neurospheres (NIM) but not primary human neurospheres have the potential to proliferate without growth factors. One possible explanation might be that hiPSC-derived neurospheres (NIM) self-produce growth factors and might therefore not be dependent on growth factor addition. However, this hypothesis remains further experiments including e.g. ELISA to analyze the released amount of growth factors.

4.2.3 Comparison of the effects of MeHgCl on hiPSC-derived and primary human neurospheres

The Neurosphere assay does not only represent a good *in vitro* model to study neurodevelopmental processes but might also predict adverse effects of chemicals on brain development (Moors et al. 2009, Baumann et al. 2015). Therefore, responses towards neurodevelopmental toxins also help characterizing the hiPSC-derived neurosphere culture.

MeHgCl is known to cause mental retardation and developmental delay if children are prenatally exposed (Grandjean and Landrigan 2006). Moreover, MeHgCl disturbs cell migration and division resulting in microcephaly and global brain disorganization (Schettler 2001). Baumann et al. (2015) could already show that MeHgCl exposure specifically inhibited migration *in vitro* in primary human neurospheres. Therefore, MeHgCl was chosen in this thesis as a model substance with known DNT potential to determine if hiPSC-derived neurospheres, similar to primary neurospheres, can also serve as a useful tool for DNT testing *in vitro*. Thus, primary human and hiPSC-derived neurospheres were treated with different concentrations of MeHgCl for 24 h and migration distance and viability were measured. The results showed that migration distance was specifically inhibited in hiPSC-derived neurospheres and primary human neurospheres due to the lower EC_{50} value (0.39 µM for hiPSC-derived neurospheres and 0.77 µM for primary human neurospheres) and the non-overlapping confidence intervals of migration compared to viability measurement (EC_{50}: 2.74 µM for hiPSC-derived neurospheres and 2.35 µM for primary human neurosphers; Fig. 3.15; Tab. 3.1). Moreover, calculated EC_{50} values and 95% confidence intervals of primary human neurospheres are in line with previously reported results (EC_{50}, migration: 0.65 µM; EC_{50}, viability: >3 µM for primary human neurospheres) (Baumann et al. 2015). The calculated EC_{50} value for migration was smaller in hiPSC-derived neurospheres (0.39 µM) compared to the primary human neurospheres (0.77 µM) and 95% confidence intervals did not overlap (Tab. 3.1). However, the values of both cell types lie within the same range and thus might not have any biological relevance. Furthermore, if concentration-response curves for migration distance were compared between hiPSC-derived neurospheres and primary human neurospheres, there was no significant difference (Fig. 3.15 C). These results suggest that differences in calculated EC_{50} values between hiPSC-derived and primary human neurospheres are rather negligible.

Current DNT testing methods are mostly based on animal experiments which do not only pose ethical concerns but are also time- and cost-intensive (Coecke et al. 2007, Lein et al. 2007). Moreover, potential species differences might result in wrong predictions for human health (Baumann et al. 2014). There are many examples for the low predictability of animal studies including different genomic responses towards inflammation between mice and human (Seok et

al. 2013). Further instances are the pharmaceuticals thalidomide or TG1412 which led to tremendous effects in human not predicted by animal studies (Stebbings et al. 2007, Leist and Hartung 2013). Therefore, alternative methods based on human cells are urgently needed and are addressed in the Neurosphere assay using primary fetal hNPCs (Moors et al. 2009, Gassmann et al. 2010, Fritsche et al. 2011, Baumann et al. 2015). However, fetal hNPCs are rather restricted and also not free of ethical concerns (Dunnett and Rosser 2014), as the cells are derived from human late abortions. hiPSCs provide a solution to overcome these ethical issues as these cells can be generated from somatic cells of adult donors and offer a theoretically inexhaustible source of cell material due to their self-renewal potential (Scott et al. 2013).

Taken together, hiPSC-derived neurospheres represent a promising tool for future DNT testing but more experiments for additional endpoints, like proliferation and neuronal differentiation are needed in order to validate this finding. Furthermore, a significant amount of chemicals has to be tested besides MeHgCl to examine further similarities and differences between hiPSC-derived neurospheres and primary human neurospheres. Moreover, to efficiently determine the predictability of hiPSC-derived neurospheres in DNT it is important to not only test DNT-positive but also –negative compounds (Baumann et al. 2015). In a previous study, 80 compounds were tested for their cytotoxicity in hiPSC, hiPSC-NPCs, hiPSC-neurons and hiPSC-astrocytes (Pei et al. 2015). However, they only tested for the endpoint cytotoxicity and used rather high concentrations (1, 10 and 100 µM). For future DNT it is necessary to include more endpoints as addressed in the Neurosphere assay because different compounds may have different modes of actions, as MeHgCl first impairs neural proliferation, migration and neuronal differentiation in primary human neurospheres before having an effect on cell viability (Baumann et al. 2015).

4.3 hiPSC-derived neurospheres as a disease model for CSB

The last aim of this thesis was the application of the established hiPSC-derived neurosphere model to study the neurodevelopmental defects of CSB patients. CSB was originally found to be a key player in TC-NER, a sub pathway of the NER (Nouspikel 2009). The deficiency in TC-NER explains the increased photosensitivity observed in CSB patients but not the severe neurological symptoms (Newman et al. 2006). These neurological defects include microcephaly, mental retardation, sensorineural deafness and retinal degeneration (Kraemer et al. 2007). Further neurological symptoms include calcification in basal ganglia and cerebral cortex as well as loss of Purkinje cells and granule neurons (Jeppesen et al. 2011). Studying the neurodevelopmental defects of CSB patients is challenging due to the limited possibilities to study the brain of the patients. The CSB mouse model, on the other hand, resembles the high photosensitivity of the patients but in contrast to the human phenotype, shows a significantly milder brain phenotype

(van der Horst et al. 1997) with reduced motor function, defects in sensorimotor coordination and the lack of demyelination (Niedernhofer 2008). Therefore, the CSB mouse model does not represent an adequate model to study the neurodevelopmental defects of CSB patients. hiPSCs enable a patient-specific approach to study the disease based on the respective genetic background of the patient. Therefore, hiPSCs derived from two different CSB patients were differentiated into neurospheres using the NIM protocol. The CSB-deficient hiPSC lines were derived from two different CSB patients with different mutations (Tab. 3.2). The first CSB-deficient hiPSC line (classic, AS548) bears a big deletion inside and in front of the CSB gene (Fig. 3.16 B+C) (Laugel et al. 2008a) and therefore completely lacks a CSB mRNA and protein (Fig. 3.16 A) (Laugel et al. 2008a). In contrast, the second CSB-deficient hiPSC line (COFS, AS789) bears a point mutation in exon 10 (Fig. 3.16 D+E) leading to a stop codon and a predicted truncated CSB protein (Laugel et al. 2008b).

Whereas both patients exhibited a mutation in the CSB gene and showed symptoms of congenital microcephaly and severe mental retardation, the kind of mutation as well as disease progression differed extensively (Tab. 2.8; Tab. 3.2). Moreover, the two different patient-specific hiPSC lines used in this study exhibited different phenotypes in undifferentiated hiPSC and NPC stage.

4.3.1 Neurosphere phenotype of hiPSC-derived NPCs derived from a CSB patient with COFS syndrome

hiPSCs derived from the CSB patient with the severe form COFS showed a decreased proliferative capacity. This phenomenon was already observed in the undifferentiated hiPSC stage when cells slowly proliferated and exhibited fewer predispositions to spontaneously differentiate. Furthermore, this proliferation phenotype was also preserved when hiPSCs were differentiated into neurospheres (Fig. 3.21 A). Moreover, if cultured in NPM without growth factors COFS hiPSC-derived neurospheres exhibited a continuous decrease in sphere size (Fig. 3.22) suggesting increased apoptosis. In accordance with this observation, COFS hiPSC-derived neurospheres migrated significantly less compared to the control if cultured in NDM without growth factors for 3 days (Fig. 3.21 B). This phenotype was rescued by culturing migrating cells in presence of EGF or bFGF (Fig. 3.21 B). Also long-term differentiation of COFS hiPSC-derived neurospheres for 28 days revealed shortened migration, but cells were nevertheless able to differentiate into βIII-Tubulin positive neurons and GFAP positive astrocytes (Fig. 3.21 C). The morphology of the GFAP positive astrocytes was altered in the COFS cells compared to the control (Fig. 3.21 C). They appeared smaller and with less processes suggesting delayed astrocyte maturation compared to the control.

Microcephaly is classified as a disorder with either decreased proliferation or increased apoptosis (Barkovich et al. 2005). Therefore, the observed decreased proliferation of COFS hiPSC-derived neurospheres might explain the microcephaly observed in the respective CSB patient (Laugel et al. 2008b, Laugel et al. 2010). Moreover, in general, apoptotic cells have been shown to be present in the cerebellum of CS patients suggesting a link between apoptosis and neurodegeneration (Kohji et al. 1998). Nevertheless, an additional apoptosis assay is needed to address the role of apoptosis in COFS hiPSC-derived neurospheres .

4.3.2 hiPSC-derived neurospheres from a CSB patient with classical CSB phenotype exhibit a defect in growth factor signaling

CSB-deficient hiPSCs obtained from a patient with classical CSB phenotype proliferated highly as hiPSCs and hiPSC-derived neurospheres, in contrast to COFS hiPSCs (Fig. 3.21 A). Furthermore, even if cultured in NPM without growth factors classical CSB-deficient hiPSC-derived neurospheres exhibited a significantly increased proliferative capacity compared to the control (Fig. 3.22). This increased proliferation seems to be contradictory to the microcephalic phenotype observed in the patient. However, if cultured in NDM without growth factors for 3 days, classical CSB-deficient hiPSC-derived neurospheres migrated significantly less compared to the control (Fig. 3.21 B). In contrast to the control and the COFS hiPSC-derived neurospheres, migration distance of classical CSB-deficient hiPSC-derived neurospheres was not increased upon EGF treatment (Fig. 3.21 B left). This observation suggests an insensitivity of classical CSB-deficient hiPSC-derived neurospheres towards EGF. Furthermore, bFGF significantly increased migration in classical CSB-deficient hiPSC-derived neurospheres but this effect was still significantly milder compared to control and COFS hiPSC-derived neurospheres (Fig. 3.21 B right). Defective neuronal migration is also linked to human microcephaly including Miller-Dieker syndrome and Hirschsprung's disease (Hurst et al. 1988, Woods 2004) and therefore, might be a possible explanation for the microcephaly observed in the classical CSB patient.

Moreover, the observed results indicate a defect in growth factor signaling in classical CSB-deficient hiPSC-derived neurospheres. This hypothesis was further confirmed by qRT-PCR analysis which revealed a significant increase of *FGFR2* expression in proliferating classical CSB-deficient hiPSC-derived neurospheres compared to control and COFS (Fig. 3.23). Growth factors play an important role in neurodevelopment, including proliferation migration and differentiation (Kuhn et al. 1997, Fortin et al. 2005, Mason 2007). Interestingly, classical CSB-deficient hiPSC-derived neurospheres failed to differentiate into GFAP positive astrocytes after 28 days of differentiation (Fig. 3.21 C). This lack of astrocytes also might be a result of defective growth factor signaling. FGF2 was found to promote astrocyte differentiation by facilitating the access of the STAT/CBP complex to the GFAP promoter (Song and Ghosh 2004). This

transcription activation is induced by Lys4 methylation and suppression of Lys9 methylation of histone H3. CSB is an important key player in transcription due to epigenetic modulation (Newman et al. 2006). However, there is nothing known about a possible role of CSB in astrocyte differentiation. Nevertheless, CSB has been found to be enriched at the MAP2 promotor site during neuronal differentiation (Ciaffardini et al. 2014). The same study showed that CSB knockdown of an hNPC line resulted in reduced differentiation potential, reduced neurite outgrowth and a decrease of *MAP2* expression. Whereas the study of Ciaffardini exhibited a clear defect in neuronal differentiation, the classical CSB-deficient hiPSC-derived neurospheres of this study seem to display an astrocytic phenotype. One explanation for these different phenotypes of CSB might be due to the difference in the cell type and kind of mutation used for the study. Whereas Ciaffardini and colleagues created a CSB knockdown in an hNPC line, the cells used in this study are generated from hiPSCs obtained from a CSB patient with a complete lack of the CSB protein. However, the study of Ciaffardini already indicates a role of CSB in neuronal differentiation upon epigenetic modulation. More studies are needed to analyze if CSB is also involved in expression of GFAP and thus astrocyte maturation.

Interestingly, FGF signaling does not only play an important role in CNS development but is also necessary for ectodermal placode development, which contributes to formation of the sense organs of the head, including the lens of the eye and the inner ear (Mason 2007). Studies with zebrafish showed that FGF signaling is required for the maintenance of photoreceptor cells of the adult retina (Hochmann et al. 2012) whereas inhibition of FGF signaling resulted in degeneration of rod cells in the mouse retina (Rousseau et al. 2000). Furthermore, the mouse deafness gene *Sprouty2* has been hypothesized to antagonize FGF8 signaling and thus, contribute to cell fate decision in the auditory sensory epithelium (Shim et al. 2005). Even though nothing is known about a role of FGF signaling in the observed symptoms of CSB patients, it is noteworthy that the CSB patient whose hiPSC-derived neurospheres exhibited the defect in growth factor signaling showed retinal degeneration and deafness whereas the COFS patient lacked these symptoms (Tab. 2.8).

Taken together, two different CSB-deficient hiPSC lines with two different *CSB* mutations resulted in distinct phenotypes. CSB is a regulator for the transcription of many genes (Newman et al. 2006). Different mutations in different regions of the *CSB* gene might have different impact on transcription resulting in potentially different expression patterns. Whereas the classical CSB-deficient hiPSC line does not express any *CSB* mRNA and no CSB protein, COFS hiPSCs are thought to exhibit a truncated CSB protein with altered function (Laugel et al. 2010). However, the existence of such a truncated CSB protein has not been proven yet.

Additionally, CSB plays a role in hypoxic response (Velez-Cruz and Egly 2013). For example, murine neurospheres showed a significant reduction of proliferation under hypoxic conditions with an even higher effect in CSB-deficient cells. Furthermore, it could be shown that CSB plays a role in the hypoxic-dependent transcription, especially in regulating the expression of the HIF-1-inducible genes *VEGF* and *Glucose Transporter 1* (*GLUT-1*) (Schumacher 2012). Previous data with CSB-deficient hiPSC-derived neurospheres cultured under hypoxic conditions, however, did not reveal any distinct results yet and require further analyses.

In this thesis, one hiPSC line each from two different CSB patients and one hiPSC line each from two different healthy individuals were analyzed. This alone is not sufficient to doubtlessly link the observed phenotypes to the respective *CSB* mutations, because genetic background or genetic instability of hiPSCs might also result in altered phenotypes.

There are some possibilities to determine if the *CSB* mutation itself results in the observed phenotypes. These possibilities involve either the usage of several hiPSC lines from each patient and multiple healthy controls or the inclusion of more comparable patients and controls. Moreover, a more reliable approach involves the correction of the mutation to rescue the phenotype (Bellin et al. 2012). This can be done by clustered regularly interspaced short palindromic repeats (CRISPR)-CRISPR-associated (Cas) systems (Okano and Yamanaka 2014). With this technique, Chang et al. (2015) were able to generate a hiPSC model of severe combined immunodeficiency (SCID) which is characterized by the absence of circulating T cells and natural killer cells together with decreased cell function of B cells. Using CRISPR-Cas9, Janus family kinase (*JAK3*) mutation, responsible for the disease, could be successfully corrected restoring normal T cell development (Chang et al. 2015).

4.4 Conclusion and Outlook

The experiments of this work led to the successful establishment of a hiPSC-derived neurosphere culture resembling the main characteristics of primary human neurospheres. These neurospheres allow studying the main processes of neurodevelopment, like proliferation, migration and differentiation on the basis of hiPSCs. Furthermore, this hiPSC-derived neurosphere culture circumvents material and ethical limitations of primary human cells and enables the study of patient-specific cells for disease modeling. Therefore, they represent an ideal model to study neurodevelopmental diseases like CSB. However, one limitation of hiPSC-derived neurospheres is their limited potential to differentiate into oligodendrocytes. In contrast to neurons and astrocytes, no oligodendrocytes were detected in our established culture. As a consequence, it was not possible to study the strong myelination phenotype of CSB patients. Recently, Wang et al. (2013) reported the differentiation of oligodendrocytes from hiPSCs. This

process required special medium supplies to direct hiPSCs exclusively to glial progenitor cell fate and took very long culture times of 4 – 5 months. By modification of our differentiation protocol it thus might be possible to also study oligodendrocyte differentiation and/or myelination phenotypes of CSB-deficient hiPSCs. Moreover, the small sample size of used hiPSC lines in this study is not sufficient to link the observed phenotype to the respective *CSB* mutation. Therefore, adequate controls are needed to guarantee that the observed phenotypes are caused by the respective *CSB* mutations. Using the CRSPR-Cas9 system, single guided RNAs (sgRNAs) are used to specifically cut the DNA double strand at the location of the mutation to produce a double strand break (Mali et al. 2013). Subsequently, a targeting construct containing the corrected DNA sequence can be inserted into the DNA strand by homologous recombination (Sander and Joung 2014). In this way, point mutations can be repaired or induced in whole organisms or cell culture (Sander and Joung 2014). CRISPR-Cas9 represents a good method to repair the point mutation of the COFS hiPSC line. To achieve this, sgRNAs and the scheme of a targeting construct were already designed by Dr. Daniel Haag (Institute for Stem Cell Biology and Regenerative Medicine, Stanford University; Appendix Fig. 6.1 and 6.2). After repairing the *CSB* mutation in COFS hiPSCs, cells have to be differentiated into neurospheres and their performance for proliferation, migration and differentiation determined. If the observed phenotypes are really caused by the *CSB* mutation, correction of the mutation should also rescue the phenotype. In case of the classical CSB-deficient hiPSC line, the deletion in front of the *CSB* gene is too big to insert the wt DNA sequence. Another possibility to determine if the observed phenotypes are caused by the *CSB* mutation is to delete the DNA sequence in control hiPSCs and thus induce the mutation. This can be done using two sgRNAs specific for either the starting or the end point of the deletion. However, even though this approach is easier as it does not require the insertion of a targeting construct, the deletion has to be induced in both chromosomes to produce a homozygous mutation.

After generating adequate controls further analyses are needed to better characterize the phenotypes observed in the CSB-deficient hiPSC-derived neurospheres. COFS hiPSC-derived neurospheres have been shown to exhibit a proliferation phenotype. This observation, however, has to be further confirmed. Proliferating COFS hiPSC-NPCs could be stained with Ki67, a marker for cell proliferation, and PI and annexin V, markers for cell death and apoptosis, respectively to distinguish the effect of decreased proliferation and increased cell death. Recently, Hibaoui et al. (2014) showed that hiPSC-derived NPCs from Down syndrome patients (DS-hiPSC-NPCs) exhibit decreased proliferation and increased apoptosis by determining the percentage of $Ki67^+$ cells and caspase-3 activity. Moreover, the study of Hibaoui showed that the differentiation potential from DS-hiPSC-NPCs was shifted from a neuronal towards a glial phenotype (Hibaoui et al. 2014). Therefore, qRT-PCR analysis could reveal if neuronal and glial markers are differently

expressed in CSB-deficient hiPSC-derived neurospheres compared to the control. Particularly, it would be interesting if the classical CSB-deficient hiPSC-derived neurospheres exhibit more neuronal and less glial gene expression compared to the control which would support the lack of GFAP positive astrocytes after 4 weeks of differentiation.

5. Literature

Aasen, T., A. Raya, M. J. Barrero, E. Garreta, A. Consiglio, F. Gonzalez, R. Vassena, J. Bilic, V. Pekarik, G. Tiscornia, M. Edel, S. Boue and J. C. Izpisua Belmonte (2008). "Efficient and rapid generation of induced pluripotent stem cells from human keratinocytes." Nat Biotechnol **26**(11): 1276-1284.

Aggarwal, S., L. Yurlova and M. Simons (2011). "Central nervous system myelin: structure, synthesis and assembly." Trends Cell Biol **21**(10): 585-593.

Alepee, N., A. Bahinski, M. Daneshian, B. De Wever, E. Fritsche, A. Goldberg, J. Hansmann, T. Hartung, J. Haycock, H. Hogberg, L. Hoelting, J. M. Kelm, S. Kadereit, E. McVey, R. Landsiedel, M. Leist, M. Lubberstedt, F. Noor, C. Pellevoisin, D. Petersohn, U. Pfannenbecker, K. Reisinger, T. Ramirez, B. Rothen-Rutishauser, M. Schafer-Korting, K. Zeilinger and M. G. Zurich (2014). "State-of-the-art of 3D cultures (organs-on-a-chip) in safety testing and pathophysiology." ALTEX **31**(4): 441-477.

Alvarez, J. I., A. Dodelet-Devillers, H. Kebir, I. Ifergan, P. J. Fabre, S. Terouz, M. Sabbagh, K. Wosik, L. Bourbonniere, M. Bernard, J. van Horssen, H. E. de Vries, F. Charron and A. Prat (2011). "The Hedgehog pathway promotes blood-brain barrier integrity and CNS immune quiescence." Science **334**(6063): 1727-1731.

Amir, R. E., I. B. Van den Veyver, M. Wan, C. Q. Tran, U. Francke and H. Y. Zoghbi (1999). "Rett syndrome is caused by mutations in X-linked MECP2, encoding methyl-CpG-binding protein 2." Nat Genet **23**(2): 185-188.

Amit, M. and J. Itskovitz-Eldor (2012). Morphology and of Human Embryonic and Induced Pluripotent Stem Cell Colonies Cultured with Feeders. Atlas of Human Pluripotent Stem Cells: Derivation and Culturing. M. Amit, Itskovitz-Eldor, J., Springer Science+Business Media.

Andersen, S. L. (2003). "Trajectories of brain development: point of vulnerability or window of opportunity?" Neurosci Biobehav Rev **27**(1-2): 3-18.

Andrade, L. N., J. L. Nathanson, G. W. Yeo, C. F. Menck and A. R. Muotri (2012). "Evidence for premature aging due to oxidative stress in iPSCs from Cockayne syndrome." Hum Mol Genet **21**(17): 3825-3834.

Araki, M., C. Masutani, M. Takemura, A. Uchida, K. Sugasawa, J. Kondoh, Y. Ohkuma and F. Hanaoka (2001). "Centrosome protein centrin 2/caltractin 1 is part of the xeroderma pigmentosum group C complex that initiates global genome nucleotide excision repair." J Biol Chem **276**(22): 18665-18672.

Aschner, M. (2000). "Neuron-astrocyte interactions: implications for cellular energetics and antioxidant levels." Neurotoxicology **21**(6): 1101-1107.

Bal-Price, A., K. M. Crofton, M. Leist, S. Allen, M. Arand, T. Buetler, N. Delrue, R. E. FitzGerald, T. Hartung, T. Heinonen, H. Hogberg, S. H. Bennekou, W. Lichtensteiger, D. Oggier, M. Paparella, M. Axelstad, A. Piersma, E. Rached, B. Schilter, G. Schmuck, L. Stoppini, E. Tongiorgi, M. Tiramani, F. Monnet-Tschudi, M. F. Wilks, T. Ylikomi and E. Fritsche (2015a). "International STakeholder NETwork (ISTNET): creating a developmental neurotoxicity (DNT) testing road map for regulatory purposes." Arch Toxicol **89**(2): 269-287.

Bal-Price, A., K. M. Crofton, M. Sachana, T. J. Shafer, M. Behl, A. Forsby, A. Hargreaves, B. Landesmann, P. J. Lein, J. Louisse, F. Monnet-Tschudi, A. Paini, A. Rolaki, A. Schrattenholz, C. Sunol, C. van Thriel, M. Whelan and E. Fritsche (2015b). "Putative adverse outcome pathways relevant to neurotoxicity." Crit Rev Toxicol **45**(1): 83-91.

Barkovich, A. J., R. I. Kuzniecky, G. D. Jackson, R. Guerrini and W. B. Dobyns (2005). "A developmental and genetic classification for malformations of cortical development." Neurology **65**(12): 1873-1887.

Baumann, J., M. Barenys, K. Gassmann and E. Fritsche (2014). "Comparative human and rat "neurosphere assay" for developmental neurotoxicity testing." Curr Protoc Toxicol **59**: 12 21 11-12 21 24.

Baumann, J., K. Gassmann, S. Masjosthusmann, D. DeBoer, F. Bendt, S. Giersiefer and E. Fritsche (2015) "Comparative human and rat neurospheres reveal species differences in chemical effects on neurodevelopmental key events." Arch Toxicol DOI: 10.1007/s00204-015-1568-8.

Beattie, G. M., A. D. Lopez, N. Bucay, A. Hinton, M. T. Firpo, C. C. King and A. Hayek (2005). "Activin A maintains pluripotency of human embryonic stem cells in the absence of feeder layers." Stem Cells **23**(4): 489-495.

Becker, K. A., P. N. Ghule, J. A. Therrien, J. B. Lian, J. L. Stein, A. J. van Wijnen and G. S. Stein (2006). "Self-renewal of human embryonic stem cells is supported by a shortened G1 cell cycle phase." J Cell Physiol **209**(3): 883-893.

Beerens, N., J. H. Hoeijmakers, R. Kanaar, W. Vermeulen and C. Wyman (2005). "The CSB protein actively wraps DNA." J Biol Chem **280**(6): 4722-4729.

Beers, J., D. R. Gulbranson, N. George, L. I. Siniscalchi, J. Jones, J. A. Thomson and G. Chen (2012). "Passaging and colony expansion of human pluripotent stem cells by enzyme-free dissociation in chemically defined culture conditions." Nat Protoc **7**(11): 2029-2040.

Bellin, M., M. C. Marchetto, F. H. Gage and C. L. Mummery (2012). "Induced pluripotent stem cells: the new patient?" Nat Rev Mol Cell Biol **13**(11): 713-726.

Bertout, J. A., S. A. Patel and M. C. Simon (2008). "The impact of O2 availability on human cancer." Nat Rev Cancer **8**(12): 967-975.

Blelloch, R., M. Venere, J. Yen and M. Ramalho-Santos (2007). "Generation of induced pluripotent stem cells in the absence of drug selection." Cell Stem Cell **1**(3): 245-247.

Bradsher, J., J. Auriol, L. Proietti de Santis, S. Iben, J. L. Vonesch, I. Grummt and J. M. Egly (2002). "CSB is a component of RNA pol I transcription." Mol Cell **10**(4): 819-829.

Breier, J. M., K. Gassmann, R. Kayser, H. Stegeman, D. De Groot, E. Fritsche and T. J. Shafer (2010). "Neural progenitor cells as models for high-throughput screens of developmental neurotoxicity: state of the science." Neurotoxicol Teratol **32**(1): 4-15.

Brennand, K. J., A. Simone, J. Jou, C. Gelboin-Burkhart, N. Tran, S. Sangar, Y. Li, Y. Mu, G. Chen, D. Yu, S. McCarthy, J. Sebat and F. H. Gage (2011). "Modelling schizophrenia using human induced pluripotent stem cells." Nature **473**(7346): 221-225.

Brooks, P. J., T. F. Cheng and L. Cooper (2008). "Do all of the neurologic diseases in patients with DNA repair gene mutations result from the accumulation of DNA damage?" DNA Repair (Amst) **7**(6): 834-848.

Catalina, P., F. Cobo, J. L. Cortes, A. I. Nieto, C. Cabrera, R. Montes, A. Concha and P. Menendez (2007). "Conventional and molecular cytogenetic diagnostic methods in stem cell research: a concise review." Cell Biol Int **31**(9): 861-869.

Chamberlain, S. J., P. F. Chen, K. Y. Ng, F. Bourgois-Rocha, F. Lemtiri-Chlieh, E. S. Levine and M. Lalande (2010). "Induced pluripotent stem cell models of the genomic imprinting disorders Angelman and Prader-Willi syndromes." Proc Natl Acad Sci U S A **107**(41): 17668-17673.

Chambers, I., D. Colby, M. Robertson, J. Nichols, S. Lee, S. Tweedie and A. Smith (2003). "Functional expression cloning of Nanog, a pluripotency sustaining factor in embryonic stem cells." Cell **113**(5): 643-655.

Chan, E. M., S. Ratanasirintrawoot, I. H. Park, P. D. Manos, Y. H. Loh, H. Huo, J. D. Miller, O. Hartung, J. Rho, T. A. Ince, G. Q. Daley and T. M. Schlaeger (2009). "Live cell imaging distinguishes bona fide human iPS cells from partially reprogrammed cells." Nat Biotechnol **27**(11): 1033-1037.

Chang, C. W., Y. S. Lai, E. Westin, A. Khodadadi-Jamayran, K. M. Pawlik, L. S. Lamb, Jr., F. D. Goldman and T. M. Townes (2015). "Modeling Human Severe Combined Immunodeficiency and Correction by CRISPR/Cas9-Enhanced Gene Targeting." Cell Rep **12**(10): 1668-1677.

Chen, Q., Y. C. Zhu, J. Yu, S. Miao, J. Zheng, L. Xu, Y. Zhou, D. Li, C. Zhang, J. Tao and Z. Q. Xiong (2010). "CDKL5, a protein associated with rett syndrome, regulates neuronal morphogenesis via Rac1 signaling." J Neurosci **30**(38): 12777-12786.

Chen, R. Z., S. Akbarian, M. Tudor and R. Jaenisch (2001). "Deficiency of methyl-CpG binding protein-2 in CNS neurons results in a Rett-like phenotype in mice." Nat Genet **27**(3): 327-331.

Cheung, A. Y., L. M. Horvath, D. Grafodatskaya, P. Pasceri, R. Weksberg, A. Hotta, L. Carrel and J. Ellis (2011). "Isolation of MECP2-null Rett Syndrome patient hiPS cells and isogenic controls through X-chromosome inactivation." Hum Mol Genet **20**(11): 2103-2115.

Chu, G. and E. Chang (1988). "Xeroderma pigmentosum group E cells lack a nuclear factor that binds to damaged DNA." Science **242**(4878): 564-567.

Ciaffardini, F., S. Nicolai, M. Caputo, G. Canu, E. Paccosi, M. Costantino, M. Frontini, A. S. Balajee and L. Proietti-De-Santis (2014). "The cockayne syndrome B protein is essential for neuronal differentiation and neuritogenesis." Cell Death Dis **5**: e1268.

Citterio, E., S. Rademakers, G. T. van der Horst, A. J. van Gool, J. H. Hoeijmakers and W. Vermeulen (1998). "Biochemical and biological characterization of wild-type and ATPase-deficient Cockayne syndrome B repair protein." J Biol Chem **273**(19): 11844-11851.

Citterio, E., V. Van Den Boom, G. Schnitzler, R. Kanaar, E. Bonte, R. E. Kingston, J. H. Hoeijmakers and W. Vermeulen (2000). "ATP-dependent chromatin remodeling by the Cockayne syndrome B DNA repair-transcription-coupling factor." Mol Cell Biol **20**(20): 7643-7653.

Coecke, S., A. M. Goldberg, S. Allen, L. Buzanska, G. Calamandrei, K. Crofton, L. Hareng, T. Hartung, H. Knaut, P. Honegger, M. Jacobs, P. Lein, A. Li, W. Mundy, D. Owen, S. Schneider, E. Silbergeld, T. Reum, T. Trnovec, F. Monnet-Tschudi and A. Bal-Price (2007). "Workgroup report: incorporating in vitro alternative methods for developmental neurotoxicity into international hazard and risk assessment strategies." Environ Health Perspect **115**(6): 924-931.

Cooke, M. J., M. Stojkovic and S. A. Przyborski (2006). "Growth of teratomas derived from human pluripotent stem cells is influenced by the graft site." Stem Cells Dev **15**(2): 254-259.

Courtot, A. M., A. Magniez, N. Oudrhiri, O. Feraud, J. Bacci, E. Gobbo, S. Proust, A. G. Turhan and A. Bennaceur-Griscelli (2014). "Morphological analysis of human induced pluripotent stem cells during induced differentiation and reverse programming." Biores Open Access **3**(5): 206-216.

Crocco, M. C., N. Fratnz and A. Bos-Mikich (2013). "Substrates and supplements for hESCs: a critical review." J Assist Reprod Genet **30**(3): 315-323.

de Hoz, L. and M. Simons (2015). "The emerging functions of oligodendrocytes in regulating neuronal network behaviour." Bioessays **37**(1): 60-69.

Denham, M. and M. Dottori (2011). "Neural differentiation of induced pluripotent stem cells." Methods Mol Biol **793**: 99-110.

Dianov, G., C. Bischoff, J. Piotrowski and V. A. Bohr (1998). "Repair pathways for processing of 8-oxoguanine in DNA by mammalian cell extracts." J Biol Chem **273**(50): 33811-33816.

Dianov, G., C. Bischoff, M. Sunesen and V. A. Bohr (1999). "Repair of 8-oxoguanine in DNA is deficient in Cockayne syndrome group B cells." Nucleic Acids Res **27**(5): 1365-1368.

Dimos, J. T., K. T. Rodolfa, K. K. Niakan, L. M. Weisenthal, H. Mitsumoto, W. Chung, G. F. Croft, G. Saphier, R. Leibel, R. Goland, H. Wichterle, C. E. Henderson and K. Eggan (2008). "Induced pluripotent stem cells generated from patients with ALS can be differentiated into motor neurons." Science **321**(5893): 1218-1221.

Dravid, G., Z. Ye, H. Hammond, G. Chen, A. Pyle, P. Donovan, X. Yu and L. Cheng (2005). "Defining the role of Wnt/beta-catenin signaling in the survival, proliferation, and self-renewal of human embryonic stem cells." Stem Cells **23**(10): 1489-1501.

Du, J., E. Campau, E. Soragni, S. Ku, J. W. Puckett, P. B. Dervan and J. M. Gottesfeld (2012). "Role of mismatch repair enzymes in GAA.TTC triplet-repeat expansion in Friedreich ataxia induced pluripotent stem cells." J Biol Chem **287**(35): 29861-29872.

Dunnett, S. B. and A. E. Rosser (2014). "Challenges for taking primary and stem cells into clinical neurotransplantation trials for neurodegenerative disease." Neurobiol Dis **61**: 79-89.

Eminli, S., A. Foudi, M. Stadtfeld, N. Maherali, T. Ahfeldt, G. Mostoslavsky, H. Hock and K. Hochedlinger (2009). "Differentiation stage determines potential of hematopoietic cells for reprogramming into induced pluripotent stem cells." Nat Genet **41**(9): 968-976.

Eriksson, P. S., E. Perfilieva, T. Bjork-Eriksson, A. M. Alborn, C. Nordborg, D. A. Peterson and F. H. Gage (1998). "Neurogenesis in the adult human hippocampus." Nat Med **4**(11): 1313-1317.

Espuny-Camacho, I., K. A. Michelsen, D. Gall, D. Linaro, A. Hasche, J. Bonnefont, C. Bali, D. Orduz, A. Bilheu, A. Herpoel, N. Lambert, N. Gaspard, S. Peron, S. N. Schiffmann, M. Giugliano, A. Gaillard and P. Vanderhaeghen (2013). "Pyramidal neurons derived from human pluripotent stem cells integrate efficiently into mouse brain circuits in vivo." Neuron **77**(3): 440-456.

Fatt, P. and B. Katz (1950). "Some observations on biological noise." Nature **166**(4223): 597-598.

Filippi, S., P. Latini, M. Frontini, F. Palitti, J. M. Egly and L. Proietti-De-Santis (2008). "CSB protein is (a direct target of HIF-1 and) a critical mediator of the hypoxic response." EMBO J **27**(19): 2545-2556.

Fortin, D., E. Rom, H. Sun, A. Yayon and R. Bansal (2005). "Distinct fibroblast growth factor (FGF)/FGF receptor signaling pairs initiate diverse cellular responses in the oligodendrocyte lineage." J Neurosci **25**(32): 7470-7479.

Fousteri, M. and L. H. Mullenders (2008). "Transcription-coupled nucleotide excision repair in mammalian cells: molecular mechanisms and biological effects." Cell Res **18**(1): 73-84.

Fritsche, E., K. Gassmann and T. Schreiber (2011). "Neurospheres as a model for developmental neurotoxicity testing." Methods Mol Biol **758**: 99-114.

Frontini, M. and L. Proietti-De-Santis (2012). "Interaction between the Cockayne syndrome B and p53 proteins: implications for aging." Aging (Albany NY) **4**(2): 89-97.

Fuchs, S. Y., V. Adler, T. Buschmann, X. Wu and Z. Ronai (1998). "Mdm2 association with p53 targets its ubiquitination." Oncogene **17**(19): 2543-2547.

Fujiwara, Y., M. Ichihashi, Y. Kano, K. Goto and K. Shimizu (1981). "A new human photosensitive subject with a defect in the recovery of DNA synthesis after ultraviolet-light irradiation." J Invest Dermatol **77**(3): 256-263.

Fukusumi, H., T. Shofuda, D. Kanematsu, A. Yamamoto, H. Suemizu, M. Nakamura, M. Yamasaki, M. Ohgushi, Y. Sasai and Y. Kanemura (2013). "Feeder-free generation and long-term culture of human induced pluripotent stem cells using pericellular matrix of decidua derived mesenchymal cells." PLoS One **8**(1): e55226.

Fuss, J. O. and J. A. Tainer (2011). "XPB and XPD helicases in TFIIH orchestrate DNA duplex opening and damage verification to coordinate repair with transcription and cell cycle via CAK kinase." DNA Repair (Amst) **10**(7): 697-713.

Garcia-Parra, P., M. Maroto, F. Cavaliere, N. Naldaiz-Gastesi, J. I. Alava, A. G. Garcia, A. Lopez de Munain and A. Izeta (2013) "A neural extracellular matrix-based method for in vitro hippocampal neuron culture and dopaminergic differentiation of neural stem cells." BMC Neurosci **14**, 48 DOI: 10.1186/1471-2202-14-48.

Gassmann, K., J. Abel, H. Bothe, T. Haarmann-Stemmann, H. F. Merk, K. N. Quasthoff, T. D. Rockel, T. Schreiber and E. Fritsche (2010). "Species-specific differential AhR expression protects human neural progenitor cells against developmental neurotoxicity of PAHs." Environ Health Perspect **118**(11): 1571-1577.

Gerrard, L., L. Rodgers and W. Cui (2005). "Differentiation of human embryonic stem cells to neural lineages in adherent culture by blocking bone morphogenetic protein signaling." Stem Cells **23**(9): 1234-1241.

Ghule, P. N., K. A. Becker, J. W. Harper, J. B. Lian, J. L. Stein, A. J. van Wijnen and G. S. Stein (2007). "Cell cycle dependent phosphorylation and subnuclear organization of the histone gene regulator p220(NPAT) in human embryonic stem cells." J Cell Physiol **213**(1): 9-17.

Gonzalez, F., S. Boue and J. C. Izpisua Belmonte (2011). "Methods for making induced pluripotent stem cells: reprogramming a la carte." Nat Rev Genet **12**(4): 231-242.

Grandjean, P. and P. J. Landrigan (2006). "Developmental neurotoxicity of industrial chemicals." Lancet **368**(9553): 2167-2178.

Greber, B., H. Lehrach and J. Adjaye (2007). "Fibroblast growth factor 2 modulates transforming growth factor beta signaling in mouse embryonic fibroblasts and human ESCs (hESCs) to support hESC self-renewal." Stem Cells **25**(2): 455-464.

Guillemin, G. J. and B. J. Brew (2004). "Microglia, macrophages, perivascular macrophages, and pericytes: a review of function and identification." J Leukoc Biol **75**(3): 388-397.
Hanawalt, P. C. (2002). "Subpathways of nucleotide excision repair and their regulation." Oncogene **21**(58): 8949-8956.
Hanawalt, P. C. and G. Spivak (2008). "Transcription-coupled DNA repair: two decades of progress and surprises." Nat Rev Mol Cell Biol **9**(12): 958-970.
Harrill, J. A., T. M. Freudenrich, B. L. Robinette and W. R. Mundy (2011). "Comparative sensitivity of human and rat neural cultures to chemical-induced inhibition of neurite outgrowth." Toxicol Appl Pharmacol **256**(3): 268-280.
Hayashi, M., M. Itoh, S. Araki, S. Kumada, K. Shioda, K. Tamagawa, T. Mizutani, Y. Morimatsu, M. Minagawa and M. Oda (2001). "Oxidative stress and disturbed glutamate transport in hereditary nucleotide repair disorders." J Neuropathol Exp Neurol **60**(4): 350-356.
Heikkila, T. J., L. Yla-Outinen, J. M. Tanskanen, R. S. Lappalainen, H. Skottman, R. Suuronen, J. E. Mikkonen, J. A. Hyttinen and S. Narkilahti (2009). "Human embryonic stem cell-derived neuronal cells form spontaneously active neuronal networks in vitro." Exp Neurol **218**(1): 109-116.
Henning, K. A., L. Li, N. Iyer, L. D. McDaniel, M. S. Reagan, R. Legerski, R. A. Schultz, M. Stefanini, A. R. Lehmann, L. V. Mayne and E. C. Friedberg (1995). "The Cockayne syndrome group A gene encodes a WD repeat protein that interacts with CSB protein and a subunit of RNA polymerase II TFIIH." Cell **82**(4): 555-564.
Hibaoui, Y., I. Grad, A. Letourneau, M. R. Sailani, S. Dahoun, F. A. Santoni, S. Gimelli, M. Guipponi, M. F. Pelte, F. Bena, S. E. Antonarakis and A. Feki (2014). "Modelling and rescuing neurodevelopmental defect of Down syndrome using induced pluripotent stem cells from monozygotic twins discordant for trisomy 21." EMBO Mol Med **6**(2): 259-277.
Hick, A., M. Wattenhofer-Donze, S. Chintawar, P. Tropel, J. P. Simard, N. Vaucamps, D. Gall, L. Lambot, C. Andre, L. Reutenauer, M. Rai, M. Teletin, N. Messaddeq, S. N. Schiffmann, S. Viville, C. E. Pearson, M. Pandolfo and H. Puccio (2013). "Neurons and cardiomyocytes derived from induced pluripotent stem cells as a model for mitochondrial defects in Friedreich's ataxia." Dis Model Mech **6**(3): 608-621.
Hochmann, S., J. Kaslin, S. Hans, A. Weber, A. Machate, M. Geffarth, R. H. Funk and M. Brand (2012). "Fgf signaling is required for photoreceptor maintenance in the adult zebrafish retina." PLoS One **7**(1): e30365.
Holcomb, P. S., T. J. Deerinck, M. H. Ellisman and G. A. Spirou (2013). "Construction of a polarized neuron." J Physiol **591**(Pt 13): 3145-3150.
Holz, R. W. and S. K. Fisher (1999). Synaptic Transmission and Cellular Signaling: An Overview. Basic Neurochemistry: Molecular, Cellular and Medical Aspects. G. J. Siegel, Agranoff, B.W., Albers, R.W., Fisher, S.K., Uhler, M.D. **6th Edition**.
Horibata, K., Y. Iwamoto, I. Kuraoka, N. G. Jaspers, A. Kurimasa, M. Oshimura, M. Ichihashi and K. Tanaka (2004). "Complete absence of Cockayne syndrome group B gene product gives rise to UV-sensitive syndrome but not Cockayne syndrome." Proc Natl Acad Sci U S A **101**(43): 15410-15415.
Hu, B. Y., J. P. Weick, J. Yu, L. X. Ma, X. Q. Zhang, J. A. Thomson and S. C. Zhang (2010). "Neural differentiation of human induced pluripotent stem cells follows developmental principles but with variable potency." Proc Natl Acad Sci U S A **107**(9): 4335-4340.
Hughes, C. S., L. M. Postovit and G. A. Lajoie (2010). "Matrigel: a complex protein mixture required for optimal growth of cell culture." Proteomics **10**(9): 1886-1890.
Hurst, J. A., M. Markiewicz, D. Kumar and E. M. Brett (1988). "Unknown syndrome: Hirschsprung's disease, microcephaly, and iris coloboma: a new syndrome of defective neuronal migration." J Med Genet **25**(7): 494-497.
Israel, M. A., S. H. Yuan, C. Bardy, S. M. Reyna, Y. Mu, C. Herrera, M. P. Hefferan, S. Van Gorp, K. L. Nazor, F. S. Boscolo, C. T. Carson, L. C. Laurent, M. Marsala, F. H. Gage, A. M. Remes, E. H. Koo and L. S. Goldstein (2012). "Probing sporadic and familial Alzheimer's disease using induced pluripotent stem cells." Nature **482**(7384): 216-220.

Itskovitz-Eldor, J., M. Schuldiner, D. Karsenti, A. Eden, O. Yanuka, M. Amit, H. Soreq and N. Benvenisty (2000). "Differentiation of human embryonic stem cells into embryoid bodies compromising the three embryonic germ layers." Mol Med **6**(2): 88-95.

Jaspers, N. G. (1996). "Multiple involvement of nucleotide excision repair enzymes: clinical manifestations of molecular intricacies." Cytokines Mol Ther **2**(2): 115-119.

Jeppesen, D. K., V. A. Bohr and T. Stevnsner (2011). "DNA repair deficiency in neurodegeneration." Prog Neurobiol **94**(2): 166-200.

Jia, F., K. D. Wilson, N. Sun, D. M. Gupta, M. Huang, Z. Li, N. J. Panetta, Z. Y. Chen, R. C. Robbins, M. A. Kay, M. T. Longaker and J. C. Wu (2010). "A nonviral minicircle vector for deriving human iPS cells." Nat Methods **7**(3): 197-199.

Jiang, X. and J. Nardelli (2015) "Cellular and molecular introduction to brain development." Neurobiol Dis DOI: 10.1016/j.nbd.2015.07.007.

Jozefczuk, J., K. Drews and J. Adjaye (2012). "Preparation of mouse embryonic fibroblast cells suitable for culturing human embryonic and induced pluripotent stem cells." J Vis Exp(64): e3854.

Jung, A. B. and J. P. Bennett, Jr. (1996). "Development of striatal dopaminergic function. III: Pre- and postnatal development of striatal and cortical mRNAs for the neurotrophin receptors trkBTK+ and trkC and their regulation by synaptic dopamine." Brain Res Dev Brain Res **94**(2): 133-143.

Kahler, D. J., F. S. Ahmad, A. Ritz, H. Hua, D. N. Moroziewicz, A. A. Sproul, C. R. Dusenberry, L. Shang, D. Paull, M. Zimmer, K. A. Weiss, D. Egli and S. A. Noggle (2013). "Improved methods for reprogramming human dermal fibroblasts using fluorescence activated cell sorting." PLoS One **8**(3): e59867.

Kaji, K., K. Norrby, A. Paca, M. Mileikovsky, P. Mohseni and K. Woltjen (2009). "Virus-free induction of pluripotency and subsequent excision of reprogramming factors." Nature **458**(7239): 771-775.

Kamenisch, Y. and M. Berneburg (2009). "Progeroid syndromes and UV-induced oxidative DNA damage." J Investig Dermatol Symp Proc **14**(1): 8-14.

Kandel, E. R., Schwartz, J.H, Jessell, T.M. (2000). Principles of neural science, Elsevier New York.

Kao, C. F., C. Y. Chuang, C. H. Chen and H. C. Kuo (2008). "Human pluripotent stem cells: current status and future perspectives." Chin J Physiol **51**(4): 214-225.

Karumbayaram, S., B. G. Novitch, M. Patterson, J. A. Umbach, L. Richter, A. Lindgren, A. E. Conway, A. T. Clark, S. A. Goldman, K. Plath, M. Wiedau-Pazos, H. I. Kornblum and W. E. Lowry (2009). "Directed differentiation of human-induced pluripotent stem cells generates active motor neurons." Stem Cells **27**(4): 806-811.

Kastenberg, Z. J. and J. S. Odorico (2008). "Alternative sources of pluripotency: science, ethics, and stem cells." Transplant Rev (Orlando) **22**(3): 215-222.

Kavalali, E. T. (2015). "The mechanisms and functions of spontaneous neurotransmitter release." Nat Rev Neurosci **16**(1): 5-16.

Keaney, J. and M. Campbell (2015). "The dynamic blood-brain barrier." FEBS J **282**(21): 4067-4079.

Kennedy, R. M., V. D. Rowe and J. J. Kepes (1980). "Cockayne syndrome: an atypical case." Neurology **30**(12): 1268-1272.

Kim, D., C. H. Kim, J. I. Moon, Y. G. Chung, M. Y. Chang, B. S. Han, S. Ko, E. Yang, K. Y. Cha, R. Lanza and K. S. Kim (2009). "Generation of human induced pluripotent stem cells by direct delivery of reprogramming proteins." Cell Stem Cell **4**(6): 472-476.

Kleinman, H. K. and G. R. Martin (2005). "Matrigel: basement membrane matrix with biological activity." Semin Cancer Biol **15**(5): 378-386.

Kohji, T., M. Hayashi, K. Shioda, M. Minagawa, Y. Morimatsu, K. Tamagawa and M. Oda (1998). "Cerebellar neurodegeneration in human hereditary DNA repair disorders." Neurosci Lett **243**(1-3): 133-136.

Kolb, B. and R. Gibb (2011). "Brain plasticity and behaviour in the developing brain." J Can Acad Child Adolesc Psychiatry **20**(4): 265-276.

Kraemer, K. H., N. J. Patronas, R. Schiffmann, B. P. Brooks, D. Tamura and J. J. DiGiovanna (2007). "Xeroderma pigmentosum, trichothiodystrophy and Cockayne syndrome: a complex genotype-phenotype relationship." Neuroscience **145**(4): 1388-1396.

Kreutzberg, G. W. (1996). "Microglia: a sensor for pathological events in the CNS." Trends Neurosci **19**(8): 312-318.

Kristensen, U., A. Epanchintsev, M. A. Rauschendorf, V. Laugel, T. Stevnsner, V. A. Bohr, F. Coin and J. M. Egly (2013). "Regulatory interplay of Cockayne syndrome B ATPase and stress-response gene ATF3 following genotoxic stress." Proc Natl Acad Sci U S A **110**(25): E2261-2270.

Kucukdereli, H., N. J. Allen, A. T. Lee, A. Feng, M. I. Ozlu, L. M. Conatser, C. Chakraborty, G. Workman, M. Weaver, E. H. Sage, B. A. Barres and C. Eroglu (2011). "Control of excitatory CNS synaptogenesis by astrocyte-secreted proteins Hevin and SPARC." Proc Natl Acad Sci U S A **108**(32): E440-449.

Kuhn, H. G., J. Winkler, G. Kempermann, L. J. Thal and F. H. Gage (1997). "Epidermal growth factor and fibroblast growth factor-2 have different effects on neural progenitors in the adult rat brain." J Neurosci **17**(15): 5820-5829.

Kurosawa, H. (2012). "Application of Rho-associated protein kinase (ROCK) inhibitor to human pluripotent stem cells." J Biosci Bioeng **114**(6): 577-581.

Lagerwerf, S., M. G. Vrouwe, R. M. Overmeer, M. I. Fousteri and L. H. Mullenders (2011). "DNA damage response and transcription." DNA Repair (Amst) **10**(7): 743-750.

Lai, Y., A. Asthana, K. Cheng and W. S. Kisaalita (2011). "Neural cell 3D microtissue formation is marked by cytokines' up-regulation." PLoS One **6**(10): e26821.

Lamb, T. M., A. K. Knecht, W. C. Smith, S. E. Stachel, A. N. Economides, N. Stahl, G. D. Yancopolous and R. M. Harland (1993). "Neural induction by the secreted polypeptide noggin." Science **262**(5134): 713-718.

Lancaster, M. A., M. Renner, C. A. Martin, D. Wenzel, L. S. Bicknell, M. E. Hurles, T. Homfray, J. M. Penninger, A. P. Jackson and J. A. Knoblich (2013). "Cerebral organoids model human brain development and microcephaly." Nature **501**(7467): 373-379.

Latini, P., M. Frontini, M. Caputo, J. Gregan, L. Cipak, S. Filippi, V. Kumar, R. Velez-Cruz, M. Stefanini and L. Proietti-De-Santis (2011). "CSA and CSB proteins interact with p53 and regulate its Mdm2-dependent ubiquitination." Cell Cycle **10**(21): 3719-3730.

Laugel, V., C. Dalloz, A. Stary, V. Cormier-Daire, I. Desguerre, M. Renouil, A. Fourmaintraux, R. Velez-Cruz, J. M. Egly, A. Sarasin and H. Dollfus (2008a). "Deletion of 5' sequences of the CSB gene provides insight into the pathophysiology of Cockayne syndrome." Eur J Hum Genet **16**(3): 320-327.

Laugel, V., C. Dalloz, E. S. Tobias, J. L. Tolmie, D. Martin-Coignard, V. Drouin-Garraud, V. Valayannopoulos, A. Sarasin and H. Dollfus (2008b). "Cerebro-oculo-facio-skeletal syndrome: three additional cases with CSB mutations, new diagnostic criteria and an approach to investigation." J Med Genet **45**(9): 564-571.

Laugel, V., C. Dalloz, M. Durand, F. Sauvanaud, U. Kristensen, M. C. Vincent, L. Pasquier, S. Odent, V. Cormier-Daire, B. Gener, E. S. Tobias, J. L. Tolmie, D. Martin-Coignard, V. Drouin-Garraud, D. Heron, H. Journel, E. Raffo, J. Vigneron, S. Lyonnet, V. Murday, D. Gubser-Mercati, B. Funalot, L. Brueton, J. Sanchez Del Pozo, E. Munoz, A. R. Gennery, M. Salih, M. Noruzinia, K. Prescott, L. Ramos, Z. Stark, K. Fieggen, B. Chabrol, P. Sarda, P. Edery, A. Bloch-Zupan, H. Fawcett, D. Pham, J. M. Egly, A. R. Lehmann, A. Sarasin and H. Dollfus (2010). "Mutation update for the CSB/ERCC6 and CSA/ERCC8 genes involved in Cockayne syndrome." Hum Mutat **31**(2): 113-126.

Laugel, V. (2013). "Cockayne syndrome: the expanding clinical and mutational spectrum." Mech Ageing Dev **134**(5-6): 161-170.

Lein, P., P. Locke and A. Goldberg (2007). "Meeting report: alternatives for developmental neurotoxicity testing." Environ Health Perspect **115**(5): 764-768.

Leist, M. and T. Hartung (2013). "Inflammatory findings on species extrapolations: humans are definitely no 70-kg mice." Arch Toxicol **87**(4): 563-567.

Levi, G., G. P. Wilkin, M. T. Ciotti and S. Johnstone (1983). "Enrichment of differentiated, stellate astrocytes in cerebellar interneuron cultures as studied by GFAP immunofluorescence

and autoradiographic uptake patterns with [3H]D-aspartate and [3H]GABA." Brain Res **312**(2): 227-241.
Li, C. and J. Wang (2013). "Quantifying Waddington landscapes and paths of non-adiabatic cell fate decisions for differentiation, reprogramming and transdifferentiation." J R Soc Interface **10**(89): 20130787.
Lim, J. W. and A. Bodnar (2002). "Proteome analysis of conditioned medium from mouse embryonic fibroblast feeder layers which support the growth of human embryonic stem cells." Proteomics **2**(9): 1187-1203.
Linderkamp, O., L. Janus, R. Linder and D. B. Skoruppa (2009). "Time Table of Normal Foetal Brain Development." Int. J. Prenatal and Prenatal Psychology and Medicine **21**: 4-16.
Llames, S., E. Garcia-Perez, A. Meana, F. Larcher and M. del Rio (2015). "Feeder Layer Cell Actions and Applications." Tissue Eng Part B Rev **21**(4): 345-353.
Longo, L. D. (1980). "Environmental pollution and pregnancy: risks and uncertainties for the fetus and infant." Am J Obstet Gynecol **137**(2): 162-173.
Lowry, R. B., R. MacLean, D. M. McLean and B. Tischler (1971). "Cataracts, microcephaly, kyphosis, and limited joint movement in two siblings: a new syndrome." J Pediatr **79**(2): 282-284.
Lowry, R. B. (1982). "Early onset of Cockayne syndrome." Am J Med Genet **13**(2): 209-210.
Lu, H. F., C. Chai, T. C. Lim, M. F. Leong, J. K. Lim, S. Gao, K. L. Lim and A. C. Wan (2014). "A defined xeno-free and feeder-free culture system for the derivation, expansion and direct differentiation of transgene-free patient-specific induced pluripotent stem cells." Biomaterials **35**(9): 2816-2826.
Ludwig, T. E., V. Bergendahl, M. E. Levenstein, J. Yu, M. D. Probasco and J. A. Thomson (2006). "Feeder-independent culture of human embryonic stem cells." Nat Methods **3**(8): 637-646.
Maitra, A., D. E. Arking, N. Shivapurkar, M. Ikeda, V. Stastny, K. Kassauei, G. Sui, D. J. Cutler, Y. Liu, S. N. Brimble, K. Noaksson, J. Hyllner, T. C. Schulz, X. Zeng, W. J. Freed, J. Crook, S. Abraham, A. Colman, P. Sartipy, S. Matsui, M. Carpenter, A. F. Gazdar, M. Rao and A. Chakravarti (2005). "Genomic alterations in cultured human embryonic stem cells." Nat Genet **37**(10): 1099-1103.
Majmundar, A. J., W. J. Wong and M. C. Simon (2010). "Hypoxia-inducible factors and the response to hypoxic stress." Mol Cell **40**(2): 294-309.
Mali, P., K. M. Esvelt and G. M. Church (2013). "Cas9 as a versatile tool for engineering biology." Nat Methods **10**(10): 957-963.
Marchetto, M. C., C. Carromeu, A. Acab, D. Yu, G. W. Yeo, Y. Mu, G. Chen, F. H. Gage and A. R. Muotri (2010). "A model for neural development and treatment of Rett syndrome using human induced pluripotent stem cells." Cell **143**(4): 527-539.
Marchetto, M. C., K. J. Brennand, L. F. Boyer and F. H. Gage (2011). "Induced pluripotent stem cells (iPSCs) and neurological disease modeling: progress and promises." Hum Mol Genet **20**(R2): R109-115.
Mason, I. (2007). "Initiation to end point: the multiple roles of fibroblast growth factors in neural development." Nat Rev Neurosci **8**(8): 583-596.
Massobrio, P., J. Tessadori, M. Chiappalone and M. Ghirardi (2015). "In vitro studies of neuronal networks and synaptic plasticity in invertebrates and in mammals using multielectrode arrays." Neural Plast **2015**: 196195.
Mayne, L. V. and A. R. Lehmann (1982). "Failure of RNA synthesis to recover after UV irradiation: an early defect in cells from individuals with Cockayne's syndrome and xeroderma pigmentosum." Cancer Res **42**(4): 1473-1478.
McMahon, A. P. and A. Bradley (1990). "The Wnt-1 (int-1) proto-oncogene is required for development of a large region of the mouse brain." Cell **62**(6): 1073-1085.
Meira, L. B., J. M. Graham, Jr., C. R. Greenberg, D. B. Busch, A. T. Doughty, D. W. Ziffer, D. M. Coleman, I. Savre-Train and E. C. Friedberg (2000). "Manitoba aboriginal kindred with original cerebro-oculo- facio-skeletal syndrome has a mutation in the Cockayne syndrome group B (CSB) gene." Am J Hum Genet **66**(4): 1221-1228.

Melis, J. P., H. van Steeg and M. Luijten (2013). "Oxidative DNA damage and nucleotide excision repair." Antioxid Redox Signal **18**(18): 2409-2419.
Mitne-Neto, M., M. Machado-Costa, M. C. Marchetto, M. H. Bengtson, C. A. Joazeiro, H. Tsuda, H. J. Bellen, H. C. Silva, A. S. Oliveira, M. Lazar, A. R. Muotri and M. Zatz (2011). "Downregulation of VAPB expression in motor neurons derived from induced pluripotent stem cells of ALS8 patients." Hum Mol Genet **20**(18): 3642-3652.
Mitsui, K., Y. Tokuzawa, H. Itoh, K. Segawa, M. Murakami, K. Takahashi, M. Maruyama, M. Maeda and S. Yamanaka (2003). "The homeoprotein Nanog is required for maintenance of pluripotency in mouse epiblast and ES cells." Cell **113**(5): 631-642.
Mohamad, O., S. P. Yu, D. Chen, M. Ogle, M. Song and L. Wei (2013). "Efficient neuronal differentiation of mouse ES and iPS cells using a rotary cell culture protocol." Differentiation **86**(4-5): 149-158.
Moors, M., J. E. Cline, J. Abel and E. Fritsche (2007). "ERK-dependent and -independent pathways trigger human neural progenitor cell migration." Toxicol Appl Pharmacol **221**(1): 57-67.
Moors, M., T. D. Rockel, J. Abel, J. E. Cline, K. Gassmann, T. Schreiber, J. Schuwald, N. Weinmann and E. Fritsche (2009). "Human neurospheres as three-dimensional cellular systems for developmental neurotoxicity testing." Environ Health Perspect **117**(7): 1131-1138.
Moreau, M. and C. Leclerc (2004). "The choice between epidermal and neural fate: a matter of calcium." Int J Dev Biol **48**(2-3): 75-84.
Moser, J., H. Kool, I. Giakzidis, K. Caldecott, L. H. Mullenders and M. I. Fousteri (2007). "Sealing of chromosomal DNA nicks during nucleotide excision repair requires XRCC1 and DNA ligase III alpha in a cell-cycle-specific manner." Mol Cell **27**(2): 311-323.
Moyer, D. B., P. Marquis, M. E. Shertzer and B. K. Burton (1982). "Cockayne syndrome with early onset of manifestations." Am J Med Genet **13**(2): 225-230.
Mummery, C. (2011). "Induced pluripotent stem cells--a cautionary note." N Engl J Med **364**(22): 2160-2162.
Munoz-Sanjuan, I. and A. H. Brivanlou (2002). "Neural induction, the default model and embryonic stem cells." Nat Rev Neurosci **3**(4): 271-280.
Nakagawa, M., M. Koyanagi, K. Tanabe, K. Takahashi, T. Ichisaka, T. Aoi, K. Okita, Y. Mochiduki, N. Takizawa and S. Yamanaka (2008). "Generation of induced pluripotent stem cells without Myc from mouse and human fibroblasts." Nat Biotechnol **26**(1): 101-106.
Nakagawa, M., Y. Taniguchi, S. Senda, N. Takizawa, T. Ichisaka, K. Asano, A. Morizane, D. Doi, J. Takahashi, M. Nishizawa, Y. Yoshida, T. Toyoda, K. Osafune, K. Sekiguchi and S. Yamanaka (2014). "A novel efficient feeder-free culture system for the derivation of human induced pluripotent stem cells." Sci Rep **4**: 3594.
Nance, M. A. and S. A. Berry (1992). "Cockayne syndrome: review of 140 cases." Am J Med Genet **42**(1): 68-84.
Nardo, T., R. Oneda, G. Spivak, B. Vaz, L. Mortier, P. Thomas, D. Orioli, V. Laugel, A. Stary, P. C. Hanawalt, A. Sarasin and M. Stefanini (2009). "A UV-sensitive syndrome patient with a specific CSA mutation reveals separable roles for CSA in response to UV and oxidative DNA damage." Proc Natl Acad Sci U S A **106**(15): 6209-6214.
Neubig, R. R., M. Spedding, T. Kenakin, A. Christopoulos, N. International Union of Pharmacology Committee on Receptor and C. Drug (2003). "International Union of Pharmacology Committee on Receptor Nomenclature and Drug Classification. XXXVIII. Update on terms and symbols in quantitative pharmacology." Pharmacol Rev **55**(4): 597-606.
Newman, A. M. and J. B. Cooper (2010). "Lab-specific gene expression signatures in pluripotent stem cells." Cell Stem Cell **7**(2): 258-262.
Newman, J. C., A. D. Bailey and A. M. Weiner (2006). "Cockayne syndrome group B protein (CSB) plays a general role in chromatin maintenance and remodeling." Proc Natl Acad Sci U S A **103**(25): 9613-9618.
Nguyen, H. N., B. Byers, B. Cord, A. Shcheglovitov, J. Byrne, P. Gujar, K. Kee, B. Schule, R. E. Dolmetsch, W. Langston, T. D. Palmer and R. R. Pera (2011). "LRRK2 mutant iPSC-derived DA neurons demonstrate increased susceptibility to oxidative stress." Cell Stem Cell **8**(3): 267-280.

Nichols, J., B. Zevnik, K. Anastassiadis, H. Niwa, D. Klewe-Nebenius, I. Chambers, H. Scholer and A. Smith (1998). "Formation of pluripotent stem cells in the mammalian embryo depends on the POU transcription factor Oct4." Cell **95**(3): 379-391.

Niedernhofer, L. J. (2008). "Nucleotide excision repair deficient mouse models and neurological disease." DNA Repair (Amst) **7**(7): 1180-1189.

Nouspikel, T. (2009). "DNA repair in mammalian cells : Nucleotide excision repair: variations on versatility." Cell Mol Life Sci **66**(6): 994-1009.

Odawara, A., Y. Saitoh, A. H. Alhebshi, M. Gotoh and I. Suzuki (2014). "Long-term electrophysiological activity and pharmacological response of a human induced pluripotent stem cell-derived neuron and astrocyte co-culture." Biochem Biophys Res Commun **443**(4): 1176-1181.

Ohtsuka, S. and S. Dalton (2008). "Molecular and biological properties of pluripotent embryonic stem cells." Gene Ther **15**(2): 74-81.

Okano, H. and S. Yamanaka (2014). "iPS cell technologies: significance and applications to CNS regeneration and disease." Mol Brain **7**: 22.

Okita, K., T. Ichisaka and S. Yamanaka (2007). "Generation of germline-competent induced pluripotent stem cells." Nature **448**(7151): 313-317.

Okita, K., M. Nakagawa, H. Hyenjong, T. Ichisaka and S. Yamanaka (2008). "Generation of mouse induced pluripotent stem cells without viral vectors." Science **322**(5903): 949-953.

Okita, K., Y. Matsumura, Y. Sato, A. Okada, A. Morizane, S. Okamoto, H. Hong, M. Nakagawa, K. Tanabe, K. Tezuka, T. Shibata, T. Kunisada, M. Takahashi, J. Takahashi, H. Saji and S. Yamanaka (2011). "A more efficient method to generate integration-free human iPS cells." Nat Methods **8**(5): 409-412.

Park, I. H., R. Zhao, J. A. West, A. Yabuuchi, H. Huo, T. A. Ince, P. H. Lerou, M. W. Lensch and G. Q. Daley (2008). "Reprogramming of human somatic cells to pluripotency with defined factors." Nature **451**(7175): 141-146.

Pei, Y., J. Peng, M. Behl, N. S. Sipes, K. R. Shockley, M. S. Rao, R. R. Tice and X. Zeng (2015) "Comparative neurotoxicity screening in human iPSC-derived neural stem cells, neurons and astrocytes." Brain Res DOI: 10.1016/j.brainres.2015.07.048.

Pena, S. D. and M. H. Shokeir (1974). "Autosomal recessive cerebro-oculo-facio-skeletal (COFS) syndrome." Clin Genet **5**(4): 285-293.

Pera, M. F. (2011). "Stem cells: The dark side of induced pluripotency." Nature **471**(7336): 46-47.

Pettinato, G., X. Wen and N. Zhang (2014). "Formation of well-defined embryoid bodies from dissociated human induced pluripotent stem cells using microfabricated cell-repellent microwell arrays." Sci Rep **4**: 7402.

Ponchio, L., L. Duma, B. Oliviero, N. Gibelli, P. Pedrazzoli and G. Robustelli della Cuna (2000). "Mitomycin C as an alternative to irradiation to inhibit the feeder layer growth in long-term culture assays." Cytotherapy **2**(4): 281-286.

Popanda, O. and H. W. Thielmann (1992). "The function of DNA polymerases in DNA repair synthesis of ultraviolet-irradiated human fibroblasts." Biochim Biophys Acta **1129**(2): 155-160.

Proietti-De-Santis, L., P. Drane and J. M. Egly (2006). "Cockayne syndrome B protein regulates the transcriptional program after UV irradiation." EMBO J **25**(9): 1915-1923.

Prokhorova, T. A., L. M. Harkness, U. Frandsen, N. Ditzel, H. D. Schroder, J. S. Burns and M. Kassem (2009). "Teratoma formation by human embryonic stem cells is site dependent and enhanced by the presence of Matrigel." Stem Cells Dev **18**(1): 47-54.

Przyborski, S. A. (2005). "Differentiation of human embryonic stem cells after transplantation in immune-deficient mice." Stem Cells **23**(9): 1242-1250.

Qiang, L., R. Fujita and A. Abeliovich (2013). "Remodeling neurodegeneration: somatic cell reprogramming-based models of adult neurological disorders." Neuron **78**(6): 957-969.

Rajala, K., B. Lindroos, S. M. Hussein, R. S. Lappalainen, M. Pekkanen-Mattila, J. Inzunza, B. Rozell, S. Miettinen, S. Narkilahti, E. Kerkela, K. Aalto-Setala, T. Otonkoski, R. Suuronen, O. Hovatta and H. Skottman (2010). "A defined and xeno-free culture method enabling the

establishment of clinical-grade human embryonic, induced pluripotent and adipose stem cells." PLoS One **5**(4): e10246.
Ransom, B. R. and C. B. Ransom (2012). "Astrocytes: multitalented stars of the central nervous system." Methods Mol Biol **814**: 3-7.
Rapin, I., K. Weidenheim, Y. Lindenbaum, P. Rosenbaum, S. N. Merchant, S. Krishna and D. W. Dickson (2006). "Cockayne syndrome in adults: review with clinical and pathologic study of a new case." J Child Neurol **21**(11): 991-1006.
Rey, S. and G. L. Semenza (2010). "Hypoxia-inducible factor-1-dependent mechanisms of vascularization and vascular remodelling." Cardiovasc Res **86**(2): 236-242.
Reynolds, B. A., W. Tetzlaff and S. Weiss (1992). "A multipotent EGF-responsive striatal embryonic progenitor cell produces neurons and astrocytes." J Neurosci **12**(11): 4565-4574.
Reynolds, B. A. and S. Weiss (1992). "Generation of neurons and astrocytes from isolated cells of the adult mammalian central nervous system." Science **255**(5052): 1707-1710.
Risher, W. C., S. Patel, I. H. Kim, A. Uezu, S. Bhagat, D. K. Wilton, L. J. Pilaz, J. Singh Alvarado, O. Y. Calhan, D. L. Silver, B. Stevens, N. Calakos, S. H. Soderling and C. Eroglu (2014) "Astrocytes refine cortical connectivity at dendritic spines." Elife **3** DOI: 10.7554/eLife.04047.
Robinton, D. A. and G. Q. Daley (2012). "The promise of induced pluripotent stem cells in research and therapy." Nature **481**(7381): 295-305.
Rousseau, B., D. Dubayle, F. Sennlaub, J. C. Jeanny, P. Costet, A. Bikfalvi and S. Javerzat (2000). "Neural and angiogenic defects in eyes of transgenic mice expressing a dominant-negative FGF receptor in the pigmented cells." Exp Eye Res **71**(4): 395-404.
Roy, A., E. Krzykwa, R. Lemieux and S. Neron (2001). "Increased efficiency of gamma-irradiated versus mitomycin C-treated feeder cells for the expansion of normal human cells in long-term cultures." J Hematother Stem Cell Res **10**(6): 873-880.
Saif, M. W., K. Kaley, M. Brennan, M. C. Garcon and G. Rodriguez (2013). "Mitomycin-C and capecitabine (MIXE) as salvage treatment in patients with refractory metastatic colorectal cancer: a retrospective study." Anticancer Res **33**(6): 2743-2746.
Sander, J. D. and J. K. Joung (2014). "CRISPR-Cas systems for editing, regulating and targeting genomes." Nat Biotechnol **32**(4): 347-355.
Sanger, F., S. Nicklen and A. R. Coulson (1977). "DNA sequencing with chain-terminating inhibitors." Proc Natl Acad Sci U S A **74**(12): 5463-5467.
Sareen, D., G. Gowing, A. Sahabian, K. Staggenborg, R. Paradis, P. Avalos, J. Latter, L. Ornelas, L. Garcia and C. N. Svendsen (2014). "Human induced pluripotent stem cells are a novel source of neural progenitor cells (iNPCs) that migrate and integrate in the rodent spinal cord." J Comp Neurol **522**(12): 2707-2728.
Sathananthan, A. H. and A. Trounson (2005). "Human embryonic stem cells and their spontaneous differentiation." Ital J Anat Embryol **110**(2 Suppl 1): 151-157.
Schettler, T. (2001). "Toxic threats to neurologic development of children." Environ Health Perspect **109 Suppl 6**: 813-816.
Schumacher, C. (2012). Die Rolle des CSB-Proteins bei der neuronalen Entwicklung und Hypoxie-induzierten Transkription, Mathematisch-Naturwissenschaftliche Fakultät der Heinrich-Heine Universität Düsseldorf.
Scott, C. W., M. F. Peters and Y. P. Dragan (2013). "Human induced pluripotent stem cells and their use in drug discovery for toxicity testing." Toxicol Lett **219**(1): 49-58.
Selby, C. P. and A. Sancar (1997). "Cockayne syndrome group B protein enhances elongation by RNA polymerase II." Proc Natl Acad Sci U S A **94**(21): 11205-11209.
Seok, J., H. S. Warren, A. G. Cuenca, M. N. Mindrinos, H. V. Baker, W. Xu, D. R. Richards, G. P. McDonald-Smith, H. Gao, L. Hennessy, C. C. Finnerty, C. M. Lopez, S. Honari, E. E. Moore, J. P. Minei, J. Cuschieri, P. E. Bankey, J. L. Johnson, J. Sperry, A. B. Nathens, T. R. Billiar, M. A. West, M. G. Jeschke, M. B. Klein, R. L. Gamelli, N. S. Gibran, B. H. Brownstein, C. Miller-Graziano, S. E. Calvano, P. H. Mason, J. P. Cobb, L. G. Rahme, S. F. Lowry, R. V. Maier, L. L. Moldawer, D. N. Herndon, R. W. Davis, W. Xiao, R. G. Tompkins, Inflammation and L. S. C.

R. P. Host Response to Injury (2013). "Genomic responses in mouse models poorly mimic human inflammatory diseases." Proc Natl Acad Sci U S A **110**(9): 3507-3512.
Sheridan, S. D., V. Surampudi and R. R. Rao (2012). "Analysis of embryoid bodies derived from human induced pluripotent stem cells as a means to assess pluripotency." Stem Cells Int **2012**: 738910.
Sherman, D. L. and P. J. Brophy (2005). "Mechanisms of axon ensheathment and myelin growth." Nat Rev Neurosci **6**(9): 683-690.
Shi, Y., P. Kirwan, J. Smith, G. MacLean, S. H. Orkin and F. J. Livesey (2012). "A human stem cell model of early Alzheimer's disease pathology in Down syndrome." Sci Transl Med **4**(124): 124ra129.
Shim, K., G. Minowada, D. E. Coling and G. R. Martin (2005). "Sprouty2, a mouse deafness gene, regulates cell fate decisions in the auditory sensory epithelium by antagonizing FGF signaling." Dev Cell **8**(4): 553-564.
Shofuda, T., H. Fukusumi, D. Kanematsu, A. Yamamoto, M. Yamasaki, N. Arita and Y. Kanemura (2013). "A method for efficiently generating neurospheres from human-induced pluripotent stem cells using microsphere arrays." Neuroreport **24**(2): 84-90.
Si-Tayeb, K., F. K. Noto, A. Sepac, F. Sedlic, Z. J. Bosnjak, J. W. Lough and S. A. Duncan (2010). "Generation of human induced pluripotent stem cells by simple transient transfection of plasmid DNA encoding reprogramming factors." BMC Dev Biol **10**: 81.
Sidman, R. L. and P. Rakic (1973). "Neuronal migration, with special reference to developing human brain: a review." Brain Res **62**(1): 1-35.
Singh, V. K., M. Kalsan, N. Kumar, A. Saini and R. Chandra (2015). "Induced pluripotent stem cells: applications in regenerative medicine, disease modeling, and drug discovery." Front Cell Dev Biol **3**: 2.
Smith, K. P., M. X. Luong and G. S. Stein (2009). "Pluripotency: toward a gold standard for human ES and iPS cells." J Cell Physiol **220**(1): 21-29.
Song, M. R. and A. Ghosh (2004). "FGF2-induced chromatin remodeling regulates CNTF-mediated gene expression and astrocyte differentiation." Nat Neurosci **7**(3): 229-235.
Stadtfeld, M., M. Nagaya, J. Utikal, G. Weir and K. Hochedlinger (2008). "Induced pluripotent stem cells generated without viral integration." Science **322**(5903): 945-949.
Stebbings, R., L. Findlay, C. Edwards, D. Eastwood, C. Bird, D. North, Y. Mistry, P. Dilger, E. Liefooghe, I. Cludts, B. Fox, G. Tarrant, J. Robinson, T. Meager, C. Dolman, S. J. Thorpe, A. Bristow, M. Wadhwa, R. Thorpe and S. Poole (2007). ""Cytokine storm" in the phase I trial of monoclonal antibody TGN1412: better understanding the causes to improve preclinical testing of immunotherapeutics." J Immunol **179**(5): 3325-3331.
Stevnsner, T., S. Nyaga, N. C. de Souza-Pinto, G. T. van der Horst, T. G. Gorgels, B. A. Hogue, T. Thorslund and V. A. Bohr (2002). "Mitochondrial repair of 8-oxoguanine is deficient in Cockayne syndrome group B." Oncogene **21**(57): 8675-8682.
Suslov, O. N., V. G. Kukekov, T. N. Ignatova and D. A. Steindler (2002). "Neural stem cell heterogeneity demonstrated by molecular phenotyping of clonal neurospheres." Proc Natl Acad Sci U S A **99**(22): 14506-14511.
Takagaki, G., S. Berl, D. D. Clarke, D. P. Purpura and H. Waelsch (1961). "Glutamic acid metabolism in brain and liver during infusion with ammonia labelled with nitrogen-15." Nature **189**: 326.
Takahashi, K. and S. Yamanaka (2006). "Induction of pluripotent stem cells from mouse embryonic and adult fibroblast cultures by defined factors." Cell **126**(4): 663-676.
Takahashi, K., K. Tanabe, M. Ohnuki, M. Narita, T. Ichisaka, K. Tomoda and S. Yamanaka (2007). "Induction of pluripotent stem cells from adult human fibroblasts by defined factors." Cell **131**(5): 861-872.
Tamm, C., S. Pijuan Galito and C. Anneren (2013). "A comparative study of protocols for mouse embryonic stem cell culturing." PLoS One **8**(12): e81156.
Tanabe, K., M. Nakamura, M. Narita, K. Takahashi and S. Yamanaka (2013). "Maturation, not initiation, is the major roadblock during reprogramming toward pluripotency from human fibroblasts." Proc Natl Acad Sci U S A **110**(30): 12172-12179.

Tantin, D., A. Kansal and M. Carey (1997). "Recruitment of the putative transcription-repair coupling factor CSB/ERCC6 to RNA polymerase II elongation complexes." Mol Cell Biol **17**(12): 6803-6814.

Tantin, D. (1998). "RNA polymerase II elongation complexes containing the Cockayne syndrome group B protein interact with a molecular complex containing the transcription factor IIH components xeroderma pigmentosum B and p62." J Biol Chem **273**(43): 27794-27799.

Thalhammer, S., U. Koehler, R. W. Stark and W. M. Heckl (2001). "GTG banding pattern on human metaphase chromosomes revealed by high resolution atomic-force microscopy." J Microsc **202**(Pt 3): 464-467.

Thomson, A., D. Wojtacha, Z. Hewitt, H. Priddle, V. Sottile, A. Di Domenico, J. Fletcher, M. Waterfall, N. L. Corrales, R. Ansell and J. McWhir (2008). "Human embryonic stem cells passaged using enzymatic methods retain a normal karyotype and express CD30." Cloning Stem Cells **10**(1): 89-106.

Thomson, J. A., J. Itskovitz-Eldor, S. S. Shapiro, M. A. Waknitz, J. J. Swiergiel, V. S. Marshall and J. M. Jones (1998). "Embryonic stem cell lines derived from human blastocysts." Science **282**(5391): 1145-1147.

Tiscornia, G., E. L. Vivas and J. C. Izpisua Belmonte (2011). "Diseases in a dish: modeling human genetic disorders using induced pluripotent cells." Nat Med **17**(12): 1570-1576.

Troelstra, C., R. M. Landsvater, J. Wiegant, M. van der Ploeg, G. Viel, C. H. Buys and J. H. Hoeijmakers (1992a). "Localization of the nucleotide excision repair gene ERCC6 to human chromosome 10q11-q21." Genomics **12**(4): 745-749.

Troelstra, C., A. van Gool, J. de Wit, W. Vermeulen, D. Bootsma and J. H. Hoeijmakers (1992b). "ERCC6, a member of a subfamily of putative helicases, is involved in Cockayne's syndrome and preferential repair of active genes." Cell **71**(6): 939-953.

Tropea, D., E. Giacometti, N. R. Wilson, C. Beard, C. McCurry, D. D. Fu, R. Flannery, R. Jaenisch and M. Sur (2009). "Partial reversal of Rett Syndrome-like symptoms in MeCP2 mutant mice." Proc Natl Acad Sci U S A **106**(6): 2029-2034.

Tropepe, V., S. Hitoshi, C. Sirard, T. W. Mak, J. Rossant and D. van der Kooy (2001). "Direct neural fate specification from embryonic stem cells: a primitive mammalian neural stem cell stage acquired through a default mechanism." Neuron **30**(1): 65-78.

Tsubooka, N., T. Ichisaka, K. Okita, K. Takahashi, M. Nakagawa and S. Yamanaka (2009). "Roles of Sall4 in the generation of pluripotent stem cells from blastocysts and fibroblasts." Genes Cells **14**(6): 683-694.

Uemura, T., K. Takamatsu, M. Ikeda, M. Okada, K. Kazuki, Y. Ikada and H. Nakamura (2012). "Transplantation of induced pluripotent stem cell-derived neurospheres for peripheral nerve repair." Biochem Biophys Res Commun **419**(1): 130-135.

Uhl, E. W. and N. J. Warner (2015). "Mouse Models as Predictors of Human Responses: Evolutionary Medicine." Curr Pathobiol Rep **3**(3): 219-223.

Valamehr, B., R. Abujarour, M. Robinson, T. Le, D. Robbins, D. Shoemaker and P. Flynn (2012). "A novel platform to enable the high-throughput derivation and characterization of feeder-free human iPSCs." Sci Rep **2**: 213.

van der Horst, G. T., H. van Steeg, R. J. Berg, A. J. van Gool, J. de Wit, G. Weeda, H. Morreau, R. B. Beems, C. F. van Kreijl, F. R. de Gruijl, D. Bootsma and J. H. Hoeijmakers (1997). "Defective transcription-coupled repair in Cockayne syndrome B mice is associated with skin cancer predisposition." Cell **89**(3): 425-435.

Velez-Cruz, R. and J. M. Egly (2013). "Cockayne syndrome group B (CSB) protein: at the crossroads of transcriptional networks." Mech Ageing Dev **134**(5-6): 234-242.

Vousden, K. H. and D. P. Lane (2007). "p53 in health and disease." Nat Rev Mol Cell Biol **8**(4): 275-283.

Wang, H. and L. C. Doering (2012). "Induced pluripotent stem cells to model and treat neurogenetic disorders." Neural Plast **2012**: 346053.

Wang, S., J. Bates, X. Li, S. Schanz, D. Chandler-Militello, C. Levine, N. Maherali, L. Studer, K. Hochedlinger, M. Windrem and S. A. Goldman (2013). "Human iPSC-derived

oligodendrocyte progenitor cells can myelinate and rescue a mouse model of congenital hypomyelination." Cell Stem Cell **12**(2): 252-264.
Wang, X. and P. Yang (2008) "In vitro differentiation of mouse embryonic stem (mES) cells using the hanging drop method." J Vis Exp DOI: 10.3791/825.
Wang, Y. and J. Adjaye (2011). "A cyclic AMP analog, 8-Br-cAMP, enhances the induction of pluripotency in human fibroblast cells." Stem Cell Rev **7**(2): 331-341.
Warren, L., P. D. Manos, T. Ahfeldt, Y. H. Loh, H. Li, F. Lau, W. Ebina, P. K. Mandal, Z. D. Smith, A. Meissner, G. Q. Daley, A. S. Brack, J. J. Collins, C. Cowan, T. M. Schlaeger and D. J. Rossi (2010). "Highly efficient reprogramming to pluripotency and directed differentiation of human cells with synthetic modified mRNA." Cell Stem Cell **7**(5): 618-630.
Watanabe, K., M. Ueno, D. Kamiya, A. Nishiyama, M. Matsumura, T. Wataya, J. B. Takahashi, S. Nishikawa, S. Nishikawa, K. Muguruma and Y. Sasai (2007). "A ROCK inhibitor permits survival of dissociated human embryonic stem cells." Nat Biotechnol **25**(6): 681-686.
Wernig, M., A. Meissner, J. P. Cassady and R. Jaenisch (2008). "c-Myc is dispensable for direct reprogramming of mouse fibroblasts." Cell Stem Cell **2**(1): 10-12.
Wesselschmidt, R. L. (2011). "The teratoma assay: an in vivo assessment of pluripotency." Methods Mol Biol **767**: 231-241.
Wilson, D. M., 3rd and V. A. Bohr (2007). "The mechanics of base excision repair, and its relationship to aging and disease." DNA Repair (Amst) **6**(4): 544-559.
Woltjen, K., I. P. Michael, P. Mohseni, R. Desai, M. Mileikovsky, R. Hamalainen, R. Cowling, W. Wang, P. Liu, M. Gertsenstein, K. Kaji, H. K. Sung and A. Nagy (2009). "piggyBac transposition reprograms fibroblasts to induced pluripotent stem cells." Nature **458**(7239): 766-770.
Woods, C. G. (2004). "Human microcephaly." Curr Opin Neurobiol **14**(1): 112-117.
Wosik, K., R. Cayrol, A. Dodelet-Devillers, F. Berthelet, M. Bernard, R. Moumdjian, A. Bouthillier, T. L. Reudelhuber and A. Prat (2007). "Angiotensin II controls occludin function and is required for blood brain barrier maintenance: relevance to multiple sclerosis." J Neurosci **27**(34): 9032-9042.
Yamanaka, S. (2012). "Induced pluripotent stem cells: past, present, and future." Cell Stem Cell **10**(6): 678-684.
Yang, J., J. Cai, Y. Zhang, X. Wang, W. Li, J. Xu, F. Li, X. Guo, K. Deng, M. Zhong, Y. Chen, L. Lai, D. Pei and M. A. Esteban (2010). "Induced pluripotent stem cells can be used to model the genomic imprinting disorder Prader-Willi syndrome." J Biol Chem **285**(51): 40303-40311.
Yoshida, Y., K. Takahashi, K. Okita, T. Ichisaka and S. Yamanaka (2009). "Hypoxia enhances the generation of induced pluripotent stem cells." Cell Stem Cell **5**(3): 237-241.
Yu, J., M. A. Vodyanik, K. Smuga-Otto, J. Antosiewicz-Bourget, J. L. Frane, S. Tian, J. Nie, G. A. Jonsdottir, V. Ruotti, R. Stewart, Slukvin, II and J. A. Thomson (2007). "Induced pluripotent stem cell lines derived from human somatic cells." Science **318**(5858): 1917-1920.
Yu, J., K. Hu, K. Smuga-Otto, S. Tian, R. Stewart, Slukvin, II and J. A. Thomson (2009). "Human induced pluripotent stem cells free of vector and transgene sequences." Science **324**(5928): 797-801.
Zhang, J., E. Nuebel, G. Q. Daley, C. M. Koehler and M. A. Teitell (2012). "Metabolic regulation in pluripotent stem cells during reprogramming and self-renewal." Cell Stem Cell **11**(5): 589-595.
Zhang, N., M. C. An, D. Montoro and L. M. Ellerby (2010). "Characterization of Human Huntington's Disease Cell Model from Induced Pluripotent Stem Cells." PLoS Curr **2**: RRN1193.
Zhang, S. and W. Cui (2014). "Sox2, a key factor in the regulation of pluripotency and neural differentiation." World J Stem Cells **6**(3): 305-311.
Zhao, H., N. Sun, S. R. Young, R. Nolley, J. Santos, J. C. Wu and D. M. Peehl (2013). "Induced pluripotency of human prostatic epithelial cells." PLoS One **8**(5): e64503.
Zhao, Y., X. Yin, H. Qin, F. Zhu, H. Liu, W. Yang, Q. Zhang, C. Xiang, P. Hou, Z. Song, Y. Liu, J. Yong, P. Zhang, J. Cai, M. Liu, H. Li, Y. Li, X. Qu, K. Cui, W. Zhang, T. Xiang, Y. Wu, Y. Zhao, C. Liu, C.

Yu, K. Yuan, J. Lou, M. Ding and H. Deng (2008). "Two supporting factors greatly improve the efficiency of human iPSC generation." Cell Stem Cell **3**(5): 475-479.

Zhou, W. and C. R. Freed (2009). "Adenoviral gene delivery can reprogram human fibroblasts to induced pluripotent stem cells." Stem Cells **27**(11): 2667-2674.

Zhou, Y. Y. and F. Zeng (2013). "Integration-free methods for generating induced pluripotent stem cells." Genomics Proteomics Bioinformatics **11**(5): 284-287.

Zonta, M., M. C. Angulo, S. Gobbo, B. Rosengarten, K. A. Hossmann, T. Pozzan and G. Carmignoto (2003). "Neuron-to-astrocyte signaling is central to the dynamic control of brain microcirculation." Nat Neurosci **6**(1): 43-50.

6. Appendix

6.1 Supplementary Figures

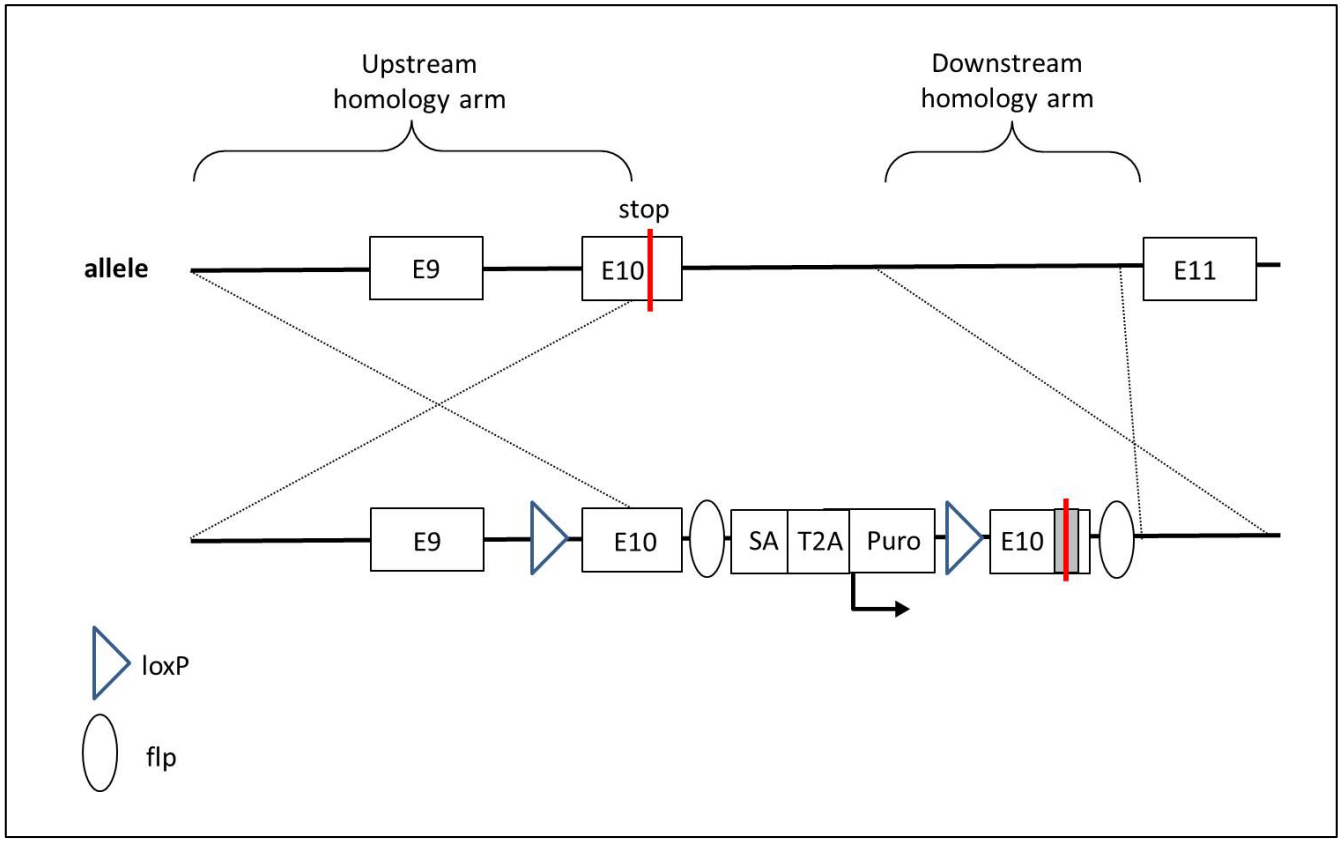

Fig. 6.1: Targeting construct to repair the point mutation of the COFS hiPSC line AS789. The COFS hiPSC line bears a point mutation in exon (E) 10 (c.2047C>T) which leads to a stop codon (upper chart). To repair this point mutation, the targeting construct (lower chart) contains the correct exon 10 sequence as well as the mutated one. The upstream homology arm includes exon 9 and the beginning of exon 10 whereas the downstream homology arm includes the intron between exon 10 and 11. The construct contains a puromycin resistance cassette (Puro) to select for positively transfected cells. By expressing the Cre protein, a DNA recombinase, the DNA double strand is cut at the loxP sites leading to the deletion of the wild type sequence. In contrast, using the recombinase flippase (flp) the mutated sequence is deleted leading to a repaired gene. The splice aceptor (SA) and Thoseaasigna virus 2 A peptide (T2A) allow the co-expression of the gene with the puromycin resistance gene. The targeting construct was designed from Dr. Daniel Haag (Institute for Stem Cell Biology and Regenerative Medicine, Stanford University).

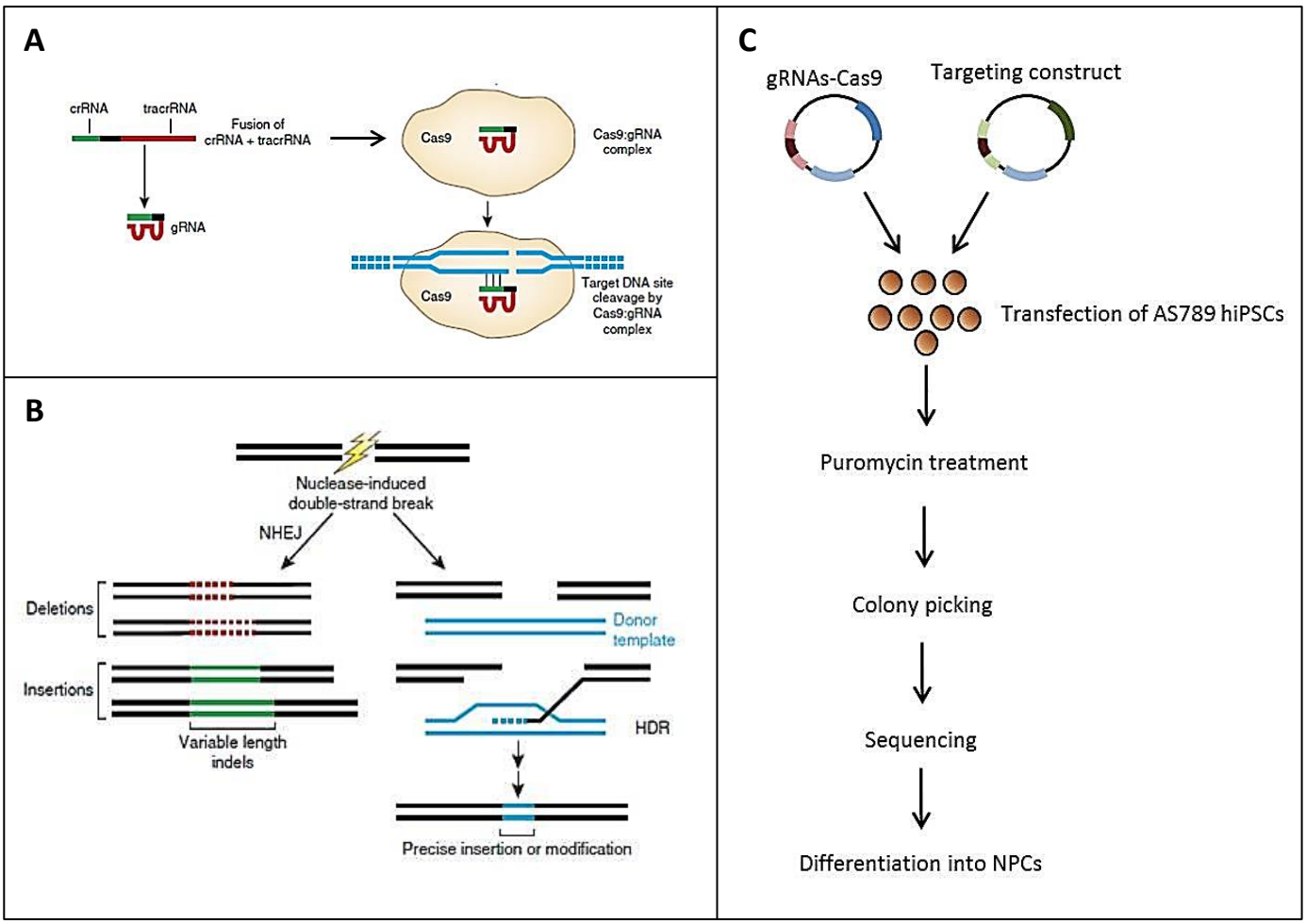

Fig. 6.2: Workflow to repair the point mutation of COFS hiPSC line AS789. A) guide RNAs (gRNAs) specific to the location of the point mutation bind the DNA and generate a specific double strand break by CRISPR-associated system (Cas) 9 activity. Taken from Sander and Joung (2014). **B)** The generated double strand break can be either repaired by non-homologous end-joining repair (NHEJ) generating deletions or insertions (indels) of variable length or by homologous directed repair (HDR) integrating a precise insertion using a donor template. Taken from Sander and Joung (2014). **C)** COFS hiPSCs need to be transfected with a vector containing the specific gRNAs and Cas9 as well as with a vector containing the specific targeting construct (Fig. 6.2). Successfully transfected cells can be selected by puromycin resistance. After selecting positive colonies, cells can be sequenced to verify the correct integration of the repaired sequence. At the end, COFS hiPSCs with successfully repaired genome can be differentiated into neural progenitor cells (NPCs) to determine if the observed phenotypes could be rescued by repairing the mutation.

6.2 List of Figures

6.3 List of Tables

6.4 Abbreviations

8-oxoG	7,8-hydroxyguanine
AD	Alzheimer's disease
AFP	Alpha-fetoprotein
ATP	Adenosine triphosphate
BER	Base excision repair
bFGF	Basic fibroblast growth factor
BMP4	Bone morphogenetic protein 4
BrdU	Bromodeoxyuridine
Cas9	CRISPR-associated
CBP	CREB-binding protein
cDNA	Copy DNA
CM	Conditional medium
C-Myc	Myelocytomatosis oncogene
CNS	Central Nervous System

COFS	Cerebro-Oculo-Facio-Skeletal
CRISPR	Clustered regularly interspaced short palindromic repeats
CS	Cockayne syndrome
CSA	Cockayne syndrome A
CSB	Cockayne syndrome B
CSPG4	Chrondritin sulfate proteoglycan 4
Ct	Control
DDB1	Damage-specific DNA binding protein 1
DMEM	Dulbecco's Modified Eagle Medium
DMSO	Dimethyl sulfoxide
DNA	Deoxyribonucleic acid
DNT	Developmental neural toxicity
DPBS	Dulbecco's Phosphate Buffered Saline
EBs	Embryoid bodies
EGF	Epidermal growth factor
EGFR	Epidermal growth factor receptor
ELISA	Enzyme-linked immunosorbent assay
ERCC1	DNA excision repair cross-complementing protein 1
ERCC6	excision-repair cross complementing group 6
ERCC8	excision-repair cross complementing group 8
FACS	Fluorescence activated cell sorting
FCS	Fetal calf serum
FGFR	Fibroblast growth factor receptor
FW	Forward Primer

GABA	Gamma-aminobutyric acid
GFAP	Glial fibrillary acidic protein
GG-NER	Global genome nucleotide excision repair
GLUT-1	Glucose transporter 1
hESCs	Human embryonic stem cells
HIF1α	Hypoxia inducible factor 1α
hiPSC	Human induced pluripotent stem cells
HIV	Human immunodeficiency virus
hNPCs	Human neural progenitor cells
HR23B	UV excision repair protein RAD23 homolog B
ICC	Immunocytochemistry
JAK3	Janus family kinase 3
kDa	kilo Dalton
Klf4	Kruppel-like factor 4
KSR	KnockOut Serum Replacement
LIF	Leukemia inhibitory factor
Lin28	Lineage protein 28
MAP2	Microtubule-associated protein 2
Mdm2	Mouse double minute 2 homolog
MEA	Multielectrode array
MEFs	Mouse embryonic fibroblasts
MeHgCl	Methyl mercury chloride
MSX1	Msh homeobox 1
NANOG	Nanog homeobox

NDM	Neural differentiation medium
NEAA	Non-essential amino acids
NER	Nucleotide excision repair
NGS	Normal goat serum
NIM	Neural induction medium
NPM	Neural proliferation medium
NSCs	Neural stem cells
OCT4	Octamer-binding transcription factor 4
OGG1	8-oxoG glycosylase 1
OPCs	Oligodendrocyte progenitor cells
PAX6	Paired-box protein 6
PBS	Phosphate Buffered Saline
PCR	Polymerase chain reaction
PD	Parkinson's disease
PDGFRα	Platelet-derived growth factor receptor alpha
PDL	Poly-D-Lysine-Hydrobromide
PFA	Paraformaldehyde
PI	Propodium iodide
Poly-HEMA	Poly-2-hydroxyethyl methacrylate
P/S	Penicillin/Streptomycin
p-value	Probability value
qRT-PCR	Quantitative realtime PCR
RNA	Ribonucleic acid
ROCK kinase	Rho-associated coiled coil forming protein serine/threonine

ROS	Reactive oxygen species
RTT	Rett syndrome
RV	Reverse Primer
SALL4	Spalt-like transcription factor 4
SD	Standard deviation
SEM	Standard error of mean
SMA	Smooth muscle actin
SOX2	Sex determining region Y-box 2
SSEA-3	Stage-specific embryonic antigen 3
SSEA-4	Stage-specific embryonic antigen 4
STAT	Signal transducer and activator of transcription
SWI2/SNF2	Switch/sucrose non-fermentable
Taq	Thermus aquaticus
TC-NER	Transcription-coupled nucleotide excision repair
TFIIH	Transcription factor IIH
TFIIS	Transcription factor IIS
TGFβ	Transforming growth factor β
TRA-1-60	Tumor rejection antigen 1-60
TRA-1-81	Tumor rejection antigen 1-81
ULA	Ultra-low attachment
UM	Unconditional medium
UTF1	Undifferentiated embryonic cell transcription factor 1
UVSS	UV-sensitive syndrome
VEGF	Vascular endothelial growth factor

Wt	Wild-type
XPA	Xeroderma pigmentosum A
XPC	Xeroderma pigmentosum C
XPF	Xeroderma pigmentosum F
XPG	Xeroderma pigmentosum G
XRCC1	X-ray repair cross-complementing protein 1
µg	Microgram
µL	Microliter
µm	Micrometer
µM	MicroMolar
°C	Degree Celsius

7. Eidesstattliche Erklärung

Eidesstattliche Erklärung zu meiner Dissertation mit dem Titel:

"Establishment of a hiPSC-based *in vitro* model to study environmental and genetic disturbances of neurodevelopmental processes"

Ich versichere an Eides Statt, dass die Dissertation von mir selbstständig und ohne unzulässige fremde Hilfe unter Beachtung der „Grundsätze zur Sicherung guter wissenschaftlicher Praxis" an der Heinrich-Heine-Universität Düsseldorf erstellt worden ist.

Ich versichere außerdem, dass ich die beigefügte Dissertation nur in diesem und keinem anderen Promotionsverfahren eingereicht habe, und dass diesem Promotionsverfahren keine gescheiterten Promotionsverfahren vorausgegangen sind.

Ort, Datum

Unterschrift

8. Danksagung

Besonders bedanken möchte ich mich bei meiner Doktormutter Prof. Dr. Ellen Fritsche für die Möglichkeit an diesem Projekt zu arbeiten. Des Weiteren möchte ich mich für die Unterstützung und die hilfreichen Diskussionen und Ratschläge bedanken, die mir stets geholfen haben, mein Projekt weiter voran zu bringen.

Mein besonderer Dank gilt Prof. Dr. Jean Krutmann, der mir ermöglichte im IUF an diesem Projekt zu arbeiten und meine Arbeit erfolgreich beenden zu können.

Prof. Dr. Dieter Willbold danke ich für die freundliche Übernahme des Zweitgutachtens.

Ich danke iBrain für die Finanzierung meines Projektes und allen Verantwortlichen für die freundliche und umfassende Betreuung.

Weiterhin möchte ich mich herzlich bei Frau Dr. Julia Tigges für die tatkräftige Unterstützung bedanken. Stets konnte ich mich an sie wenden und von ihrer umfangreichen wissenschaftlichen Erfahrung profitieren. Darüber hinaus stand sie mir auch bei allen anderen Angelegenheiten immer zur Seite.

Muchas gracias a Dr. Marta Barenys por su ayuda, los consejos y su optimismo. También agradesco el tiempo libre, la cocina y las clases de espaňol.

Ich bedanke mich ganz herzlich bei der gesamten AG Fritsche und allen Ehemaligen, die meinen Weg kreuzten, für die tolle Zeit. Dabei gilt mein ganz besonderer Dank Herrn Dr. Martin Schmuck für viele wissenschaftliche, tiefgründige und nicht ganz so tiefgründige Gespräche. Bedanken möchte ich mich auch bei Frau Dr. Katharina Dach, die mich mit ihrer energischen Art und ihrem Perfektionismus immer sehr beeindruckt hat. Für die angenehme Atmosphäre innerhalb und außerhalb des Büros bedanke ich mich besonders bei Denise de Boer, Farina Bendt und Diane Schmiegelt. Ulrike Hübenthal danke ich vor allem für die tolle Unterstützung mit zahlreichen PCRs und in der Zellkultur. Vielen Dank auch an Laura Nimtz und Yaschar Kabiri, die mir mit ihrer unkomplizierten und freundlichen Art meine Betreuerpflichten immer sehr angenehm gestaltet haben. Ein ganz besonderer Dank gilt ebenfalls Frau Dr. Susanne Giersiefer für die kompetente und freundliche Unterstützung bei der Sequenzierung. Danken möchte ich außerdem Stefan Masjosthusmann, Dr. Jenny Baumann und Dr. Janette Goniwiecha für die freundliche Unterstützung.

Dr. Marc Majora danke ich für seine Unterstützung und seine stets freundliche Art. Auch der gesamten AG Krutmann gilt mein besonderer Dank für die freundliche Aufnahme und Hilfe während meines Projektes.

Ich bedanke mich bei Prof. Dr. James Adjaye und Prof. Dr. Jean-Marc Egly für die Bereitstellung der hiPS Zellen. Außerdem bedanke ich mich ganz herzlich bei Frau Dr. Friederike Schröter für die umfassende Einführung in die hiPS Zellkultur. Bedanken möchte ich mich auch bei Herrn Dr. Alexey Epantchintsev für die Unterstützung mit den hiPS Zellen.

Ich bedanke mich bei Prof. Dr. Luc Stoppini für die interessante und schöne Zeit in Genf und bei Herrn Dr. Youssef Hibaoui und Herrn Dr. Maxime Feyeux für die kritische Diskussion über mein Projekt.

Außerdem bedanke ich mich bei Herrn Dr. Daniel Haag für die umfassende Unterstützung während der Planung für die Erstellung endogener Kontrollen mittels CRISPR/Cas-9.

Ein ganz besonderer Dank gilt Katerina Kefalakes für ihre ansteckende Fröhlichkeit.

Bei meinen iBrain Kolleginnen Klaudia Lepka und Christine Baksmeier möchte ich mich für die leckeren Treffen bedanken, in denen über wichtige und unwichtige Themen diskutiert wurde.

Ein herzlicher Dank gilt meinen Eltern, die mir das Studium ermöglicht haben und mich immer unterstützen.

Ein großes Dankeschön geht außerdem an Helge für seine Geduld und seine unermüdliche Unterstützung.